

**Climate, vegetation and  
lake development at Sokli  
(northern Finland) during  
early MIS 3 at ~ 50 kyr:**

**Revising earlier concepts on climate,  
glacial and vegetation dynamics in  
Fennoscandia during the Weichselian**

Karin F Helmens, Department of Physical Geography  
and Quaternary Geology, Stockholm University

August 2009

**Svensk Kärnbränslehantering AB**

Swedish Nuclear Fuel  
and Waste Management Co

Box 250, SE-101 24 Stockholm  
Phone +46 8 459 84 00



**Climate, vegetation and  
lake development at Sokli  
(northern Finland) during  
early MIS 3 at ~ 50 kyr:**

**Revising earlier concepts on climate,  
glacial and vegetation dynamics in  
Fennoscandia during the Weichselian**

Karin F Helmens, Department of Physical Geography  
and Quaternary Geology, Stockholm University

August 2009

This report concerns a study which was conducted for SKB. The conclusions and viewpoints presented in the report are those of the author. SKB may draw modified conclusions, based on additional literature sources and/or expert opinions.

A pdf version of this document can be downloaded from [www.skb.se](http://www.skb.se).

## Preface

This document contains information on climate and environmental conditions during part of the Weichselian glaciation, to be used in the safety assessment SR-Site. The information will be used in e.g. the report "Climate and climate-related issues for the safety assessment SR-Site".

Stockholm, August 2009

*Jens-Ove Näslund*

Person in charge of the SKB climate programme

## Summary

Long sediment records that register environmental changes in formerly glaciated regions such as Fennoscandia in the period preceding the Last Glacial Maximum (LGM) at ~ 20 kyr are rare. The Weichselian history of Fennoscandia is based on the long-distance correlation of poorly dated stratigraphic fragmentary evidence and studies on glacial geomorphology. Environmental conditions during ice-free intervals have been mostly reconstructed based on low resolution palynological analysis only. Here we present the results of a detailed study of a for Fennoscandia unusually long and continuous sediment sequence that has been recovered from the Sokli basin in northern Finland. The Sokli sequence consists of tills, glacio-fluvial beds, and fluvial beds, interlayered with fossil-rich lacustrine sediments that according to multiple accelerator mass spectrometer (AMS)  $^{14}\text{C}$  and optically stimulated luminescence (OSL) datings extend from the present into the Penultimate Glacial representing the last ~ 130 kyr.

This report focuses on the youngest Weichselian interstadial interval with ice-free conditions at Sokli dated to ~ 50 kyr in the early part of Marine Isotope Stage (MIS) 3. A comprehensive environmental reconstruction is made based on multi-proxy analysis on a two meter thick laminated, lacustrine clay-silt sequence, including lithological characteristics; organic content (loss-on-ignition, LOI); plant microfossils (pollen, spores, algal and fungal remains); macrofossils of plants (e.g. seeds, moss remains) and of aquatic animals (e.g. statoblasts of Bryozoa); head-capsules of chironomids (i.e. aquatic insects); and diatoms and other siliceous microfossils (e.g. phytolites, chrysophyte stomatocysts). Additionally, geomorphic evidence and analysis of Digital Elevation Model (DEM) data are employed in the environmental reconstruction. Mean July temperatures are reconstructed by applying transfer functions to the pollen, chironomid and diatom records.

The results have been surprising in various aspects, seriously challenging the present concept on environmental conditions during early MIS 3 in the near-central area of the Fennoscandia glaciations. Traditionally, the area is thought to have been ice covered throughout MIS 4-2 from ~ 70 kyr to the deglaciation at 10 kyr ago. Our study shows not only ice-free conditions but also warming to present-day temperatures. The laminated sediments seem to have been deposited in a sheltered embayment of a glacial lake impounded along the ice front of the Fennoscandian Ice Sheet. Throughout the deposition of the lacustrine sediments, the reconstructed terrestrial ecosystem on the deglaciated land is low-arctic shrub tundra very similar in composition to modern tundra in the continental sector of northern Fennoscandia. The distributional ranges of pine and tree birch were probably only few hundred kilometres south or south-east of Sokli. This is concordant with the sparse evidence for the presence of boreal tree taxa during MIS 3 in the Baltic countries and further east in Europe but contradicts with the commonly inferred treeless tundra or grass-dominated steppe conditions in central Europe.

Mean July air temperatures in the magnitude of present-day values are reconstructed by the chironomid and diatom records as well as by fossils from aquatic plants and Bryozoa. Temperature inferences based on the terrestrial pollen are consistently lower than the temperatures reconstructed from the fossil aquatic assemblages. It is possible that the regional terrestrial and the local aquatic systems responded differently to the climatic and landscape features at the time of MIS 3. Warmest and moistest conditions are recorded in the lower part of the laminated lacustrine sequence. This is consistent with the pattern of the Greenland millennium-scale Dansgaard-Oeschger (D/O) interstadials in which abrupt warming is followed by a gradual cooling. The chironomid-inferred mean July air temperatures amount to around  $13^{\circ}\text{C}$  (i.e. current value)  $\pm 1.15^{\circ}\text{C}$  in the lower part of the lake sequence and to around  $12 \pm 1.15^{\circ}\text{C}$  in the upper part. The mean July air temperatures inferred from the terrestrial pollen data lie within the range of around  $12 \pm 1.5^{\circ}\text{C}$  (lower part of sequence) and around  $11 \pm 1.5^{\circ}\text{C}$  (higher part of sequence). High summer temperatures are ascribed in part to enhanced July insolation compared to present at the high latitude site of Sokli.

Comparison with recently published, well-dated sediment sequences in eastern and western Finland suggest ice-free and warm conditions in major part of eastern Fennoscandia at ~ 50 kyr. Open birch forest seems to be registered in eastern Finland during part of the warming event. Direct evidence is lacking to reconstruct the total time span with ice-free conditions at the studied sites. It is argued that the Sokli site was glaciated during the overall colder late MIS 3. The absence of well-dated geological data in northern Sweden hampers a reconstruction of the total ice-marginal retreat in the continental sector of the Fennoscandian Ice Sheet during the 50 kyr warming event.

# Contents

|          |  |    |
|----------|--|----|
| <b>1</b> | <b>Introduction</b>  | 9  |
| 1.1      | Background   | 9  |
| 1.2      | Project description and objectives   | 9  |
| 1.3      | This report  | 14 |
| <b>2</b> | <b>Present environmental setting of the study area</b>   | 17 |
| <b>3</b> | <b>The Sokli B-series borehole</b>   | 19 |
| 3.1      | Coring and sub-sampling  | 19 |
| 3.2      | Lithology and dating   | 20 |
| <b>4</b> | <b>Reconstruction of lake development, sedimentation and ecosystem composition</b>             | 23 |
| 4.1      | Reconstructions based on multi-proxy evidence  | 23 |
| 4.1.1    | Methods  | 23 |
| 4.1.2    | Lake development and sedimentation   | 25 |
| 4.1.3    | Ecosystem composition  | 29 |
| 4.1.4    | Comparison of the multi-proxy data   | 34 |
| 4.2      | Reconstruction of glacial lake evolution using digital elevation model and geomorphologic data | 38 |
| <b>5</b> | <b>Quantitative climate reconstructions</b>  | 41 |
| 5.1      | Proxy-based reconstructions  | 41 |
| 5.1.1    | The chironomid record  | 41 |
| 5.1.2    | The terrestrial pollen record  | 45 |
| 5.1.3    | The diatom record  | 46 |
| 5.1.4    | Comparison of the multi-proxy based climate reconstructions                                    | 48 |
| 5.2      | Climate model simulations  | 49 |
| <b>6</b> | <b>Early MIS 3 lacustrine sequences in Finland</b>   | 51 |
| 6.1      | Stratigraphy and dating  | 51 |
| 6.1.1    | Ruunaa (eastern Finland)   | 51 |
| 6.1.2    | Hitura (western Finland)   | 52 |
| 6.2      | Environmental reconstructions  | 53 |
| 6.2.1    | Ruunaa (eastern Finland)   | 53 |
| 6.2.2    | Hitura (western Finland)   | 53 |
| <b>7</b> | <b>Discussions</b>   | 55 |
| 7.1      | Vegetation and climate in Finland during early MIS 3   | 55 |
| 7.2      | Timing and duration of the early MIS 3 ice free interval in Finland                            | 57 |
| 7.3      | Configuration of the Fennoscandian Ice Sheet during early MIS 3                                | 58 |
|          | <b>Acknowledgements</b>  | 60 |
|          | <b>References</b>  | 61 |
|          | <b>Appendix I</b> List of chironomid-taxa encountered in the MIS 3 sediments at Sokli          | 73 |
|          | <b>Appendix II</b> List of diatom-taxa encountered in the MIS 3 sediments at Sokli             | 75 |

# 1 Introduction

## 1.1 Background

Long sediment records that register environmental and climatic changes in formerly glaciated regions such as Fennoscandia in the period preceding the Last Glacial Maximum (LGM) at ~ 20 kyr are rare. Consecutive glacial events by the continental Fennoscandian Ice Sheet seem to have erased most of the Quaternary sedimentary geological record in Fennoscandia, leaving scattered and highly fragmented sedimentary sequences. The environmental history of Fennoscandia during the Last Glacial cycle (or Weichselian in the northwestern European mainland climate-stratigraphy), between 115 and 10 kyr, has been mostly reconstructed based on long-distance correlation of the often poorly-dated stratigraphic fragmentary evidence.

The nature of terrestrial ecosystems in Fennoscandia during relatively warm, ice-free intervals of the Last Glacial cycle (interstadials) has been deduced from pollen analysis of organic-bearing beds. In the absence of absolute dating, age assignments have been based on correlation with long pollen records from the northwest European mainland. As clearly outlined in /Donner 1996/, this correlation has been fraught with uncertainties: 1) Pollen-bearing interstadial beds are usually not found in sequence with sediments of Last Interglacial age (Eemian at around 120 kyr), in other words, the interstadial sediment could belong to an older cold stage than the Weichselian. 2) Sediment beds are mostly truncated, covering only part of an interstadial (or interglacial such as the Eemian Interglacial) sequence. 3) The distance of correlation is large (including an area with a great range of climatic conditions due to differences in latitude and altitude). 4) The differences in vegetational history between the Early Weichselian interstadials, and between the Middle Weichselian interstadials, on the European mainland are very small, making correlation very difficult.

The glacial history of Fennoscandia during the Weichselian relies heavily on correlation with the deep-sea record. The marine record suggests relatively large global ice volumes during Marine Isotope Stages (MIS) 4-2. As such, the classic notion has been that large parts of Fennoscandia were glaciated by the Fennoscandian Ice Sheet throughout MIS 4-2, from ~70 kyr to the deglaciation at 15–10 kyr ago. Relative extensive ice cover over Fennoscandia has also been postulated for MIS 5d (at around 110 kyr) and 5b (90 kyr) following correlation with the deep-sea record /e.g. Andersen and Mangerud 1989, Mangerud 1991, Lundqvist 1992, Donner 1995/.

It has long been acknowledged, however, that the oxygen-isotope record obtained from deep-sea foraminifera carries a composite signal of global ice volume and ocean water temperature /Chappell and Shackleton 1986, Shackleton 1987/. Relatively high sea levels and small global ice volumes during MIS 3 between 60–28 kyr are suggested by dated coral terraces around the world /e.g. Linsley 1996/. In addition, during recent years, high-resolution marine and ice core records are providing a climatic background of abrupt, large magnitude changes in climate and oceanic circulation during the Weichselian /e.g. Dansgaard et al. 1993, Bond et al. 1993, Johnsen et al. 2001, NorthGRIP Members 2004, Huber et al. 2006/ and increasing evidence shows that these millennium-scale changes impacted the terrestrial environment on the European continent as well /e.g. Sirocko et al. 2005, Spötl et al. 2006, Wohlfarth et al. 2008/.

## 1.2 Project description and objectives

In 2006, a project co-financed by Svensk Kärnbränslehantering AB (SKB) and POSIVA (Finland) entitled “**Weichselian climate variability in Scandinavia based on a unique sediment sequence preserved at Sokli**” was launched at Stockholm University (Sweden) with principal investigator Dr. Karin F. Helmens. The main objective of this project is to make a detailed climate and environmental reconstruction for different time intervals of the Weichselian when ice-free conditions prevailed at the Sokli site in northeastern Finland (Figure 1-1). The Sokli basin contains a for Fennoscandia unusually long and continuous sediment sequence. The sequence consists of tills, glacio-fluvial beds, and fluvial beds, interlayered with fossil-rich lacustrine sediments that extend from the present into the Penultimate Glacial (Late Saalian or MIS 6), representing the last ~ 130 kyr /Helmens et al. 2000, 2007a/. The Sokli sediments have been protected from glacial erosion due to their sheltered position in a

depression formed in deeply weathered rocks of a carbonate-rich magma intrusion /Ilvonen 1973/ and to sustained cold-based sub-glacial conditions during the LGM /Kleman et al. 1997, 1999, Boulton et al. 2001/. The Sokli sediment sequence is dated by independent accelerator mass spectrometer (AMS)  $^{14}\text{C}$  and optically stimulated luminescence (OSL) dating which is in agreement with stratigraphic dating based on correlation with the deep-sea record /Helmens et al. 2000, 2007a, Alexanderson et al. 2008/.

A reconnaissance study of the entire Sokli sequence has revealed a more dynamic glacial environment with less extensive and more variable ice cover during the Weichselian /Helmens et al. 2000, 2007a/ than previously reconstructed based on long-distance correlation of fragmented litho- and bio-stratigraphic data /Korpela 1969, Hirvas 1991, Donner 1995/. It shows that Sokli became glaciated for the first time during the second cold stage of the Early Weichselian (MIS 5b). Thereafter the region became ice-free twice including during the early part of MIS 3. The reconnaissance study has also revealed the unique fossil content of the non-glacial sediments including abundant and well-preserved micro- and macrofossils of a large variety of plants and aquatic animals. Therefore, the Sokli sedimentary sequence provides a unique opportunity to study in detail environmental changes and climate variability in Fennoscandia for a series of ice-free intervals during the last 130 kyr. Sokli is situated in the relatively flat Precambrian Shield region at ~ 500 km east of the Scandinavian mountain chain (Figure 1-1). Its climate is representative for the climate over central Finnish Lapland (Figure 1-2). Its location in the near-central area of the Fennoscandian glaciations (Figure 1-3) makes it a key-site for understanding the dynamics of the Fennoscandian Ice Sheet through the Last Glacial cycle.

The project “Weichselian climate variability in Scandinavia based on a unique sediment sequence preserved at Sokli” reconstructs in detail climate and environmental conditions for three different time intervals of the Weichselian. Based on the reconnaissance study of the Sokli sequence, the climate conditions during these intervals ranged from 1) cold and possibly dry, peri-glacial during the stadial interval dated to MIS 5d (115–105 kyr); to 2) almost as warm as today in the Sokli area (interstadial of MIS 5c age, 105–95 kyr); to 3) relatively warm in an ice-marginal environment (interstadial dated to early part of MIS 3, ~ 50 kyr). These conditions are thought to cover the full range of Weichselian stadial-interstadial climate variability, during ice-free conditions, which could be expected in the Sokli area in case of future climate cooling and glaciation.

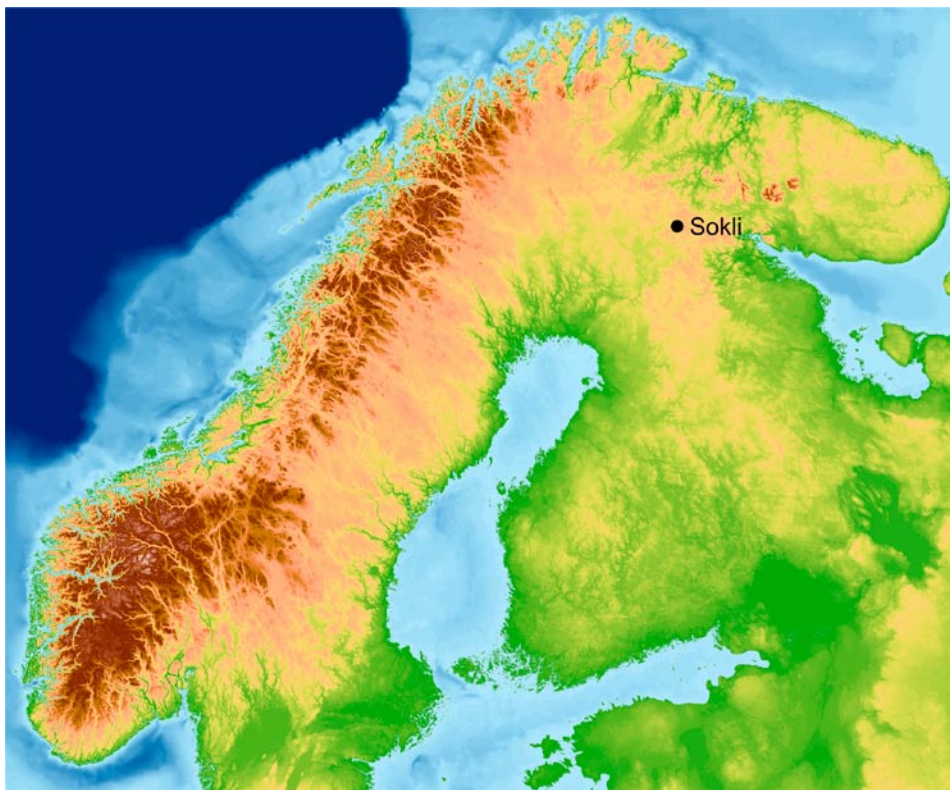


**Figure 1-1.** Location of the study site Sokli (lat. 67°48'N, long. 29°18'E, elevation 220 m.a.s.l.) in the relatively flat Precambrian Shield region of northeastern Fennoscandia.

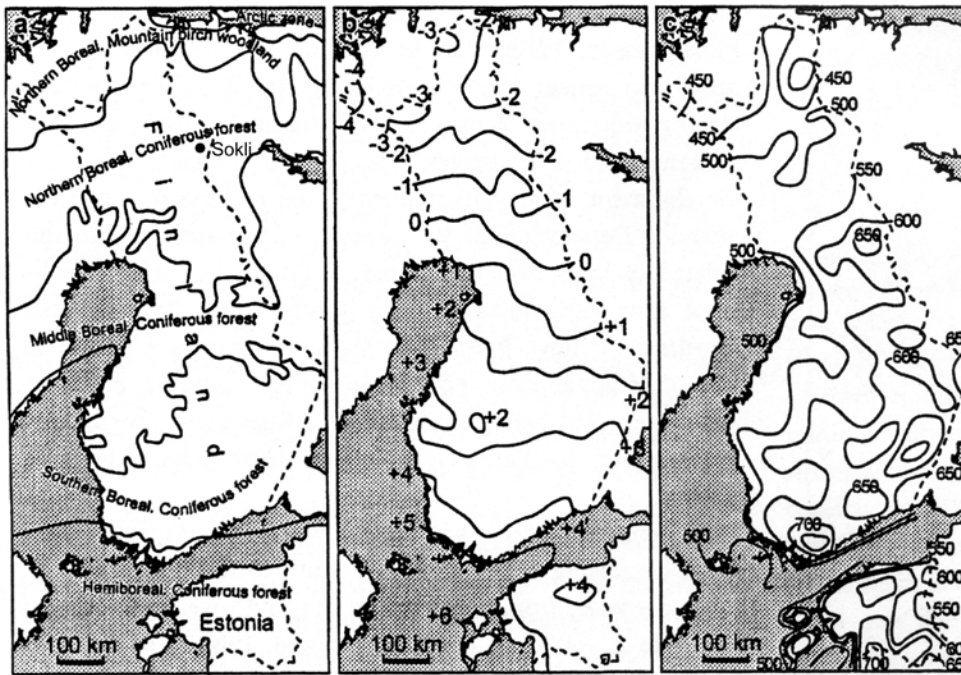


**Figure 1-2.** Vegetation zones of Finland (left panel), distribution of annual mean temperature ( $^{\circ}\text{C}$ ; middle panel), and distribution of annual precipitation (mm; right panel). From /Seppä et al. 2004/. The study site Sokli is indicated. Temperature patterns in Finland are relatively simple with decreasing values from the south ( $+5^{\circ}\text{C}$ ) to the north ( $-3^{\circ}\text{C}$ ). July is the warmest month (not shown). Finland is located on the lee side of the Scandes Mountains (see Figure 1-1), where the influence of Atlantic air flow on precipitation is subdued and the annual precipitation values are relatively low. Highest values, 650–700 mm, are recorded in southern and eastern Finland. On the west coast of Finland and in Lapland values are lower, 450–550 mm. The vegetation zonation in Finland follows the main south-north climatic gradient.

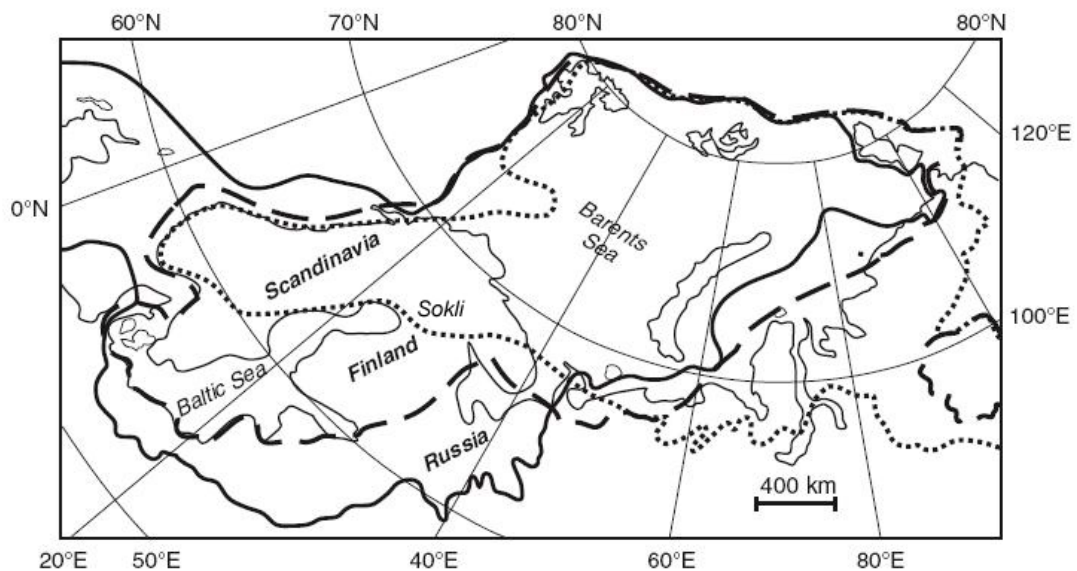


**Figure 1-3.** The location of Sokli in the near-central area of the Fennoscandian glaciations. The figure shows the extent of the Eurasian Ice Sheet, including the Fennoscandian Ice Sheet to the southwest (over Scandinavia and Finland (i.e. Fennoscandia), the Baltic countries and the northwestern Russian plain) and the Barents Sea Ice Sheet to the northeast (over the Barents Sea, Novaya Zemlya and the northernmost part of the northwestern Russian lowland), during three different time slices in the Weichselian,  $\sim 95\text{--}85$  kyr (MIS 5b, stippled line),  $\sim 75\text{--}60$  kyr (MIS 4, dashed line) and the LGM extent  $\sim 20$  kyr (MIS 2, solid line). From /Lunkka et al. 2008/, modified after /Svendsen et al. 2004/.

The methods applied in this project are similar to those being used during recent years to reconstruct environmental and climate conditions during the Present Interglacial (Holocene, last 10 kyr). The non-glacial sediments in the Sokli sequence (Figure 1-4) are subjected to high-resolution, multi-proxy analyses (Figure 1-5) including the analysis of: 1) lithological characteristics; 2) organic content (as assessed by loss-on-ignition (LOI)); 3) plant microfossils (pollen, spores, algal and fungal remains); 4) macrofossils of plants (e.g. seeds, moss remains) and of aquatic animals (e.g. statoblasts of Bryozoa); 5) head-capsules of chironomids (i.e. aquatic insects); and 6) diatoms and other siliceous microfossils (e.g. phytolites, chrysophyte stomatocysts). Multi-proxy analysis allows a comprehensive reconstruction of the past environmental conditions such deposition environment, the nature of lake, wetland and terrestrial ecosystems and catchment erosion. A transfer function approach /e.g. Birks 2003/ is used to infer quantitatively mean July air temperatures from the fossil record. The transfer functions make use of modern-day animal/plant-climate calibration sets from northern Europe /Brooks and Birks 2001, Seppä and Birks 2001, Weckström et al. 2006/. In addition, minimum mean July air temperatures are estimated based on information of the present distribution of certain plant/animal species ('indicator species') in northern Europe /e.g. Kolstrup 1980/.

Multi-proxy analysis minimizes problems related to the interpretation of single proxies. Furthermore, the multi-proxy-inferred comprehensive reconstruction of past environmental conditions is important for the evaluation of the quantitative climate reconstructions /e.g. Heiri and Lotter 2005, Walker and Cwynar 2006, Weckström et al. 1997a, b/. Climate and other environmental factors may produce similar signals in a proxy record, such as both cooling and wetland expansion can increase herb percentages in the pollen record, and the multi-proxy data allows discriminating between the different environmental factors.

Environmental reconstruction is also made on the landscape level (e.g. glacial lake evolutions) using aerial photo- and satellite image-interpretation and analysis of Digital Elevation Model data. Additionally, the proxy-based climate reconstructions are compared with climate model simulations.

**Different specialists and institutions in Europe are collaborating on the application of the multi-proxy and transfer function approaches to the study of the Sokli sediments, and on geomorphology/GIS, including:**

*University of Helsinki (Finland):*

Prof. Dr. Heikki Seppä (pollen-climate transfer function), Dr. Minna Väliranta (macrofossil analysis), Dr. Jan Weckström (diatom-climate transfer function).

*Geological Survey of Finland:*

Dr. Peter Johansson (geomorphology).

*University of Bergen (Norway):*

Prof. Dr. John Birks (pollen-climate transfer function, ecosystem reconstruction), Dr. Hilary Birks (macrofossil identification).

*Vrije Universiteit Amsterdam (The Netherlands):*

Dr. Hanneke Bos (macrofossil analysis), Dr. Sjoerd Bohncke (paleo-ecology), Dr. Stefan Engels (chironomid analysis).

*Utrecht University (The Netherlands):*

Dr. Olivier Heiri (chironomid identification and interpretation).

*The Natural History Museum, London (U.K.):*

Prof. Dr. Steve Brooks (chironomid-climate transfer function).

*Stockholm University (Sweden):*

Dr. Jonas Bergman (pollen analysis), Mrs. Annika Berntsson (MSc; diatom analysis), Dr. Krister Jansson (GIS), Mrs. Päivi Kaislahti Tillman (MSc; diatom analysis), Mr. Martin Margold (MSc; geomorphology; GIS), Dr. Jan Risberg (diatom identification).

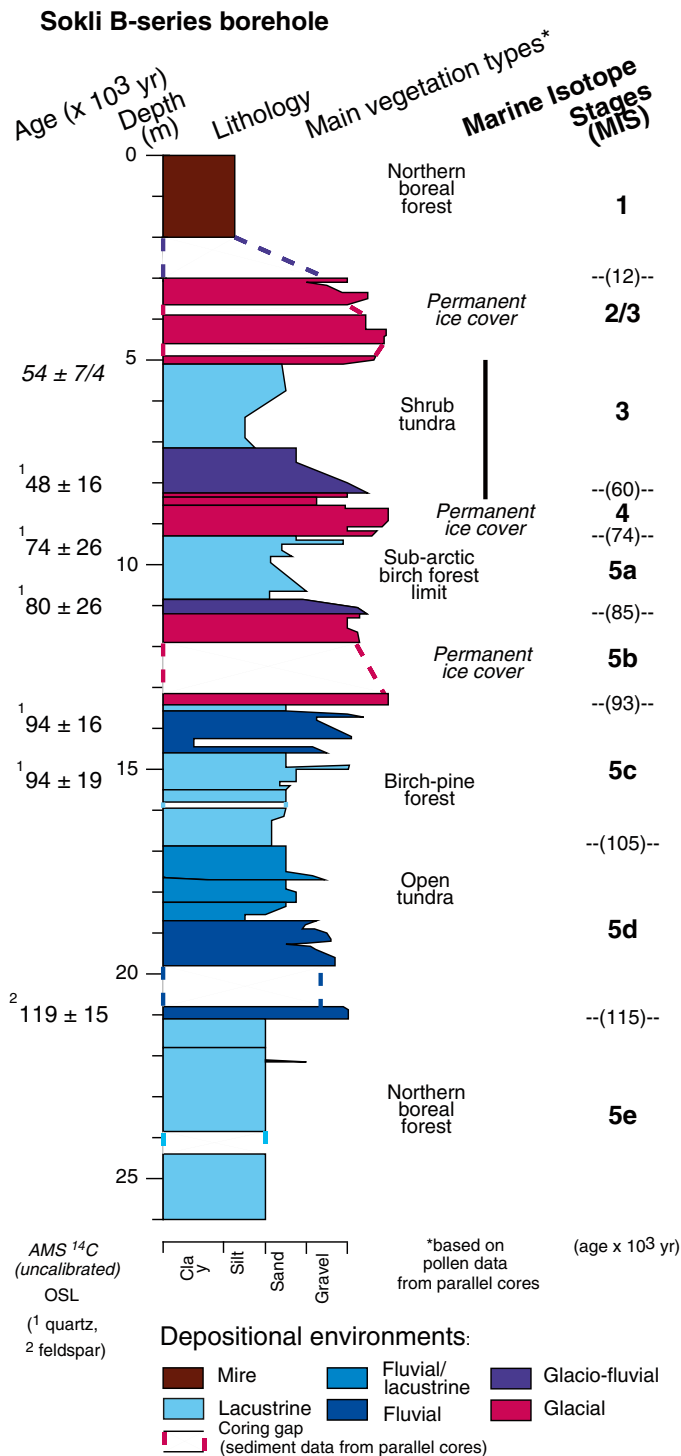


**Figure 1-4.** The Late Quaternary sedimentary sequence at Sokli as recorded in the Sokli B-series borehole. This borehole represents the most complete sediment recovery from the central Sokli basin; it reaches into the Last Interglacial (MIS 5e) lacustrine bed and has only minor gaps corresponding with the coarsest sediment layers. The independent AMS <sup>14</sup>C and OSL chronology for the Sokli B-series borehole is indicated to the left of the column showing simplified lithology and inferred depositional environments, and inferred vegetation/ice-cover and correlations with the deep-sea record /Martinson et al. 1987/ are on the right. The present study focuses on the ice-marginal and overlying lacustrine sediments dated to the early part of MIS 3 at ~ 50 kyr (highlighted in figure).

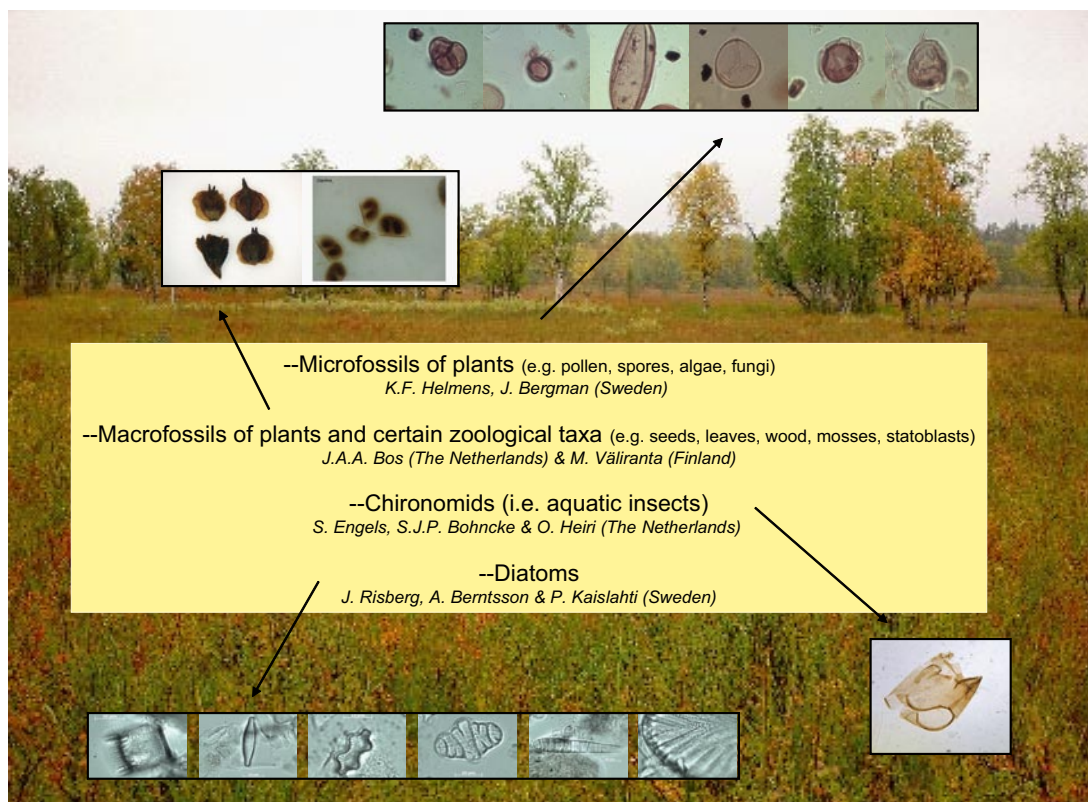


**Figure 1-5.** Illustrations of different biotic proxies analyzed in the non-glacial sediments at Sokli with specialists.

### 1.3 This report

This report presents the results from the interstadial deposit in the Sokli basin dated to the early part of MIS 3 at ~ 50 kyr. The climate reconstructions for the early MIS 3 interstadial at Sokli have been discussed in the workshop “Quantitative climate reconstruction for MIS 3 based on multi-proxy evidence from Sokli (northern Finland)”, Helsinki University, Finland, November 15–16, 2007 (funded by Nordic Network of Palaeoclimatology (NEPAL), NordForsk). Part of the analyses of the MIS 3 deposit at Sokli were carried out in the scope of the European Science Foundation (ESF) EUROCORES on EuroCLIMATE project ‘RESOLuTION’: “Rapid climatic and environmental shifts during Oxygen Isotope Stages 2 and 3 – linking high-resolution terrestrial, ice core and marine archives” coordinated by Prof. Dr. Barbara Wohlfarth (Stockholm University; 2005–2008).

#### **This report is a compilation of the following papers (with summaries):**

- 1) *Present-day temperatures in northern Scandinavian during the Last Glaciation*. Authors: Helmens K F, Bos, J A A, Engels S, Van Meerbeeck C J, Bohncke S J P, Renssen H, Heiri O, Brooks S J, Seppä H, Birks H J B, Wohlfarth B. *Geology*: 35, 987–990 (2007).

This paper gives a first integration of the multi-proxy data obtained from the Sokli early MIS 3 lacustrine deposit and presents the pollen- and chironomid-inferred temperature curves. The chironomids, as well as fossils from aquatic plants and Bryozoa, reconstruct surprisingly high, present-day mean July air temperatures. Comparison with a climate-model simulation with a MIS 3 interstadial setup (carried out in the scope of the RESOLuTION project) confirms the high mean July temperatures northeast of the Fennoscandian Ice Sheet in response to high insolation values during MIS 3 and dry winds blowing off the ice sheet. The early MIS 3 interstadial at Sokli is correlated with Interstadial (IS) 14 in the Greenland ice core record. The paper not only provides evidence for a highly dynamic Fennoscandian Ice Sheet during the middle part of the Last Glacial cycle, resulting in extensive deglaciation during early MIS 3 around 50 kyr, but also demonstrates a clear response by biotic proxies to rapid climate warming.

- 2) *Chironomid-based palaeotemperature estimates for northeast Finland during Oxygen Isotope Stage 3*. Authors: Engels S, Bohncke S J P, Bos J A A, Brooks S J, Heiri O, Helmens K F. *Journal of Paleolimnology*: 40, 49–61 (2008).

The paper presents the chironomid diagram for the early MIS 3 deposit at Sokli (reflecting a diverse fauna) and the chironomid-inferred temperature curve. A careful evaluation of the temperature curve is presented, i.e. discussing different mechanism that could potentially have influenced the chironomid-based temperature reconstructions. The chironomid-inferred mean July air temperatures reach values similar to the current temperature at the Sokli site. This is the first study showing chironomid-derived palaeotemperature estimates for a deposit predating the Late Glacial – Holocene (MIS 1) in northwestern Europe.

- 3) *Flora, vegetation, and climate at Sokli, north-eastern Fennoscandia, during the Weichselian Middle Pleniglacial*. Authors: Bos J A A, Helmens K F, Bohncke S J P, Seppä H, Birks H J B. *Boreas*: 38, 335–348 (2009).

The nature of the terrestrial, wetland and lake ecosystems at Sokli during the early MIS 3 interstadial is reconstructed based on the plant microfossil and plant/aquatic animal macrofossil diagrams. The terrestrial vegetation was probably low-arctic shrub tundra. The tundra vegetation seems to have had a markedly similar composition to modern tundra in the continental sector of northern Fennoscandia. The distributional ranges of pine and tree birch were probably only few hundred kilometres south or south-east of Sokli. This is concordant with the sparse evidence for the presence of boreal tree taxa during MIS 3 in the Baltic countries and further east in Europe but contradicts with the commonly inferred treeless tundra or grass-dominated steppe conditions in central Europe. The paper also discusses the pollen-inferred temperature curve. Warmest and moistest conditions (with birch trees possibly present in sheltered spots in the Sokli area) are recorded in the lowermost part of the lake sequence. This is consistent with the pattern of the Greenland millennium-scale Dansgaard-Oeschger interstadials in which abrupt warming is followed by a gradual cooling. Temperature inferences based on the terrestrial pollen are consistently lower than temperatures reconstructed from the chironomid and other aquatic fossil assemblages. One of the possible hypotheses to account for these differences is that the regional terrestrial and the local aquatic systems responded differently to the climatic and landscape features at the time of MIS 3.

- 4) *Early MIS 3 glacial lake evolution, ice-marginal retreat pattern and climate at Sokli (northeastern Fennoscandia)*. Authors: Helmens K F, Risberg J, Jansson K N, Weckström J, Berntsson A, Kaislahti-Tillman P, Johansson P W, Wastegård S. *Quaternary Science Reviews*: 28, 1880–1894 (2009).

This paper gives a detailed description of the lithology of the early MIS 3 deposit in the Sokli basin, presents the results of the siliceous microfossil analysis, discusses geomorphologic evidence and analysis of Digital Elevation Model (DEM) data, and presents a quantitative climate reconstruction based on the diatom record. The fossil record registers distinct changes in lake level and size which provide an explanation for the sudden appearance and then disappearance of macrofossils in the middle part of the lacustrine sediment sequence. The lake level/size curve together with lithology, a low LOI and the DEM-based landscape reconstruction indicate that major part of the early MIS 3 minerogenic, laminated clay-silt sequence was probably deposited in a glacial lake impounded along the margin of the Fennoscandian Ice Sheet. The DEM-based reconstructions place the coring-site in a sheltered lake embayment and show that several large rivers draining most probably non-glaciated terrain flowed into the glacial lake. This explains a limited influence of the ice sheet at the coring-site, resulting in a proxy record that in detail registers the biotic environment around the coring-site and reconstructs the regional climate. The combined micro- and macrofossil evidence indicates that the upper more sandy laminated sediments were most probably deposited in an isolated lake of greatly diminished size. An increased influence of the local carbonate bedrock at Sokli on runoff might explain certain characteristics of the diatom assemblage in the sandy sediment. The diatom record reconstructs high, present-day mean July air temperatures similar as the chironomid record and other aquatic indicator species. The diatom-based reconstructions also suggest that high temperatures already prevailed during the earliest part of lacustrine sedimentation from which macrofossils are scarce. The paper highlights the importance of multi-proxy analysis for making detailed environmental and climate reconstructions. It notes that the study of the early MIS 3 deposit at Sokli is the first study of a pre-LGM deposit in northern Europe in which pollen, macrofossils, chironomids and diatoms are combined and transfer functions are used to quantitatively reconstruct climate.

5) *Ice-free conditions during early Marine Isotope Stage 3: lacustrine records from eastern Fennoscandia*. Authors: Helmens K F, Engels S. Boreas (in revision).

In this final paper, the environmental reconstructions based on the early MIS 3 deposit at Sokli are compared with those inferred from recently published, well-dated sediment sequences in western and eastern Finland and on the Timan ridge in northwestern Russia (which is located outside all Weichselian glacial limits). All Finnish records start with an important phase of glacio-lacustrine sedimentation. Pollen data from the eastern Finnish site suggest the presence of open birch forest close to the early MIS 3 retreating ice-margin of the Fennoscandian Ice Sheet in agreement with the presence of shrub tundra vegetation and the proximity of the distributional limit of tree birch at the more northerly site Sokli. Open birch forest with spruce is reconstructed for early MIS 3 on the Timan ridge. The Finnish interstadial sediments are all dated to ~ 50 kyr and possibly correlate to the prominent IS 14 in the Greenland ice core record. Warm conditions on Greenland during IS 14 lasted for about 2,500 years. In the speleotherm record from the Austrian Alps, the prominent IS 14 is dated by high-precision U-series thermal ionization mass spectrometry dates to 54.5–52 kyr. Direct evidence is lacking to estimate the total time span with ice-free conditions in Finland during MIS 3. It is argued that late MIS 3 is generally reconstructed as colder than early MIS 3 in a variety of proxy records from the North Atlantic region and it is possible that glaciation in the continental sector of the Fennoscandian Ice Sheet had resumed during late MIS 3, leading to maximum ice build-up during the LGM at ~ 20 kyr (MIS 2). This paper presents strong evidence for ice-free and warm conditions in major part of Finland during early MIS 3. Dated evidence is lacking in northern Sweden to reconstruct the total ice marginal-retreat in the continental sector of the Fennoscandian Ice Sheet during the early MIS 3 warming event.

## 2 Present environmental setting of the study area

The study site (lat. 67°48'N, long. 29°18'E, elevation 220 m.a.s.l.) in the Sokli wetland area (Sokliaapa), northeastern Finland, is situated on the main water divide that separates drainage into the Barents and White Seas to the east and the Baltic Sea to the southwest (Figures 1-1 and 2-1). The Sokli rivulet (Soklioja), which flows through the Sokli wetland, forms part of the drainage basin of the Nuortti River that drains into the Barents Sea (Figure 2-1).

The small sedimentary basin (~ 2 km<sup>2</sup>) along the lower course of the Sokli rivulet is formed in the central part of the Sokli Carbonatite Massif where two fracture zones cross (Figure 2-1). The Sokli Massif represents a Palaeozoic carbonate-rich magma intrusion of only limited extent (diameter ~ 6 km) into the surrounding crystalline rocks of the Precambrian Shield. The top of the carbonatite is almost entirely weathered, which has resulted in a regolith rich in apatite and francolite /Vartiainen 1980/.

Sokli is located in the northern boreal forest (Figure 1-2) with *Betula* (*B. pubescens* and *B. pendula*), *Pinus sylvestris* and *Picea abies* as the dominant tree species. The highest peaks (~ 500 m.a.s.l.) in the region reach just above the altitudinal tree-line which is formed by *Betula*. Mires of the aapa-type (i.e. patterned fen with strings and flarks) with *Sphagnum*, *Rubus chamaemorus*, Ericaceae, *Betula nana*, *Salix* spp. and *Carex* spp. are extensively present. Only the extent of the Sokliaapa mire near the coring-site, however, is indicated in Figure 2-1. Present climate is cold boreal with a mean July temperature of ~ 13°C, mean February temperature of ~ -14°C and mean annual temperature of ~ -2°C. Mean annual precipitation amounts to ~ 500–550 mm (Atlas of Finland, 1992; Figure 1-2).

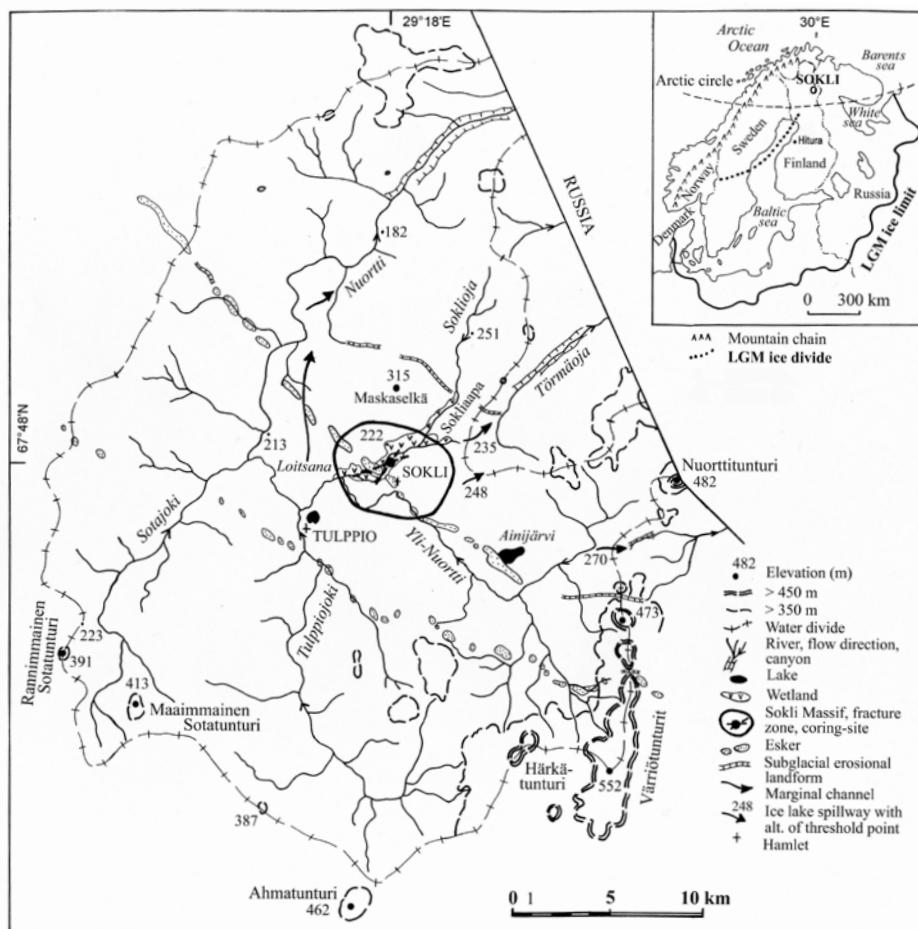


**Figure 2-1.** Drainage basin of the Nuortti River in northeastern Finland with indicated the coring-site in the central part of the Sokli Carbonatite Massif. Note that only the Sokli mire (Sokliaapa) around the coring-site is indicated. The extent of other wetlands in the area is not shown. Glacio-fluvial landforms are according to /Johansson 1995/.

Large eskers and meltwater channels are present in the study area /Johansson 1995; Figure 2-1/. A series of canyons near the Russian border (such as the canyon of the Törmäoja in Figure 2-1) are interpreted by /Johansson 1995/ as drainage channels and spillways for glacial lakes formed during the last deglaciation of the Fennoscandian Ice Sheet. The size of these canyons suggests that during the Quaternary they repeatedly served as glacial lake drainage sites of lakes formed by meltwater impounded between higher ground towards SE and the retreating ice margin towards NW.

Figure 2-2 shows photos of the Sokli wetland with the coring-locality (A), the northern boreal forest in the Sokli region with aapa mires (B), the deeply weathered rocks of the Sokli Carbonatite Massif (C), and the canyon of the Törmäoja (D).

Sokli is situated in a zone, which stretches over northern Sweden and Finland and onto the Kola Peninsula in Russia, in which an array of Quaternary landforms in loose material and sediments pre-dating the LGM is found /e.g. Lagerbäck 1988, Lagerbäck and Robertsson 1988, Kleman et al. 1997, Hättestrand and Clark 2006/. The preservation of relict landforms is ascribed to frozen bed conditions under the LGM Fennoscandian Ice Sheet extending well into the last deglaciation phase /Kleman et al. 1999/. Weak glacial erosion in northern Finland is reflected by the extensive occurrence of a pre-glacial weathering mantle, a distinct concentration of findings of till-covered organic beds, and the preservation of till beds and eskers of different ages /e.g. Hirvas 1991, Johansson 1995, Johansson and Kujansuu 2005/. At least three cross-cutting esker systems have been mapped in northeastern Finland /Johansson 1995/. The till-covered esker system B, of which remnants are found just south of the Nuortti River drainage basin, has been dated to the deglaciation phase of the early MIS 3 interstadial based on correlation with the Weichselian stratigraphy in the Sokli basin /Helmens et al. 2007a/. The early MIS 3 age assignment is supported by an OSL date of  $65 \pm 13$  kyr that was recently obtained on sand covering the glacio-fluvial sediment /Johansson 2007/. The eskers of system B follow on general a north-south direction, changing into a northwest-southeast trend further south.



**Figure 2-2.** A Sokli mire with coring-site. B Northern boreal forest with aapa mires in the Sokli region. C Deeply weathered rocks of the Sokli Carbonatite Massif. D The canyon of the Törmäoja (Figure 2-1) is deeply eroded into crystalline rocks and is today only occupied by a small rivulet. It is interpreted to have served as a glacial lake spillway and drainage site during the last deglaciation of the Sokli area /Johansson 1995/ and during early MIS 3 (present report;  $x^2$  in Figure 4-7).

## 3 The Sokli B-series borehole

### 3.1 Coring and sub-sampling

The detailed study of the Sokli early MIS 3 deposit, which forms the subject of the present report, was carried out on the Sokli B-series borehole. This borehole represents the most complete sediment recovery from the central part of the Sokli Basin. It reaches into the Eemian gyttja bed (MIS 5e) and has only minor gaps corresponding with the coarsest sediment layers (Figure 1-4). Coring was performed in the winter of 2002 using a hydraulic piston corer (GM 100). Cores were taken into a PVC tube, 2 m long and 4 cm in diameter, which was driven by vibration into the sediment while inserted in a steel tube (Figure 3-1). The coring was carried out by the Geological Survey of Finland. For a compilation of borehole lithologies from the Sokli basin and the Late Quaternary stratigraphic sequence in the basin the reader is referred to /Helmens et al. 2007a/.

Detailed sub-sampling of the B-series borehole (Figure 3-2) was carried out in 2003. Only half cylinders were available for proxy analysis, as the other half of each tube was used for a detailed luminescence dating program. The early MIS 3 deposit was sub-sampled at five cm intervals (and 2.5 cm in fine-grained sediment between depths 6.75–6.85 m). Central parts of each sample interval were used for pollen, diatom and loss-on-ignition (LOI) analyses, whereas the sediment in the lower and upper parts of each interval was used for macrofossil and chironomid analyses. The outer portions of the sediment core were disregarded in view of possible contamination. Samples were directly stored at  $-20^{\circ}\text{C}$  to prevent fungal growth. The sub-sampling was carried out by Dr. Karin Helmens at the Arctic Centre, University of Lapland, Finland.



*Figure 3-1. Coring of the Sokli sediments.*



**Figure 3-2.** The Sokli B-series cores. The Eemian (MIS 5e) diatom gyttja deposit is on the right and the glacial till bed of MIS 3-2 age on the left.

### 3.2 Lithology and dating

A simplified lithological column of the Sokli B-series borehole, with depositional environments, is given in Figure 1-4. Lithological characteristics and inferred depositional environments are discussed in more detail in /Helmens et al. 2007a/. The early MIS 3 deposit occurs at 5.0–8.5 m depth below the Sokli wetland surface (Figure 1-4). It consists of a 1.5 metre thick layer of upward fining gravely to sandy ice-marginal sediment overlain by a two metre thick upward fining and then upward coarsening minerogenic, laminated lacustrine clay-silt sequence. These sediments are intercalated in-between two till beds representing glaciation during MIS 4 and late MIS 3-2. A detailed lithological column of the sediment sequence is given to the left of the diagrams in Figures 4-3 till 4-6, and the lithology of the early MIS 3 deposit will be described in detail in section 4.1.2. The multi-proxy analysis was focused on the laminated lacustrine sediments. In addition, one sample interval from the uppermost part of the sandy ice-marginal sediment was included in the analysis. The underlying, remaining part of the ice-marginal sediment has a brownish colour caused by inter-mixing with organic debris re-deposited from the Eemian interglacial gyttja bed in the Sokli basin /Helmens et al. 2000/. As such, no reliable proxy analysis could be performed on the latter sediments.

Pollen in the lacustrine sediment near the base of the Sokli sequence show an interglacial vegetation sequence similar as registered in the Holocene surface peat deposit and has been correlated with the Eemian Interglacial (MIS 5e; Figure 1-4 /Ilvonen 1973, Forsström 1990, Helmens et al. 2000/). Above the interglacial lacustrine sediment, sediment and pollen reflect progressively colder conditions upward in the sequence, indicating a climate evolution similar to the deep-sea record for the Last Glacial cycle /Helmens et al. 2000, 2007a/.

OSL dating, using the single aliquot regeneration (SAR) protocol to estimate equivalent doses /Murray and Wintle 2000/, was performed on fluvial and glacio-fluvial sediments in the Sokli sequence, that were likely to have been reasonably bleached at deposition /Alexanderson et al. 2008/. The results obtained from dating feldspar are more or less uniform throughout the entire Last Glacial sequence and show ages in the order of 100–130 kyr. Five quartz OSL ages, on the other hand, follow stratigraphic order showing successively older ages with depth (Figure 1-4). In addition, the youngest of these quartz OSL dates matches two AMS <sup>14</sup>C dates from the same interstadial sediment (see below). Since feldspar is less quickly and easily zeroed than quartz /Godfrey-Smith et al. 1988, Fuchs et al. 2005/, the feldspar dates most probably overestimate the true age of sediment-deposition due to incomplete bleaching. One feldspar date on fluvial sediment in the lowermost part of the Last Glacial sequence, however, is indicated in Figure 1-4. This age is in line with the quartz ages. It sup-

ports the idea that incomplete bleaching seemed to be less of a problem during glacial build-up than during glacial decay and deglaciation, when deposition generally took place more rapidly /Hansen et al. 1999/. One relatively old quartz OSL date in the upper part of the Last Glacial sequence has been rejected due to very poor OSL characteristics of the sample. In addition, the latter sediment was most probably deposited in a lacustrine environment, which may explain reduced sunlight exposure and subsequent incomplete bleaching /Alexanderson et al. 2008/. The absolute ages obtained for the three Weichselian interstadial sediment intervals in the Sokli basin, i.e.  $\sim 94$  kyr,  $\sim 74\text{--}80$  kyr and  $\sim 42\text{--}54$  kyr, are in agreement with the stratigraphic correlations to the Brørup (MIS 5c) and Odderade (MIS 5a) Interstadials and an interstadial of Middle Weichselian age (early MIS 3), respectively, in the northwest European mainland climate-stratigraphy and the marine oxygen-isotope record (Figure 1-4 /Helmens et al. 2007a, Alexanderson et al. 2008/).

The ice-marginal sediment of early MIS 3 age has yielded a quartz OSL date of  $48 \pm 16$  kyr (Figure 1-4 /Alexanderson et al. 2008/), whereas AMS  $^{14}\text{C}$  dating on mostly terrestrial macrofossils from the uppermost part of the overlying laminated lacustrine sediments has provided uncalibrated ages of  $42.5 \pm 3.5$  kyr (parallel borehole /Helmens et al. 2000/) and  $54 \pm 7/4$  kyr (Figure 1-4 /Helmens et al. 2007b/). Differences in radiocarbon ages are attributed to uncertainties near the limit of the radiocarbon dating method /Alexanderson et al. 2008/. The lacustrine sediment has been additionally analyzed for cryptotephra, but no volcanic glass shards were detected and a correlation with ash zones dated to MIS 3 in the North Atlantic /Wastegård et al. 2006/ could not be achieved /Helmens et al. 2009/. If the laminations in the lacustrine sediment have an annual origin, then some 400 years of sedimentation is recorded /Helmens et al. 2000/.

## 4 Reconstruction of lake development, sedimentation and ecosystem composition

### 4.1 Reconstructions based on multi-proxy evidence

#### 4.1.1 Methods

##### ***Organic content***

A LECO TGA-601 oven was used to determine loss-on-ignition (LOI). In order to measure the dry weight of the sampled sediment ( $W_{dr}$  (g)), samples were heated to 105°C until constant weight was achieved. Subsequently, temperature was raised to 335°C at a ramp rate of 10°C per minute and organic matter was burned in an atmosphere of 100% oxygen. In order to determine the “classic” loss-on-ignition, the temperature in the oven was further raised to 550°C at a ramp rate of 10°C per minute. Afterwards, the residue was weighed ( $W_{gl}$  (g)) and  $W_{550}$  was calculated using:  $W_{550} = ((W_{dr} - W_{gl}) / W_{dr}) \times 100\%$ . The LOI measurements were carried out by Ir. Martin Konert at the Department of Palaeoclimatology and Geomorphology, Vrije Universiteit Amsterdam, The Netherlands. The organic content of the sediment is given in Figures 4-3 till 4-6 and is discussed in detail in section 4.1.4.

##### ***Chironomid (aquatic insect) analysis***

Wet sediment samples ranging in weight 3.65–38.54 gram were used for chironomid analysis. To remove fine particles from the samples, the sediments were deflocculated in cold 10% KOH for at least four hours and subsequently rinsed through a 100 µm sieve. Using a dissecting microscope, chironomid head capsules were hand-picked at 35 × magnification using fine forceps and permanently mounted on glass slides using Euparal® mounting medium. The chironomid head capsules were identified following /Wiederholm 1983, Heiri et al. 2004, Makarchenko and Makarchenko 1999, Moller Pillot 1984, Schmid 1993, Rieradevall and Brooks 2001/ and /Oliver and Rousset 1983/. Head capsules were generally well preserved. The average count sum in the samples above 6.75 m core depth was 89 head capsules (hc) per sample (range: 54–199 hc), although fewer counts were present in the lowermost part of the profile (2–24 hc). A chironomid percentage diagram was constructed using the computer programs TILIA and TG.VIEW /Grimm 1991–2004/. Zonation of the chironomid diagram was carried out using the optimal sum-of-squares partitioning method as implemented in the program ZONE /Lotter and Juggins 1991/; the significant number of zones was assessed by a broken stick model /Bennett 1996/. The chironomid analysis was carried out by Dr. Stefan Engels at the Department of Palaeoclimatology and Geomorphology, Vrije Universiteit Amsterdam, The Netherlands.

##### ***Analysis of diatoms and other siliceous microfossils***

Not all sub-samples from the minerogenic clay-silt sequence were analyzed for siliceous microfossils (see section 3.1). A high sample resolution was maintained in the lower part of the sequence as here the diatom-based climate reconstruction was aimed to extend the chironomid-inferred climate reconstruction into the lowermost part of the sequence where head capsules are scarce (see above). The sample interval was decreased in the upper sediments. Preparation of siliceous microfossil samples followed a procedure based on the compilation by /Battarbee 1986/. Two gram of wet sediment was put in 100 ml beakers and 10% HCl was added to remove carbonates (no visible reaction). Organic matter was oxidised by boiling a few days in 17–35% H<sub>2</sub>O<sub>2</sub>. Clay particles were removed by repeated decanting from 100 ml beakers in two hours intervals and once after dispersion in weak NH<sub>3</sub> solution. The residue was mounted in Naphrax®. The analyses were carried out under LM using oil immersion and ×1000 magnification. Diatom identification was mostly based on /Cleve-Euler 1951–1955, Mölder and Tynni 1967–1973, Tynni 1975–1980/ and /Krammer and Lange-Bertalot 1986, 1988, 1991ab/. Additional information on diatom identification and living habitat (i.e. benthic, tychoplanktonic, planktonic, aerophilous and rheophilous) was found in /Cholnoky 1968, Haworth 1988, Pässe et al. 1988, Round and Håkansson 1992, Khursevich 1994, Korhola and Tikkanen 1996, Siver and Kling 1997, Corner et al. 1999, Laing et al. 1999, Bigler et al. 2000, Philibert and Praire 2002, Rühland et al. 2003, Weckström et al. 2003, Cremer and Van de Vijver 2006/ and /Stachura-Suchoples and Khursevich 2007/.

Diatom frustules were generally well-preserved, although fragments occurred in all samples analyzed. A total sum of ~ 125–200 valves was achieved in the silty samples where diatom concentrations were low. For the remaining sediment, ~ 250–500 diatom valves were counted per sample. The identification of *Aulacoseira* spp. to species level was hampered by numerous poor observations in valve views. It is probable that a large portion of the *Aulacoseira* spp. frustules that were not identified to species level belong to either *A. italica* v. *valida* or *A. lirata* v. *lirata* considering the large similarities between the curves for *Aulacoseira* spp. and the mentioned species. In addition to one re-deposited silicoflagellate, Tertiary diatom taxa were encountered. The latter include marine and freshwater diatoms that were found heavily silicified and coarsely structured. They are derived from Tertiary and/or interglacial sediment as in e.g. /Tynni 1982, Niemelä and Tynni 1979, Corner et al. 1999, Round and Håkansson 1992/ and /Cremer and Van de Vijver 2006/. These observations are exemplified by species like *Pliocaenicus costatus*, a relict freshwater taxon from the Pliocene, and *Paralia sulcata*, and the genera *Hemiaulus* spp., the latter two diatom taxa being of marine origin. Diatom fossils that could not be identified because of poor preservation/view, and those that could only be identified to genus level precluding a reconstruction of preferred living habitat, were grouped as ‘unknown ecology’. Other siliceous microfossils that were encountered in the analysis include phytoliths, chrysophyte stomatocysts and sponge spiculae. A numerical zonation was applied to the diatom data based on optimal partitioning /Birks and Gordon 1985/, and the statistical significance of the identified diatom assemblage zones was determined by comparison of the suggested partitions with the broken stick model /Bennett 1996/. In order to stabilize the variance in the diatom data, diatoms were square root transformed using the program C2 /Juggins 2007/.

The variations in the percentage abundance of the groups ‘planktonic’ and ‘tychoplanktonic diatom taxa’ were used to reconstruct relative lake level fluctuations /cf Kienel et al. 1999, Selby et al. 2005/. In order to get a general overview of the water chemistry history, a quantitative pH reconstruction was made by applying a diatom calibration dataset consisting of 53 lakes from northwestern and 45 lakes from northeastern Finnish Lapland /Seppä and Weckström 1999, Korhola et al. 1999/ to our data. pH has been shown to be one of the most important limnological factors determining the diatom composition /e.g. Birks et al. 1990, Weckström et al. 2003/ and diatom-based reconstructions of pH are generally reliable /e.g. Weckström et al. 2003/. The one component weighted averaging partial least squares (WA-PLS) diatom-pH model is relatively robust with  $r^2 = 0.68$  and a prediction error of 0.31 pH units.

The siliceous microfossil analysis was performed by Dr. Jan Risberg, Mrs. Annika Berntsson and Mrs. Päivi Kaislahti Tillman at the Department of Physical Geography and Quaternary Geology, Stockholm University, Sweden. The pH reconstruction was made by Dr. Jan Weckström at the Department of Biological and Environmental Sciences, University of Helsinki, Finland.

### **Palynological (plant microfossil) analysis (pollen, spores, algal and fungal remains)**

Microfossil samples were prepared following /Fægri and Iversen 1989/ with additional sodium polytungstate heavy-liquid separation to remove clastic material. Subsequently, the material was sieved over a 7–8  $\mu\text{m}$  nylon mesh to remove fine particles, mounted in glycerine jelly, and sealed with paraffin wax. *Lycopodium* spores were added to estimate microfossil concentrations. The pollen and spore analysis was performed at the lowest possible taxonomic level. The nomenclature of pollen and spore types in general follows /Moore et al. 1991/.

To calculate the percentage curves of the individual taxa a pollen sum consisting of trees, shrubs, dwarf shrubs (Ericaceae), herbs, and terrestrial Pteridophytes, was employed, similar to the one that was used in the modern pollen-climate-data-set (see section 5.1.2). Pollen sums varied between 299 and 479. Because of the ecological significance of the different *Betula* species that are present in the region, an attempt was made to separate them on the basis of their pollen. *Betula nana* (dwarf birch) was separated from *Betula pubescens/pendula* (tree birch) using a combination of size and morphological characteristics /e.g. Terasmaä 1951, Birks 1968, Usinger 1977, Kolstrup 1982, Mäkela 1996, Blackmore et al. 2003/. The division is not absolute, since size ranges overlap. Previous investigations, however, gave consistent results when the pollen proportions are compared within the different pollen assemblages and with the occurrences of macrofossils of these taxa /Helmens et al. 2000, Bos et al. 2006/. A numerical zonation was applied to the microfossil data based on optimal partitioning /Birks and Gordon 1985/, and the statistical significance of the proposed pollen assemblage zones was determined by comparison of the proposed partitions with the broken stick model /Bennett

1996/. Two divisions are indicated as statistically significant in the numerical zonation and these form the basis for distinguishing pollen assemblage zones 1, 2, and 3. Subzones 2a and 2b are based on visual inspection and are distinguished to facilitate ease of discussion and interpretation of the diagrams.

Pollen slide preparation was made by Ir. Martin Konert at the Department of Palaeoclimatology and Geomorphology, Vrije Universiteit Amsterdam, The Netherlands. The palynological analysis was carried out by Dr. Karin Helmens at the Department of Physical Geography and Quaternary Geology, Stockholm University, Sweden.

### Macrofossil analysis of plants and zoological taxa

Macrofossil samples, varying between 7–48 g wet weights and 8–22 ml, were washed over a 100 µm sieve. Fossil remains were picked out from the sieve residue. The nomenclature of plant macroremains follows /Berggren 1969, 1981, Anderberg 1994/ and /Körber-Grohne 1964, 1991/ and, for *Potamogeton*, /Cappers 1993/. The macrofossil analysis was carried out by Dr. Hanneke Bos at the Department of Palaeoclimatology and Geomorphology, Vrije Universiteit Amsterdam, The Netherlands.

## 4.1.2 Lake development and sedimentation

### The chironomid record

A total of 65 chironomid taxa were identified in the early MIS 3 sediments and a summarized chironomid sequence is presented in Figure 4-1. The full chironomid taxon list is provided in Appendix I. The high number of lacustrine taxa with a preference for littoral to sub-littoral habitats suggests that, with the exception of the earliest phase of lacustrine sedimentation, a shallow lake was present at the Sokli site. The chironomid diagram is mostly interpreted in terms of changing air temperatures and its main application is in the quantitative climate reconstructions (see section 5.1.1). Nevertheless, the record gives some information on lake development and trophic conditions. Therefore, the chironomid assemblage zones (Zone Sokli-Chironomids: Zone S-Ch) will be discussed here.

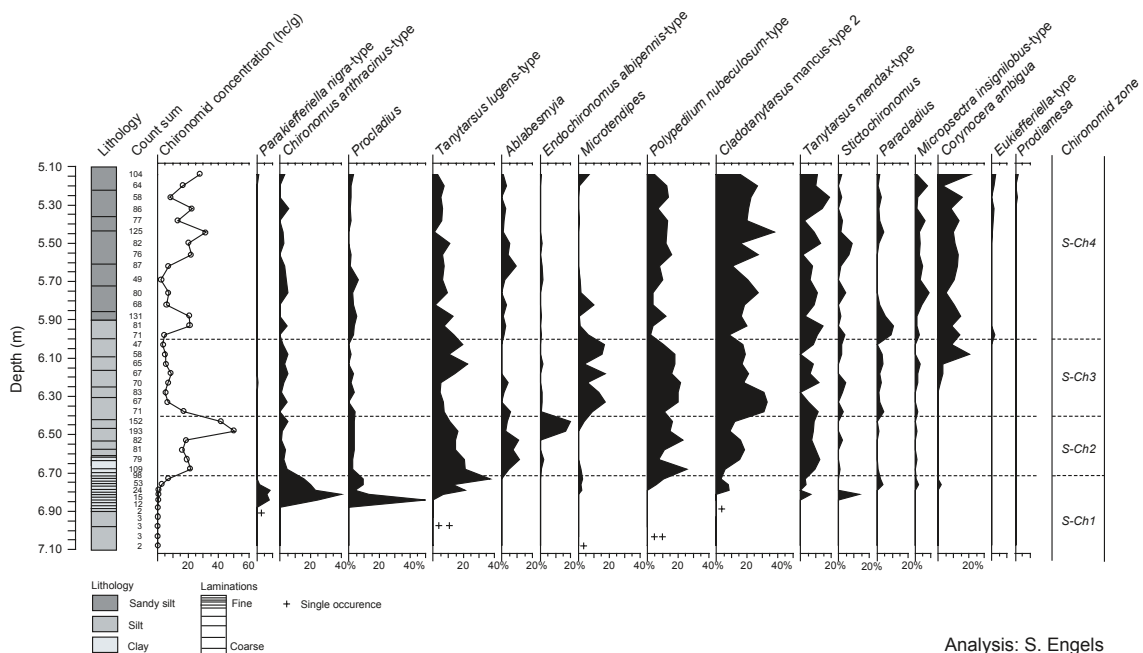


**Figure 4-1.** Summary diagram showing selected chironomid taxa recovered from the early MIS 3 sediments at Sokli. Abundances for the individual taxa are given as percentages, the head capsule count-sum in numbers, and the chironomid concentration in the number of head capsules per gram wet sediment. The samples below 6.79 m core depth yielded limited numbers of chironomid head capsules, and individual findings are indicated with (+).

### **Zone S-Ch1 (7.10–6.71 m core depth)**

*Tanytarsus lugens*-type, *Microtendipes* and *Polypedilum nubeculosum*-type were among the taxa that first appeared at Sokli. The chironomid concentration does not rise above 1 head capsule (hc) per gram. In the upper part of zone S-Ch1, count sums increase to values above 50, and *Chironomus anthracinus*-type (20%), *T. lugens*-type (15–40%) and *Procladius* (10%) are the most abundant taxa. Both *C. anthracinus*-type and *Procladius* have a broad distribution along the temperature gradient in the Norwegian training set (see section 5.1.1): *Procladius* has a large temperature tolerance, as it was found in lakes with mean July air temperatures ranging from 4.5°C to 16.0°C. The abundances of *C. anthracinus*-type show a bimodal distribution in the modern calibration set, with a small optimum in abundances at 8.5°C, and a large optimum in abundances around 14.6°C. *T. lugens*-type, the third taxon to show high numbers, also has a large temperature-tolerance, but has been considered to be indicative for cool and oligotrophic conditions /e.g. Brooks 2006/. All these taxa might be indicative of a relatively deep lake.

### **Zone S-Ch2 (6.71–6.40 m)**

The onset of zone S-Ch2 is indicated by a sharp increase in the concentration of chironomid remains, reaching values of 50 hc/g wet sediment. The assemblages are initially dominated by *T. lugens*-type, with abundances of 40% at the onset of this zone. *Ablabesmyia* shows its highest occurrences in the middle part of this zone (10%). Toward the top of zone S-Ch2, the abundance of *T. lugens*-type declines and *Tanytarsus mendax*-type, *Polypedilum nubeculosum*-type and *Cladotanytarsus mancus*-type 2 become the dominant taxa. The latter two taxa (values above 20%) are indicative of higher July air temperatures and the transition to a chironomid-assemblage that is dominated by these two taxa could be the result of a steadily increasing summer temperature at Sokli. At the end of zone S-Ch2 there is a peak in the occurrence of *Endochironomus albipennis*-type, which temporarily becomes the dominant taxon with an abundance of 20%. This might indicate rising temperatures too, but could also be related to an increased nutrient availability in the lake.

### **Zone S-Ch3 (6.40–6.00 m)**

*Endochironomus albipennis*-type and *T. lugens*-type show lower abundances at the onset of S-Ch3, while *Microtendipes* returns to the lake and reaches abundances of 5–15%. *P. nubeculosum*-type and *Cladotanytarsus mancus*-type 2 remain the dominant taxa with an abundance of 20% and 20–30% respectively. *Ablabesmyia* shows declining abundances and temporarily disappears from the sequence during zone S-Ch3, while *Corynocera ambigua* appears in the middle of the zone. The concentration of chironomid head capsules is low throughout zone S-Ch3, between 5 and 10 hc/g. The occurrence of *Microtendipes* could indicate temperatures that are best classified as intermediate to warm /Bedford et al. 2004, Brooks and Birks 2000/ and the gradual warming trend that was observed in zone S-Ch2 was probably interrupted.

### **Zone S-Ch4 (6.00–5.10 m)**

At the onset of S-Ch4, *Microtendipes* disappears from the sequence, whereas *C. ambigua* shows a constant abundance of 15%. This latter species was formerly considered to be a true cold-water stenotherm, but those ideas have recently been questioned by /Brodersen and Lindegaard 1999/, as they found *C. ambigua* in temperate, eutrophic Danish lakes. In the Norwegian training set, this species has a narrow temperature tolerance ( $\pm 1$ –2°C) with a temperature optimum of 9.9°C. *Paracladius* shows its first phase of high abundance, reaching values of 10%. At 5.83 m core depth, values of *Paracladius* decline and the head capsule density decreases to values below 10 hc/g. In the uppermost part of the core, between 5.10–5.50 m, this taxon reappears in the chironomid assemblage, but in much lower numbers. This genus is considered to be a true cold-water stenotherm, and its presence is possibly the result of a colder temperature at the study site.

At 5.60 m core depth, the head capsule density increases again to approximately 50 hc/g. *Stictochironomus* reaches abundances of up to 10% in the upper part of the record. However, *P. nubeculosum*-type and *Cladotanytarsus mancus*-type 2 are still the dominant taxa in the assemblage. An interesting feature of the upper part of zone S-Ch4 is the occurrence of stream-inhabiting taxa such as *Eukiefferiella* and *Prodiamesa*.

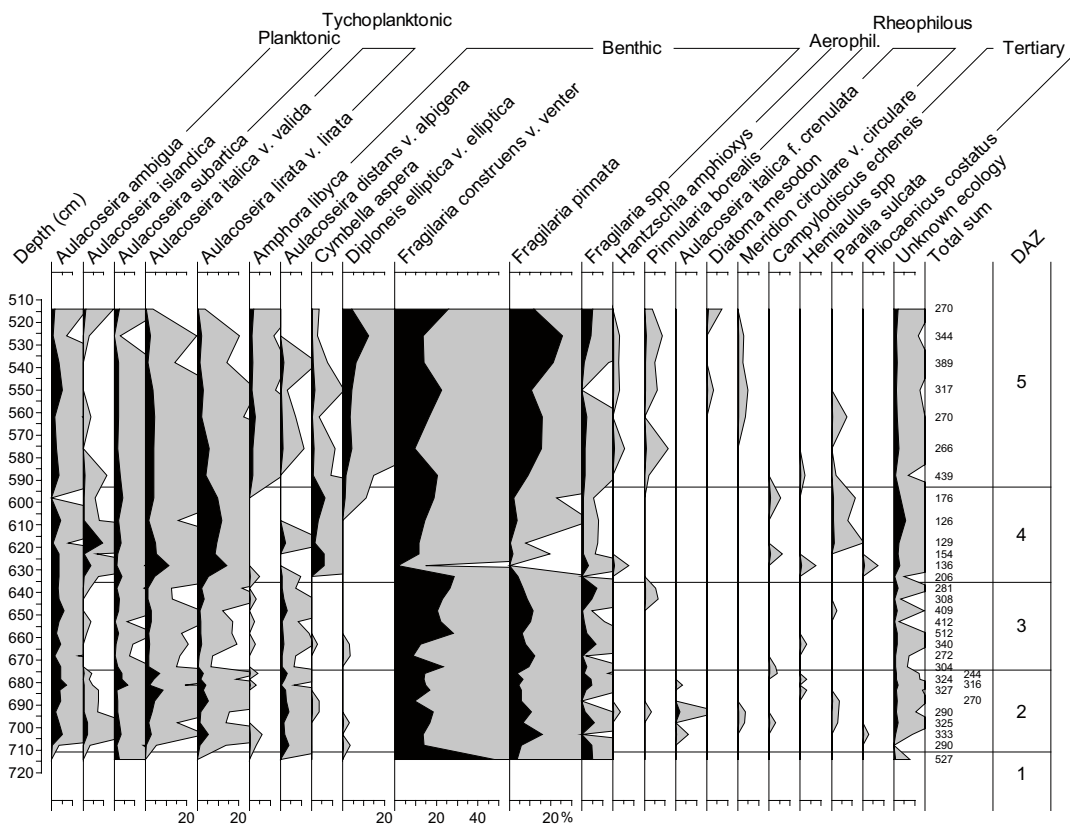
### The diatom and lithological records

A total of 211 diatom taxa and 47 genera were identified and a simplified percentage diagram showing diatom taxa that are mentioned in the text, grouped according to living habitat, is given in Figure 4-2. The full diatom taxon list is provided in Appendix II. The diatom flora is dominated by *Aulacoseira* spp. and *Fragilaria* spp. Observed taxa within these genera indicate the presence of a water body deep enough to support the growth of planktonic and tychoplanktonic species and a somewhat enhanced pH. The groupings of diatoms according to living habitat, the relative percentages of other siliceous microfossils to diatoms, the diatom-inferred lake level curve (see below) and pH curve, which averages around a value of 7.4, are given at the left side of Figure 4-6. Next follows a description and interpretation of the diatom assemblage zones (DAZ) and lithology. The detailed lithological column is indicated to the left of the proxy diagrams in Figure 4-6.

#### DAZ 1 (7.15–7.10 m)

This zone is represented by one sample only. The sample is derived from a ~ 5 cm thick layer of greenish coloured silty sand to fine gravel (uppermost part of the ice-marginal sediment sequence; see section 3.2). Diatoms, mainly benthic forms such as *Fragilaria* spp. especially *F. construens* v. *venter*, dominate the siliceous microfossil record.

The dominance of pioneering benthic *Fragilaria* spp. is a typical feature in diatom assemblages during the initial phase of Holocene lake development in Finnish Lapland /e.g. Seppä and Weckström 1999/. Their dominance may reflect their opportunism, adaptation ability to rapidly changing environments, high reproductive rate /Risberg et al. 1996, Lotter et al. 1999/, and their ability to tolerate poor light conditions in, for instance, turbid waters /Bigler et al. 2003/. This agrees with the proglacial setting of the lake environment at the onset of our record. The relatively high reconstructed pH concurs with a high influx of minerogenic material into the lake from the non-leached soils surrounding the lake.



Analysis: P. Kaislahti Tillman, A. Berntsson, J. Risberg

**Figure 4-2.** Simplified percentage diagram showing a selection of diatom taxa analyzed in the early MIS 3 deposit at Sokli and the subdivision into Diatom Assemblage Zones (DAZ). Percentages are calculated as percentages of the total sum of diatoms counted per sample. The solid curves show the actual percentages, the hatched curves show an  $\times 10$  exaggeration. The lithological column is given to left in Figure 4-6.

### **DAZ 2 (7.10–6.75 m)**

Relative abundances of planktonic diatom taxa (e.g. *Aulacoseira ambigua*, *A. islandica* and *A. subarctica*) and tychoplanktonic taxa (e.g. *A. italica* v. *valida* and *A. lirata* v. *lirata*) increase with respect to benthic taxa. Rheophilous taxa, represented by *Aulacoseira italica* f. *crenulata*, and re-deposited Tertiary taxa (e.g. *Paralia sulcata*, *Campylodiscus echeneis* and *Pliocaenicus costatus*) appear in low percentages. Phytoliths are relatively abundant showing strongly fluctuating percentages in the upper part of the zone. Sponge spiculae show a low but almost continuous occurrence. One re-deposited silicoflagellate was encountered in the analysis.

The sediment in this 35 cm thick layer gradually fines up from silt; to clayey silt and silty clay that contain 2–0.5 mm thick dark coloured laminae; to very finely laminated silty clay in which the dark coloured clay laminae are less than 0.25 mm thick and the light coloured silty laminae ~ 0.75 mm. Some coarser, up to 2–3 mm thick, light coloured laminae are recorded in the uppermost part of the layer.

The diatom flora shows a rapid diversification at the beginning of DAZ 2 and this together with the distinct change in lithology recorded here (i.e. from gravely sand to silt) most probably reflects a greater distance of the ice margin to the coring-site. A progressive ice-marginal retreat throughout the zone seems to be indicated by the gradual transition to finely laminated clayey sediment. The diatom record reflects the development of a relatively deep lake at the coring-site. The fluctuating pattern between diatoms and phytoliths in the upper part of DAZ 2 might indicate variations in terms of water inflow from streams, which is supported by the occurrence of rheophilous diatom taxa, and/or windy conditions.

### **DAZ 3 (6.75–6.35 m)**

At the beginning of DAZ 3 there is a sudden increase in benthic taxa, mainly *Fragilaria* spp. Percentages of the tychoplanktonic *Aulacoseira* spp. decrease significantly, while the benthic *Aulacoseira distans* v. *alpigena* remains stable. The relative abundance of phytoliths decreases. Sponge spiculae are absent from the record in the lower part of the zone. The lithology of the 40 cm thick layer changes through a transitional zone, in which both the sediment and laminations have coarsened up compared with the underlying clayey sediment of DAZ 2, to fine silt that is coarsely interlayered with ~ 3 mm thick clay laminae.

The diatom assemblage zone indicates a sudden lowering of the lake level. This change might have been caused by the opening of a spillway as the ice front withdrew further away from the Sokli basin, allowing drainage of the glacial lake. As the water level fell, coarser sediment fractions were able to accumulate at the coring-site.

### **DAZ 4 (6.35–5.93 m)**

A sudden increase in abundance of tychoplanktonic diatom taxa characterises the start of this zone, and DAZ 4 shows peaks in occurrences of both tychoplanktonic and planktonic taxa. Among the benthic taxa, besides *Fragilaria* spp., there is a peak in occurrence of *Cymbella aspera*. Sponge spiculae are most common in this zone and the relative abundances of phytoliths and Tertiary taxa are at their highest. The sediment in the ~ 40 cm thick layer consists of coarsely laminated silt.

A deeper lake is again suddenly established at the coring-site, possibly caused by re-blocking of the earlier opened spillway. Transgression caused flooding of formerly vegetated areas, resulting in erosion and reworking of phytoliths from grassy vegetation and Tertiary diatom taxa from underlying soil (mostly till), the robust structure of the Tertiary taxa allowing multiple phases of re-working. Large amounts of silt derived from the shores were deposited at the coring-site. The slight decrease in pH recorded during DAZ 4 is most probably due to the inwash of organic matter.

### **DAZ 5 (5.93–5.10 m)**

A continuous decrease in percentages of planktonic and tychoplanktonic taxa is recorded during DAZ 5. The benthic genus *Fragilaria* spp. dominates the assemblages and several species such as *Diploneis elliptica* v. *elliptica* and *Amphora libyca* increase and show steady occurrences upwards

in the zone. Different aerophilous taxa (e.g. *Hantzschia amphioxys* and *Pinnularia borealis*) and rheophilous taxa (e.g. *Meridion circulare* v. *circulare* and *Diatoma mesodon*) are found. The abundance of phytoliths decreases gradually while the relative occurrence of chrysophyte cysts increases. The sediment has changed to fine sands and sandy silts that are only very coarsely laminated (i.e. only few up to 5 mm thick clay laminae are recorded in the ~ 80 cm thick sediment layer).

DAZ 5 reflects a gradual lowering in lake level at the coring-site. The presence of an extensive littoral zone is suggested by the abundance of *Fragilaria pinnata*, the continuous registration of aerophilous taxa, and the increased abundance of chrysophyte stomatocysts. /Douglas and Smol 1995/ compared the relative percentage of chrysophyte stomatocysts to diatoms from epiphytic (moss), epilithic, and surface sediments from high arctic ponds and found the highest percentage of cysts in semi-aquatic mosses. The influence of flowing water closer to the coring-site is indicated by the rheophilous taxa and the coarse sandy lithology.

During this zone, the ice margin probably retreated and the glacial lake was entirely drained leaving an isolated lake in the Sokli basin. The occurrences of *Diploneis elliptica* v. *elliptica* and *Amphora libyca* are notable and might be related to enhanced pH values /e.g. Whitmore 1989, Jones and Birks 2004, Davies et al. 2005/ as the lake size decreased and the influence of the local carbonate-rich bedrock on run-off increased. Along the lake shore, wetland vegetation developed and extended. The dropstone found in the upper part of DAZ 5, and pieces of wood, were probably transported by river-ice.

#### 4.1.3 Ecosystem composition

##### ***The palynological and macrofossil records***

The terrestrial pollen and spore percentage diagram, a microfossil diagram for algae, other aquatics, wetland elements and fungi, and the plant and aquatic animal macrofossil diagram are given in Figures 4-3 till 4-5. The diagrams form the basis for the reconstruction of the terrestrial, lake and wetland ecosystems discussed below.

##### **Reconstruction of the terrestrial ecosystem**

Overall, total tree pollen percentages vary between 30–50% (Figure 4-3). *Betula* generally dominates the tree pollen spectra with values between 15–30%. *Pinus* reaches percentages of 15–20%. *Picea* is represented in low values throughout the record. Non-aboreal taxa (NAP) are abundant and diverse, including shrubs and dwarf-shrubs such as *Salix*, *Betula nana*, *Juniperus*, and Ericaceae, and a rich herb flora with a variety of arctic-alpine and heliophilous, pioneer elements (e.g. Caryophyllaceae, *Rumex-Oxyria*, *Artemisia*, Chenopodiaceae, and *Polygonum viviparum*-type). Polypodiaceae and Lycopodiaceae (*Lycopodium annotinum*, *Diphasiastrum*, and *Huperzia selago*) are also well-represented throughout the record (sum of pteridophytes 10–20%). The general pollen and spore values suggest the presence of low-arctic tundra throughout the sequence. The moderately high values of Cyperaceae, Poaceae, shrubs, and dwarf-shrubs are typical for modern and Holocene pollen assemblages and modern plant assemblages from the Fennoscandian tundra /Prentice 1978, Haapasaari 1988, Oksanen and Virtanen 1995, Seppä et al. 2002, 2004, Bjune et al. 2004, Bergman et al. 2005/. The tundra vegetation during early MIS 3 appears to have been remarkably similar to the tundra of the present interglacial in northern Fennoscandia.

The pollen values of *Pinus* and *Betula* suggest that the distributional limits of tree *Betula* and *Pinus* may not have been far away from Sokli. In modern pollen samples from northern Fennoscandia, the threshold pollen percentage values for the local presence of *Pinus* trees is about 40% whereas values of *Pinus* pollen of about 20% occur some 100 km north of the present *Pinus* tree-line. The latter values are similar to the Sokli data. Thus, the Sokli early MIS 3 palynological record shows overall similarities with pollen values from the modern ecotonal tundra in northern Fennoscandia, where *Betula* is the northernmost tree taxon and *Pinus* is the northernmost conifer species.

There is the possibility that some of the tree pollen may be secondarily derived from older deposits at Sokli formed under more temperate conditions (e.g. Eemian, early Weichselian interstadials). There is, however, no evidence to support this hypothesis in the form of pollen of thermophilous taxa (e.g. *Quercus*, *Ulmus*, *Tilia*) or macrofossils of any boreal or thermophilous trees /cf. Cushing 1964/.

Although the inferred vegetation type is low-arctic tundra throughout the study period, some changes of ecological relevance took place. The highest percentages of tree *Betula* pollen values are recorded in pollen assemblage zone (PAZ) 1, suggesting the smallest distance to the range limit of this taxon. They may have been a reflection of local pockets of tree *Betula* present in sheltered spots in the Sokli region. PAZ 1 is further characterized by relatively high percentages of Polypodiaceae (*Athyrium*-type). It is thus possible that the basal PAZ represents the warmest and moistest part of the Sokli early MIS 3 sequence. This interpretation is consistent with the pattern of the Greenland Dansgaard-Oeschger interstadials in which abrupt warming is followed by a gradual cooling /e.g. Johnsen et al. 1992, Bond et al. 1993, Dansgaard et al. 1993/.

The percentages of tree *Betula* and Polypodiaceae decrease during PAZ 2a, whereas percentages of Poaceae pollen increase. The latter may be related to changes in the telmatic vegetation due to water-level changes. The diatom record obtained from the Sokli early MIS 3 lacustrine sequence shows a phase with distinctly low water-levels during this zone (see under 4.1.2 and Figure 4-6).

During PAZ 2b there is a gradual decrease in the *Pinus* and *Alnus* values and a gradual increase in Cyperaceae percentages. This may reflect the start of a slow southward retreat of the tree-line and thus gradual cooling during this zone. The mycorrhizal (soil) fungus *Glomus* /van Geel et al. 1989/ appears in PAZ 2b (Figure 4-4), which may reflect the onset of soil erosion in the lake's catchment as a result of cooling. *Pinus* values continue to decrease during PAZ 3. PAZ 3 is further characterized by relatively low tree *Betula* values and relatively high Cyperaceae and *Salix* values. It is possible that the trends in pollen percentage values during PAZ 3 reflect further cooling. However, the presence of nutlets of *Carex* spp. (Figure 4-5) and spores of *Gaeumannomyces* (Figure 4-4) indicates that part of the high Cyperaceae values during PAZ 3 can be attributed to a local wetland source. The latter is a fungus that is parasitic on *Carex* spp. /van Geel et al. 1983/. A distinct phase with wetland extension is reflected in the upper part of the lacustrine sequence (see below).

Furthermore, during PAZ 3 plant macrofossil types (Figure 4-5), such as *Tripleurospermum inodorum*, *Rumex acetosella*, *Arenaria norvegica*, and *Juncus balticus* appear, which suggests that those 'pioneer' taxa colonized unstable, mineral soils possibly exposed as a result of climate cooling in PAZ 3. Finds of fragmented leaves of *Dryas octopetala*, a typical component of modern tundra on base-rich soils in northernmost and alpine Fennoscandia, support this interpretation. PAZ 3 further shows the representation of soil fungi, i.e. spores of *Glomus* (Figure 4-4 /van Geel et al. 1989/) and macrofossils of *Cenococcum geophilum* (Figure 4-5 /Birks 2000, Walker et al. 2003/). Although these findings support the hypothesis of a gradual cooling trend as suggested by the pollen data, that resulted in a more open vegetation and increased soil erosion, they might also be related (at least in part) to changes in the local depositional environment. The diatom record indicates a distinct decrease in lake size during the upper PAZ, and the sandy lithology and occurrence of stream-inhabiting diatoms and chironomids reflect an increased fluvial input into the lake (see section 4.1.2 and Figure 4-6). The change in local environment might have led to a more efficient transport of fossils from the surrounding slopes to the coring-site. Remains of *Cenococcum* are only usually found in lake sediments when there is an input of material from the surrounding soils /Walker et al. 2003/.

### Reconstruction of the lake and wetland ecosystem

The presence of algae, such as *Botryococcus* and *Pediastrum*, indicate lacustrine conditions at the coring-site throughout the record (Figure 4-4). Similarly, spores and macroremains of *Sphagnum* and other mosses suggest some mires and peaty telmatic communities around the lake (Figures 4-4 and 4-5). The lake was probably fringed by peaty shores, as are many Fennoscandian northern boreal forest and low-arctic tundra lakes today. In addition, high pollen values of Cyperaceae and Poaceae may be partly related to wetland areas in the vicinity of the lake, and tall herbs such as *Filipendula* and *Sanguisorba officinalis* (Figures 4-3 and 4-5) suggest relatively moist conditions locally.

Aquatic macrofossils (Figure 4-5), including head capsules of chironomids (see Figure 4-1), are virtually absent in zone 1, whereas their concentrations are relatively low during zone 2b. This is probably due to a relatively high lake-level and large lake-size as reconstructed by the diatom record for these parts of the early MIS 3 lacustrine sequence (see section 4.1.2 and Figure 4-6), resulting in a larger distance from the coring-site to the shore.

Sokli B-series borehole  
N Finland  
Terrestrial pollen and spore percentage diagram

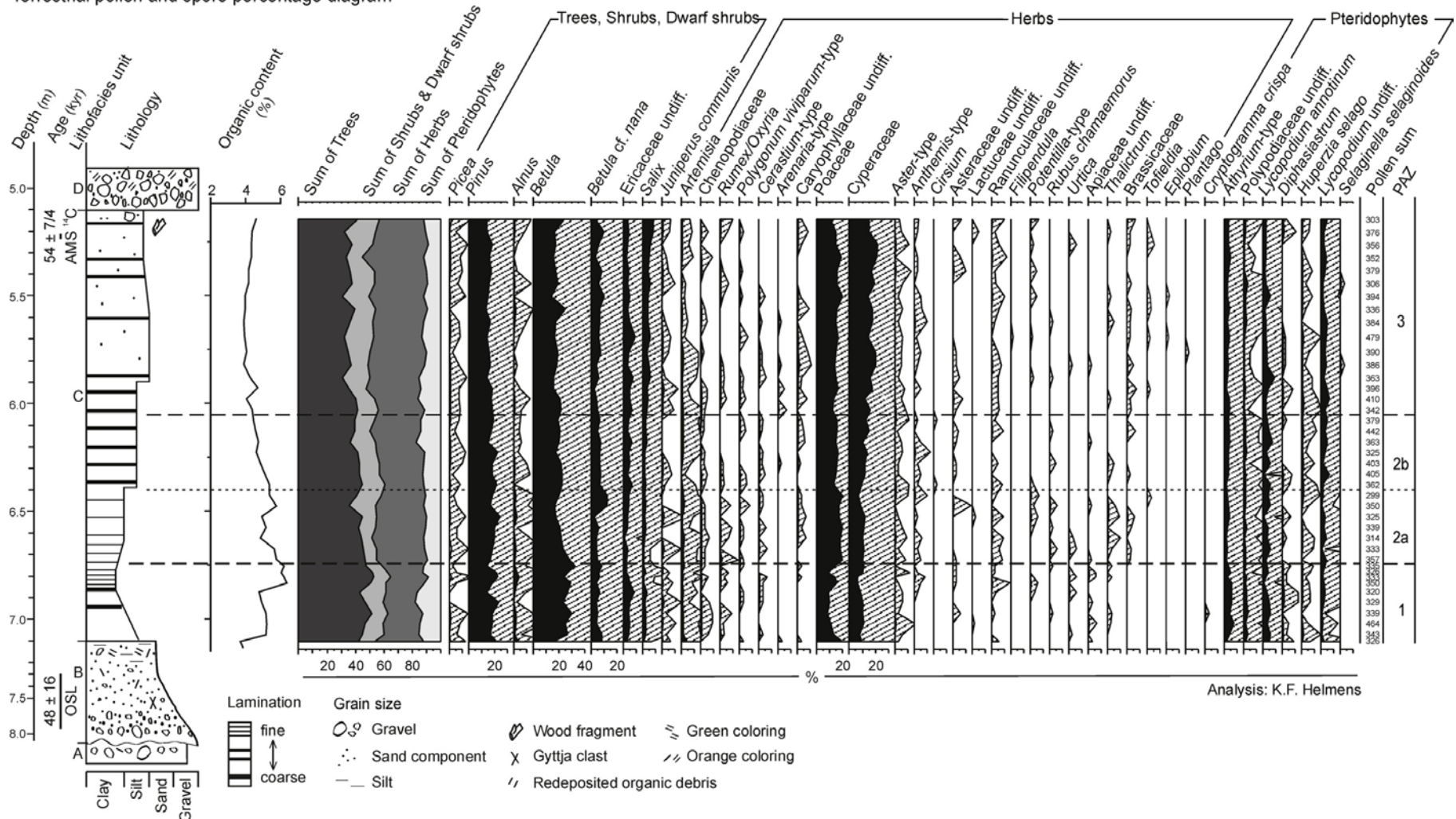
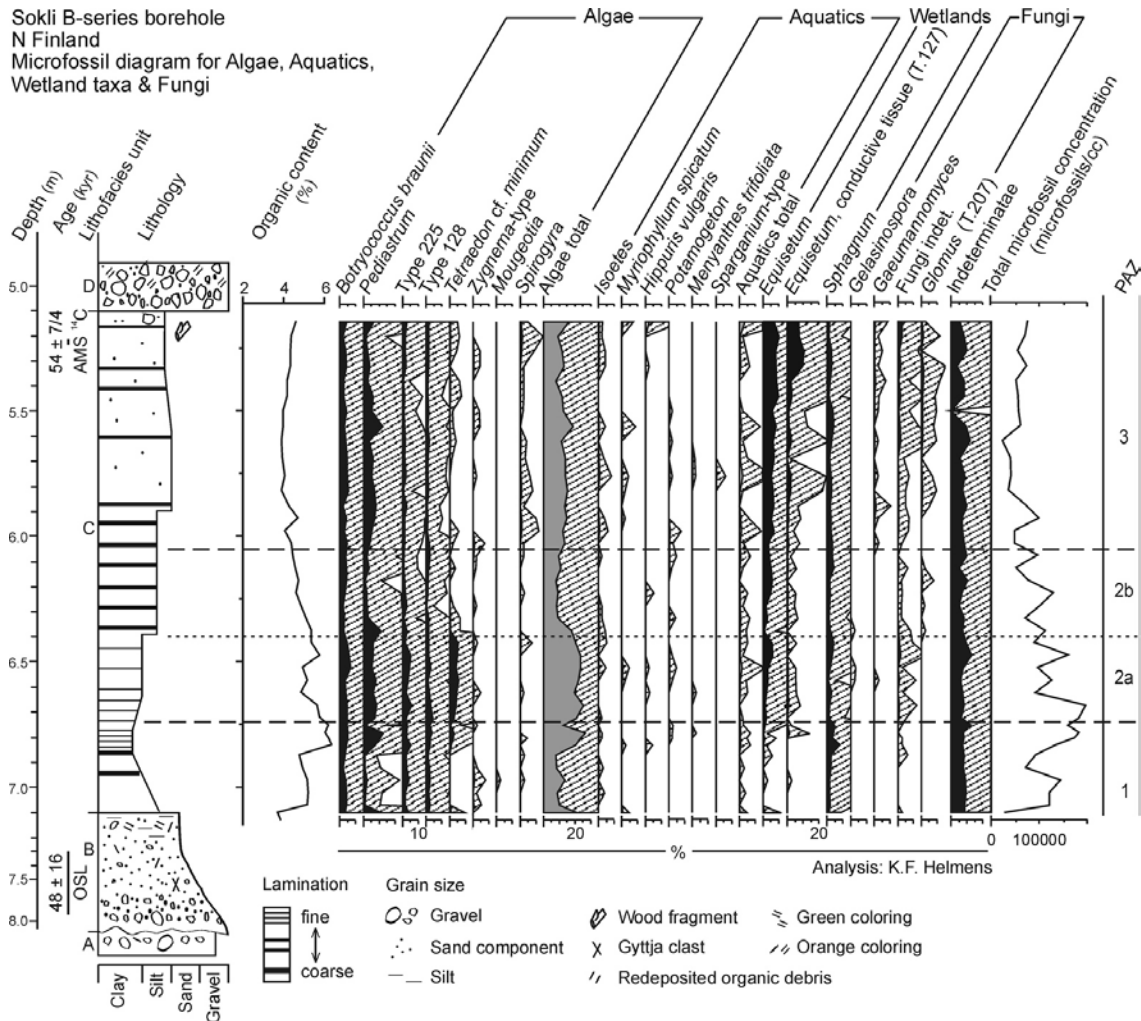


Figure 4-3. Terrestrial pollen and spore percentage diagram for the early MIS 3 deposit at Sokli. Percentages are calculated as percentages of total tree, shrub, dwarf-shrub, and herb pollen and pteridophyte spores. The solid curves show the actual percentages, the hatched curves show an  $\times 10$  exaggeration. The ages and sediment lithology and organic content are also shown.



**Figure 4-4.** Microfossil diagram for algae, other aquatics, *Sphagnum*, *Equisetum*, and fungi for the early MIS 3 deposit at Sokli. Percentages are calculated as percentages of total terrestrial pollen and spores (Figure 4-3). The solid curves show the actual percentages, the hatched curves show an  $\times 10$  exaggeration. The ages, sediment lithology and organic content, and total microfossil concentration are also shown. The total microfossil concentration shows considerable variation within the record, which is probably due to changes in the sedimentation rate (see section 4.1.4). High concentrations and relatively high organic content (LOI) values are recorded in the finely laminated clayey sediment around core depth  $\sim 6.75$  m. The total microfossil concentration and LOI values overall decrease as the sedimentation rates increases towards the top and bottom of the lacustrine sequence as the sediment becomes more coarse-grained.

Shallow-water conditions throughout zone 2a are indicated by the large amounts of macroremains (stem fragments) of *Equisetum*, reflecting the local presence of this wetland element (probably *E. fluviatile*) at or close to the coring-site. Zone 2a records abundant and diverse aquatic biota. It shows an abundance of resting eggs of the cladoceran genus *Daphnia* and, in the lower part of the zone, statoblasts of the bryozoan *Fredericella indica* (Figure 4-5). An increase in aquatic macrophyte vegetation is registered in the upper part of the zone which may in part explain the decline in *Fredericella indica*, as this benthic invertebrate prefers lakes with low aquatic vegetation and stony shores (Økland and Økland 2001). The aquatic macrophyte vegetation during zone 2a included both submerged (i.e. *Potamogeton mucronatus*, *Nitella*, *Isoetes*, *Myriophyllum spicatum*), emergent (*Hippuris vulgaris* and *Menyanthes trifoliata*), and floating taxa such as *Callitriche hermaphroditica*. Furthermore, the bryozoan *Plumatella*, Acari (mites), Trichoptera (insects), and Chironomidae (see section 4.1.2) are recorded. Algae were abundant and diverse (Figure 4-4), including *Botryococcus braunii*, *Pediastrum*, *Zygnema*-type, and *Spirogyra* (Zygnemataceae), the algal types T.225 and T.128 /van Geel et al. 1983, 1989/, and, especially confined to this zone, *Tetraedon cf. minimum*.

Sokli B-series borehole  
N Finland  
Macrofossil diagram

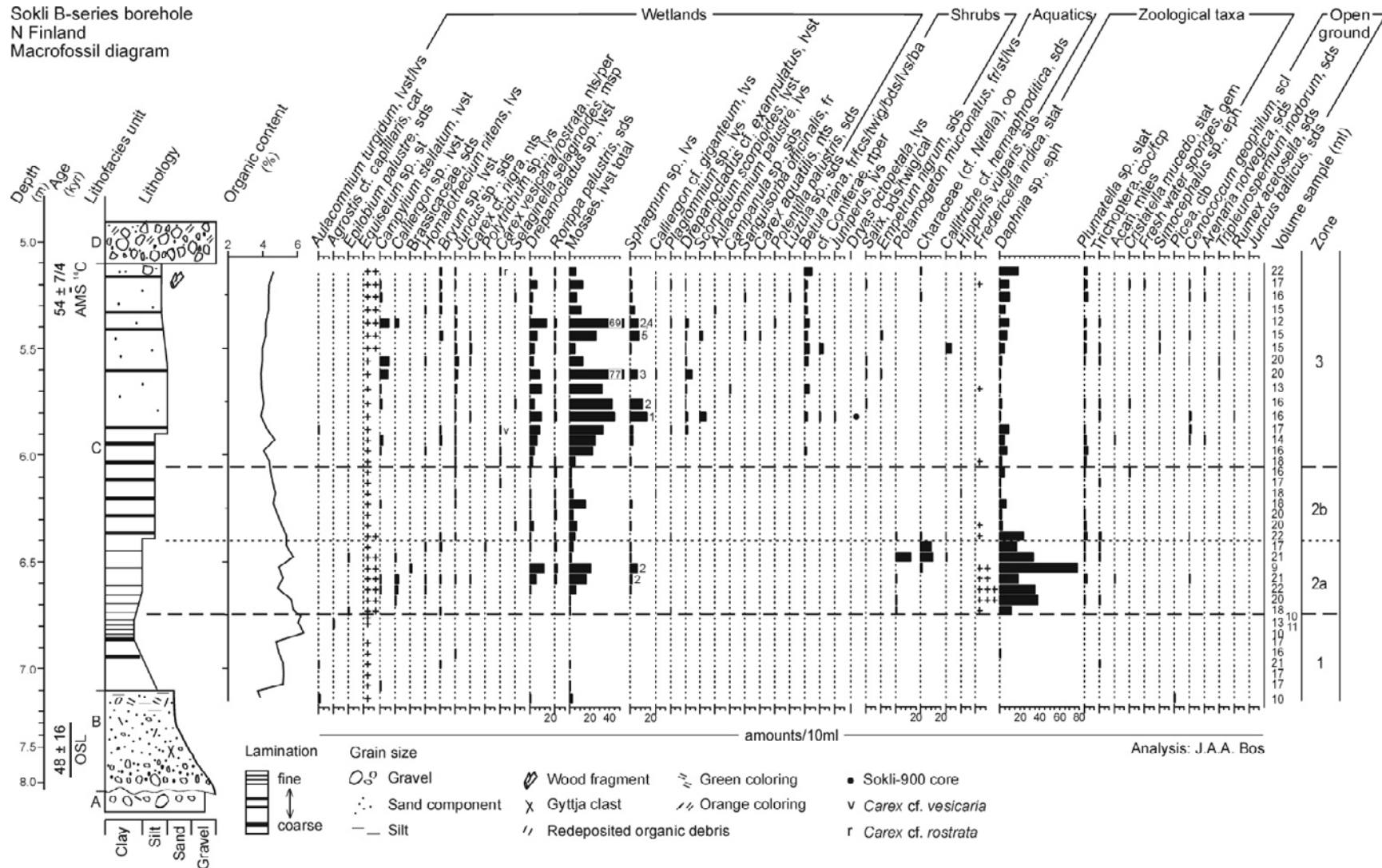


**Figure 4-5.** Diagram of plant macrofossils and animal remains for the early MIS 3 deposit at Sokli. Macrofossils are expressed as concentrations (amounts/10 ml) and drawn as histograms or as presence (+) or high abundance (+++). Type of remains: ba = bark, bds = budscales, cal = calytra, car = caryopses, coc = cocoons, eph = ephippia, f = fruits, fcp = frontoclypeus, gem = gemmulae, lvs = leaves, lvst = leavy stems, msp = megaspores, nts = nutlets, oo = oogonia, per = perigynia, rtper = root periderm, scl = sclerotia, sds = seeds, st = stems, stat = statoblasts. Macrofossils are near absent in the lowermost part of the sequence. Remains of *Sphagnum* 1 = *S. teres/squarossum*, 2 = *Sect. Acutifolia*, 3 = *Sect. Sphagnum*, 4 = *S. warnstorffii*, 5 = *Sect. Squarrosa*. The zones indicated are the pollen assemblage zones from Figures 4-3 and 4-4. The ages and sediment lithology and organic content are also shown.

*Potamogeton mucronatus* and *Callitriche hermaphroditica* prefer shallow waters and eutrophic to mesotrophic conditions /Oberdorfer 1994, van der Meijden 2005/. Similar nutrient conditions are favoured by *Tetraedon* cf. *minimum* and the algal T.225 /van Geel et al. 1989/, whereas nutrient-poor, oligotrophic waters are preferred by *Fredericella indica*. An increased nutrient availability in the lake during the upper part of the zone is suggested by a peak in the occurrence of the aquatic insect *Endochironomus albipennis*-type (see section 4.1.2), the appearances of *Rorippa palustris*, *Callitriche hermaphroditica*, and *Nitella*, and higher abundances of *Potamogeton mucronatus* (Figure 4-5), and a higher percentage representation of the alga *Tetraedon* cf. *minimum* (Figure 4-4).

The presence of pollen and plant macrofossils of Poaceae, *Rubus chamaemorus*, *Epilobium palustre*, *Potentilla palustris*, *Juncus*, *Carex acuta/nigra*, *Urtica dioica*, and *Rorippa palustris*, and the mosses *Bryum*, *Drepanocladus*, *Polytrichum*, *Homalothecium nitens*, *Campylium stellatum*, and *Sphagnum* suggests that the shallow lake during zone 2a was fringed by wet meadows and poor- to rich-fens, as are many shallow lakes in northern boreal and sub-arctic Fennoscandia today.

The bryozoan *Cristatella mucedo* appears in the uppermost part of zone 2b. This species is less strict in its ecological requirements and is indifferent towards aquatic macrophyte vegetation and sediment, but it prefers more coloured water with less wave action than *Fredericella indica* /Økland and Økland 2000, 2005/. High algal percentages during the upper part of zone 1 and during zone 2a (Figure 4-4) are probably related to clear water. In the preceding and following parts of the record (including during zone 2b), suspended silts causing a turbid water column may have limited algal growth (see section 4.1.2 and Figure 4-6).

During zone 3, an increased wetland zone is registered both in the micro- and macrofossil records (Figures 4-3 till 4-5), reflected by high pollen percentages of Cyperaceae combined with hyphopodia of *Gaeumannomyces* (see above) and macrofossils of *Carex* spp., high spore percentages and (in the upper part of the zone) conductive tissue (T.217 /van Geel et al. 1989/) and stem fragments of *Equisetum*, and abundant moss fragments. Macrofossils of woody plants such as *Betula nana*, *Salix*, and *Empetrum* suggest their local presence in the wetland. Taxa that appear for the first time during zone 3 are *Tofieldia*, *Filipendula*, *Sanguisorba officinalis*, *Campanula*, *Carex* cf. *rostrata*, *C. aquatilis*, *Selaginella selaginoides*, *Calliargon* cf. *giganteum*, *Scorpidium scorpioides*, and *Drepanocladus exannulatus*. *Carex aquatilis* and *Rorippa palustris* may suggest seasonally fluctuating water-levels /Weeda et al. 1987, 1994/. In the lake fauna, Porifera and *Simocephalus* appear (Figure 4-5). The latter indicates shallow, open water, eutrophic conditions and dense stands of vegetation /van Geel et al. 1983/.

#### 4.1.4 Comparison of the multi-proxy data

A combined proxy diagram for the early MIS 3 sediments is given in Figure 4-6: A presents lithology, lithofacies units (units A-D), and datings; B groupings of diatoms according to living habitat and relative percentages of other siliceous microfossils to diatoms; C diatom-inferred lake level and pH curves; and D a selection of other proxy indicators. The early MIS 3 interstadial at Sokli has been defined as the Tulppio Interstadial (Figure 4-6 A /Helmens et al. 2007a/).

In this section, changes in lake level and extent and the possible ice-dammed nature of the lake in the Sokli basin during the Tulppio Interstadial, as inferred from the siliceous microfossil and lithological records (section 4.1.2), are discussed in the light of the combined proxy record obtained from the Sokli early MIS 3 sediments.

#### **Changes in lake level and extent**

The diatom record reconstructs sudden changes in lake level during the deposition of the early MIS 3 sediments (Figure 4-6 C). The classification of diatom taxa according to living habitat that we employed in order to reconstruct the lake level fluctuations (Figure 4-6 B), however, is not absolute. The search of ecological preferences in the literature may give contradictory information or be vague /e.g. Philibert and Prairie 2002/. Therefore, lake level reconstructions based on diatoms should be used with caution. Nevertheless, the combined siliceous microfossil record seems to give a coherent reconstruction. Changes in the abundance of phytoliths and re-deposited Tertiary diatoms, as well as diatom-inferred pH, are in general concurrence with the lake level curve. Rises in lake level

and associated transgressions caused flooding of formerly vegetated areas, resulting in erosion and reworking of phytoliths and Tertiary diatoms. Although variations in reconstructed pH are small and within the model-based error margin, pH is generally lowered during phases with high lake level probably due to inwash of organic matter.

The phases with relatively high lake levels (DAZ 2 and 4) coincide with parts of the sediment sequence in which fossils of chironomids and other macrofossils (Figures 4-5 and 4-6 D) are nearly absent (DAZ 2) or scarce (DAZ 4). As no major trends are visible in the relative abundances of aquatic plant pollen throughout the sediment sequence ('aquatic plant' curve in Figure 4-6 D), /Engels et al. 2008/ assumed that the variations in chironomid concentration are not due to major changes in available micro-habitats for the aquatic insects as a result of changing aquatic vegetation. It is most likely that the scarcity of macrofossils during DAZ 2 and 4 are related to the large lake size indicated by the siliceous microfossil record. Changes in the distance between sampling point and shoreline have been shown to significantly influence the amount of macrofossils in lake sediments, where a high lake level and a remote location of the shoreline sharply reduce the abundance of macrofossils at the sampling location /e.g. Hannon and Gaillard 1997, Väiranta 2006/.

Although counts of chironomid head capsules are low in the lowermost part of the sediment sequence, the chironomid taxa found in the depth interval corresponding to DAZ 2 might also be indicative of a relatively deep lake (to a depth of ~ 10 m; section 4.1.2 and Stefan Engels pers. comm. 2008). The chironomid taxa percentage diagram does not reflect a distinct increase in lake depth during DAZ 4. Lake depth at the coring-site during DAZ 3-5 can be estimated at around 5 m based on the chironomid record /Stefan Engels pers. comm. 2008/.

Whereas the phases with high lake level provide an explanation for a scarcity of macrofossil findings, the late phase with low lake levels is also very clearly registered by the non-siliceous microfossil records. The siliceous microfossil record depicts for DAZ 5 in addition to a low lake level, an extensive littoral zone (e.g. indicated by the continuous registration of aerophilous diatom taxa in Figure 4-6 B) and increased fluvial influence near the coring-site (rheophilous taxa). Percentages of microfossils of wetland plants (Figure 4-6 D; e.g. *Sphagnum* and *Equisetum*), and macrofossil counts of for instance mosses (Figure 4-5), for instance, show highest values in this uppermost part of the sediment sequence, and the registration of spores from *Gaeumannomyces* indicates that also part of the high abundances of sedge pollen (see main pollen diagram in Figure 4-6 D) can be attributed to a local wetland source, as the latter fungus parasites on *Carex* spp. /Van Geel et al. 1983/. The chrysophyte stomatocysts curve in Figure 4-6 B parallels the wetland curve in Figure 4-6 D supporting the occurrence of the chrysophytes in an epiphytic habitat (see section 4.1.2) Also in concordance with the diatom record, stream-inhabiting chironomids (e.g. *Eukiefferiella*-type, *Prodiamesa*, and *Rheotanytarsus*), various soil fungi (*Glomus* and *Cennococcus*) and a sandy lithology suggest increased fluvial influence during DAZ 5. Furthermore, the registration of the diatom taxa *Diploneis elliptica* v. *elliptica* and *Amphora libyca* during DAZ 5 (Figure 4-6 B) are probably related to the largely diminished lake size during this latest part of the record and as such an increased influence of the local carbonate-rich bedrock on run-off. In addition, during the low lake level phase DAZ 3, the main pollen diagram shows relatively high percentage values for grass pollen, most probably related to the low lake level and the presence of an extended littoral zone.

### **Ice-dammed nature of lake and sedimentation rates**

Here, factors that could have caused the changing lake levels during the deposition of the early MIS 3 minerogenic, laminated sediment sequence, and information on sedimentation rates in the lake, are further explored. Although the exact time span of lacustrine sedimentation is unknown (i.e. if the laminations in the sediment have an annual origin, then some 400 years of sedimentation is recorded; section 3.2), the changes in lake level generally seem to have been sudden, leaving a distinct impact on the lake surroundings and the lake ecosystem. The apparent sudden changes in lake level and extent, combined with changes in sediment lithology (see section 4.1.2), and the fact that distinct glacio-fluvial landforms in the Sokli area suggest the existence of ice-dammed lakes during the last deglaciation (see section 2 /Johansson 1995/), make it likely that the changing lake levels/sizes reflect different stages in glacial lake evolution related to the retreating ice front of the Fennoscandian Ice Sheet from its MIS 4 position. This is further supported by a low LOI and the fact that Digital Elevation Model (DEM) data combined with morphological evidence is able to recon-



struct the proxy-inferred glacial lake evolution (see below). It can not be totally ruled out, however, that (part) of the lake level fluctuations are caused by changes in precipitation. However, changes in terrestrial vegetation during deposition of the early MIS 3 sediments seem to have been minor (see section 4.1.3), making it unlikely that major changes in precipitation (which can be expected to leave an imprint on the terrestrial ecosystem) occurred during the time interval recorded. The DEM-based landscape reconstructions place the coring-site in a sheltered lake embayment and show that several large rivers draining most probably non-glaciated terrain flowed into the glacial lake (see section 4.2 and Figure 4-7). This explains a limited influence of the ice sheet at the coring-site, resulting in a proxy record that in detail registers the biotic environment around the coring-site and reconstructs the regional climate.

A low organic content (LOI) of less than 5% in the early MIS 3 Sokli sediments is striking (Figure 4-6 D). The pollen assemblages in the early MIS 3 lacustrine sequence are similar to those currently recorded in surface samples from the shrub tundra region close to the sub-arctic birch forest limit in northern Fennoscandia (see section 4.1.3.). LOI measured in the sediment of a typical Fennoscandian sub-arctic lake is ~ 30%, whereas values of ~ 10% are recorded in tundra lakes with a barren catchment, and < 5% in Late Glacial or Early Holocene sediments, i.e. glacial clays and silts deposited in recently deglaciated lake environments /Korhola and Weckström 2004/. The low LOI in the Sokli sediments therefore supports the idea of the presence of a glacial lake at Sokli with sources for minerogenic matter including the extensive catchment that drained into the ice-dammed lake (see Figure 4-7), the inundated lake shores during phases of sudden lake level rise, and the near-by ice sheet. The low LOI in the uppermost sandy sediment (DAZ 5) can be ascribed to an increased fluvial influence (see above).

Reconstructions by /Johansson and Kujansuu 2005/ for the last deglaciation show that in northern Finland, lakes impounded along the northeastern margin of the Fennoscandian Ice Sheet were small and isolated. The results of a detailed study on one of these lakes, the relatively large (~ 1,000 km<sup>2</sup>) but highly irregularly outlined Glacial Lake Inari /Kujansuu et al. 1998/, show many similarities to those obtained on the early MIS 3 sediments at Sokli. The pollen record obtained from the one–two meter thick minerogenic, laminated lacustrine sequence at Inari, although influenced to some degree by re-working of older fossils, reconstructs a contemporaneous vegetation of park-like birch forests and open-land vegetation. This vegetation is similar as reconstructed by the pollen record from the small lake basin Akuvaara that is situated just north of the Inari Lake Basin and above the highest shoreline in the area /Hyvärinen 1975/. The deglaciation sediments at Akuvaara consist of sands and that in Glacial Lake Inari of laminated silt/clay fining up to very finely laminated clay and then coarsening up to laminated clay/silt. In case the laminations at Inari have an annual origin, then some 300–500 years of sedimentation is recorded /Kujansuu et al. 1998/.

Information on sedimentation rate is provided by the concentrations of pollen and spores from the terrestrial vegetation calculated in the sediment ('pollen sum taxa concentration' curve in Figure 4-6 D). As the main pollen diagram depicts little variation in regional vegetation cover in the Sokli area during the deposition of the lacustrine sediment sequence, we can assume that pollen production remained rather constant during the time interval studied. Therefore, the considerable variations in pollen/spore concentration values are most probably due to changes in sedimentation rate. High concentrations and relatively high LOI values in the finely laminated clayey sediments around ~ 6.75 m depth (Figure 4-6 D) seem to reflect a relatively low sedimentation rate. Sedimentation rates overall increase (and microfossil concentrations and LOI decrease) both towards the bottom and top of the record as the sediment coarsens to silts and sands.

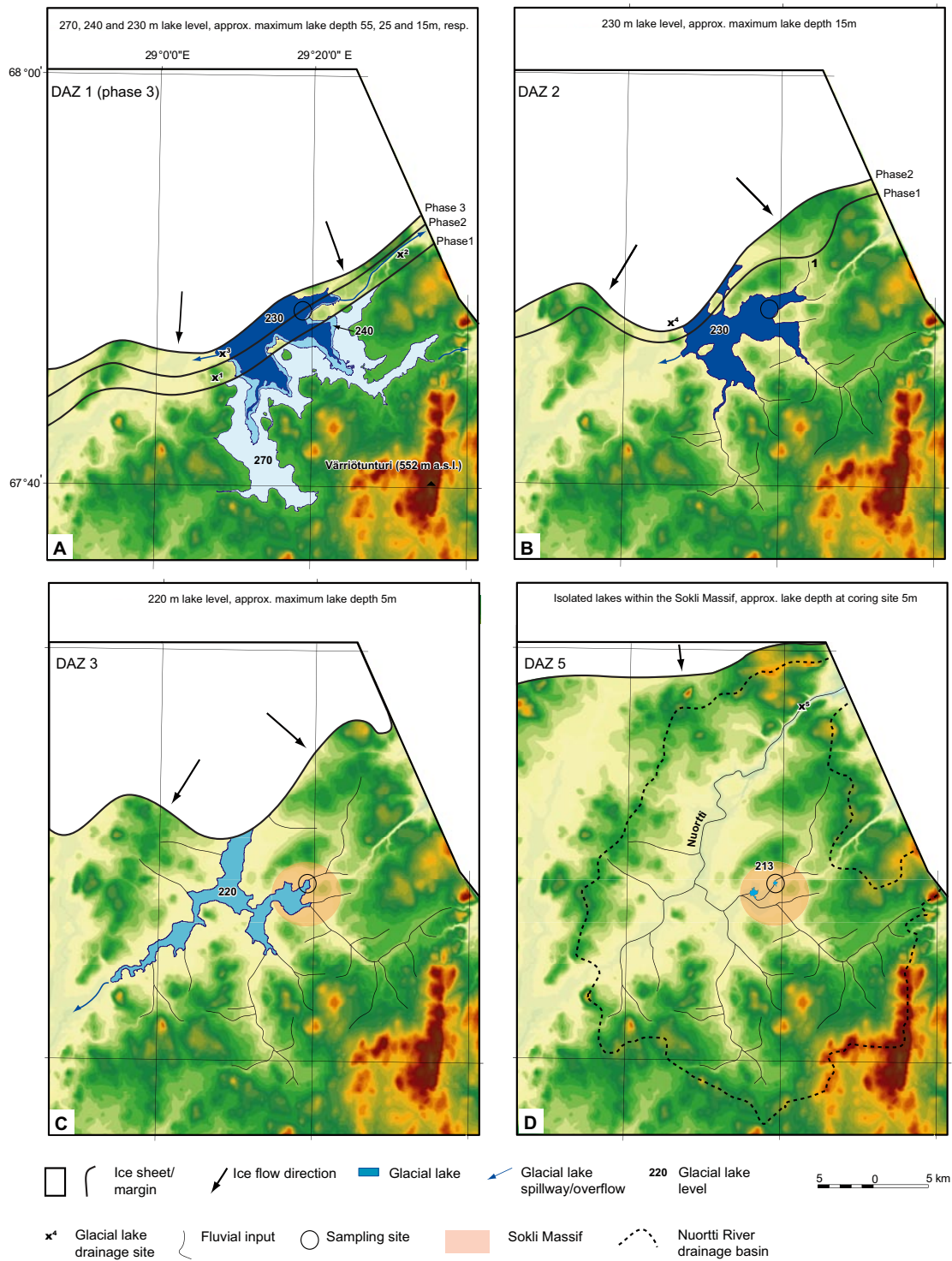
Similar trends as in pollen/spore concentrations are observed in the concentration of algal remains encountered in the pollen analysis (e.g. *Pediastrum*, *Botryococcus braunii*, *Tetraedon*, *Zygnema*, and *Spirogyra*; Figure 4-6 D). The algae concentration values, however, rise and then fall more abruptly at the lithological transitions from silts to clays and back to silts (depths 6.85 m in the upper part of DAZ 2 and 6.35 m at the transition from DAZ 3 to 4, respectively). It is likely that high amounts of suspended silty sediment in the turbid water column limited algae growth during the early part of DAZ 2 and during DAZ 4, i.e. when the ice margin was relatively close to the coring-site and lake shores were inundated (section 4.1.2).

## 4.2 Reconstruction of glacial lake evolution using digital elevation model and geomorphologic data

A Digital Elevation Model (DEM) of the National Land Survey of Finland (licence no. MYY/223/06) was used to reconstruct the evolution of the early MIS 3 Glacial Lake Sokli at the landscape level. The DEM has a spatial resolution of 25×25 m and a vertical resolution of one meter. No correction was made for non-uniform rebound effects due to a lack of data on isostatic uplift at the time of glacial lake formation. The area is relatively small (~ 30×30 km) and possible generated errors are considered to be insignificant for reconstructed glacial lake outlines /Jansson 2003/. N-S trending eskers of early MIS 3 age, that have been identified in the region just south of the Nuortti River drainage basin (see section 2), were used for the general direction of ice margin retreat. The set of deglacial landforms in northeastern Finland /Johansson 1995/, including abundant eskers on hill slopes and lateral meltwater channels, and the absence of landforms typical of the disintegration of stagnant ice in the Sokli region, supports the interpretation of the deglacial environment as a frontal deglaciation instead of aerial downwasting.

Two-dimensional reconstructions were generated for different stages in the evolution of Glacial Lake Sokli during the deposition of the early MIS 3 sediments (Figure 4-7 A–C). The reconstructions are described in the figure caption. The reconstructions are based on damming of tributaries in the upper drainage basin of the Nuortti River (Figure 2-1) between higher ground to the southeast and a retreating ice margin to the north, and topographic cols that control maximum lake-level altitudes. A northwards ice-marginal retreat as indicated by the eskers was not strictly followed. This would have resulted in open drainage routes towards the west, which in turn would have prevented the formation of relatively deep lake stages. It is assumed that the high terrain around Sokli influenced the ice retreat direction locally and that the margin was irregular with tongues extending into valleys.

We focused our reconstructions on stages in glacial lake evolution during the early part of the early MIS 3 interstadial (shown in Figure 4-7 A–C), i.e. when the proxy record from the Sokli sediments seems to register a detailed ice-marginal retreat and distinct phases in glacial lake configurations (DAZ 1–3 in section 4.1.2). During DAZ 4, when an ice-marginal re-advance appears to be recorded, it is possible that a glacial lake was generated similar as during DAZ 2 (Figure 4-7 B). Figure 4-7 D depicts a lake without ice-damming (DAZ 5). The DEM based reconstructions were prepared by Dr. Krister Jansson at the Department of Physical Geography and Quaternary Geology, Stockholm University, Sweden.



K.N. Jansson

**Figure 4-7.** Suggested early MIS 3 glacial lake evolution at the Sokli basin. Digital Elevation Model-based reconstructions are compared with the proxy record (Figure 4-6). The DEM is sourced from the National Land Survey of Finland (licence no. MYY/223/06) Note that the glacial lake outline during DAZ 4 (Figure 4-6) is not separately shown, as during this apparent ice-marginal re-advance phase a glacial lake similar as shown in B might have formed.

**Figure 4-7. Continued.**

A) Early stages of glacial lake formation in the valleys of the Yli-Nuortti and Tulppiojoki (Figure 2-1). At phase 1 (270 m), the coring-site at Sokli was ice-covered (lower till bed, or lithofacies unit A, in Figure 4-6 A) and the maximum lake depth of ~ 55 m was controlled by the col in the northernmost part of the Värriö-Nuortti Tunturit mountain ridge.  $x^1$  indicates the drainage site at which the 270 m lake was drained and lowered to 260 m and  $x^2$  where the lake level was lowered to 240 m. The 240 m level at phase 2 (lake depth maximal ~ 25 m) was controlled by the col at the head of the Törmäoja valley (Figure 2-2 D). The ice-margin was situated within the Sokli basin and proglacial sediment inter-mixed with re-deposited Eemian gyttja was deposited at the coring-site (lower part of coarse-grained ice-marginal sediment, lithofacies unit B, in Figure 4-6 A).

As the ice margin retreated further, the phase 2 lake drained at  $x^3$ , lowering the maximum water depth at the coring-site to ~ 15 m. At phase 3 (230 m), with the ice-front situated north of the Sokli basin, pioneering *Fragilaria* spp. is registered in more fine-grained proglacial sediment (DAZ 1 in the uppermost part of lithofacies unit B (Figure 4-6 A); see also section 4.1.2).

B) This stage of glacial lake evolution marks a stable situation in terms of water depth. An ice tongue developed over lower ground, blocking a new drainage site ( $x^4$ ) and maintaining the maximum lake depth at ~ 15 m as in A stage 3. Progressive ice-marginal retreat greatly increased the distance between the coring-site and the ice-margin – glacial lake contact, and positioned the Sokli basin in a sheltered lake embayment. Distinctly more fine-grained, laminated silt-clay accumulated at the coring-site (lowermost part of lithofacies C in Figure 4-6 A) showing a rich diatom flora (DAZ 2 in Figure 4-2). As the ice-front moved from phase 1 to 2, also the influence of the ice sheet through proglacial streams (1 in figure) was greatly diminished at the coring-site. The upper part of DAZ 2 records abundant algae in more transparent water (Figure 4-6 D).

C) This stage followed the opening of the drainage path in the Sotajoki valley ( $x^4$  in B), lowering the lake level down to 220 m. After the drainage, the maximum water depth at the coring-site was ~ 5 m (DAZ 3 in section 4.1.2). The lowering in lake level greatly diminished the distance between the coring-site and shore. This allowed the registration of abundant and diverse aquatic biota in the proxy record (Figures 4-5 and 4-6 D).

D) As the ice margin retreated north of the Nuortti River drainage basin, the glacial lake finally drained through the canyon of the Nuortti River (Figure 2-1;  $x^5$ ). Only scattered lakes remained (DAZ 5 in section 4.1.2). In contrast to A-C, when a large catchment drained into the Glacial Lake Sokli, the catchment of the isolated lake that remained in the central Sokli basin is limited to the Soklioja valley (Figure 2.1). This caused an increased influence of the local carbonate-rich bedrock (Sokli Carbonatite Massif) on run-off, allowing diatom taxa such *Diploneis elliptica* v. *elliptica* and *Amphora libyca* to flourish.

## 5 Quantitative climate reconstructions

### 5.1 Proxy-based reconstructions

In order to obtain quantitative paleo-temperature estimates, climatic reconstructions were carried out using mathematical transfer functions that express past values of the environmental variable of interest as a function of the fossil biological data /e.g. Birks 2003/. The use of these transfer functions requires a collection of modern surface samples (calibration set) that is mathematically correlated with an associated set of modern climatic parameters.

The transfer function approach requires information about the modern climate preferences and tolerances of the taxa found as fossil. The basic assumption throughout is methodological uniformitarianism /Birks and Birks 1980, Birks 2003/, namely that modern-day observations and relationships can be used as a model or analogue for past conditions and, more specifically, that fossil taxa – climate relationships have not changed with time, at least in the Late Quaternary /see further Birks and Seppä 2004/.

Transfer functions using modern-day animal/plant-climate calibration sets from northern Europe /Brooks and Birks 2001, Seppä and Birks 2001, Birks 2003, Weckström et al. 2006/ were applied to the chironomid, pollen and diatoms records obtained from the Sokli early MIS 3 deposit in order to infer mean July air temperatures. Reconstructions were carried out by Dr. Stefan Engels, Department of Palaeoclimatology and Geomorphology, Vrije Universiteit Amsterdam, The Netherlands, and Prof. Dr. Steve Brooks, Department of Entomology, The Natural History Museum, London, U.K. (chironomids); Prof. Dr. Heikki Seppä, Department of Geology, University of Helsinki, Finland, and Prof. Dr. John Birks, Department of Biology and Bjerknes Centre for Climate Research, University of Bergen, Norway (pollen); and Dr. Jan Weckström, Department of Biological and Environmental Sciences, University of Helsinki, Finland (diatoms). In addition, minimum mean July air temperatures were estimated based on information of the present distribution of certain plant/animal species ('indicator species') in northern Europe /e.g. Kolstrup 1980/ (Dr. Hanneke Bos, Department of Palaeoclimatology and Geomorphology, Vrije Universiteit Amsterdam, The Netherlands).

#### 5.1.1 The chironomid record

Chironomids (or non-biting midges) are recognized as a powerful proxy for inferring past climatic changes /e.g. Walker et al. 1991, Brooks and Birks 2001, Barley et al. 2006/ and in recent years have been widely used to infer quantitative mean July air temperatures on both late-glacial and Holocene timescales /e.g. Ilyashuk et al. 2005, Brooks 2006, Walker and Cwynar 2006/.

A Norwegian chironomid-temperature calibration data set was used as a modern analogue for the fossil chironomid assemblages encountered in the early MIS 3 deposit at Sokli. This training set contains 153 Norwegian lakes and spans a mean July air temperature range of 3.5–15.6°C (unpublished data and /Brooks and Birks 2001/). The samples for the training set were retrieved from the centres of all the lakes, and surface sediment samples were analysed for chironomid remains. Modern temperature values were calculated for the individual sites using 30-year averaged measurements of all meteorological stations situated close to the lakes (usually 10–20), with a correction for altitude (using local lapse rates) and distance to the coast (using local regression models).

A three-component weighted-averaging partial least squares (WA-PLS) model was selected as the inference model with the best predictive power, using mean July air temperatures as the response variable and chironomid taxa as the predictor variables. Using leave-one-out cross-validation (jack-knifing), the predictive powers of the model were estimated /Birks 1995/. Our inference model had a RMSEP of 1.01°C, an  $r^2$  of 0.91 and a maximum bias of 1.05°C. A bootstrap cross-validation with 499 cycles was performed to calculate sample-specific error estimates. Using the modern analogue technique described by /Birks et al. 1990/, the occurrence of non-analogues in the fossil samples was calculated, where “no close” or “no good” analogues with the modern data were defined as the cut-level of the 2<sup>nd</sup> and 5<sup>th</sup> percentile of all chi-square distances in the modern calibration data. A cut-level of the 95<sup>th</sup> and the 90<sup>th</sup> percentile of the modern residual chi-square distances was used as

an estimate of the fit of the fossil samples to temperature (“very poor” and “poor” respectively /Heiri et al. 2003a/). The percentage of rare taxa in the fossil samples was calculated, where a rare taxon has a Hill’s  $N_2$  (Hill, 1973) of five or less in the modern data set. /Brooks and Birks 2001/ state that the temperature optima of taxa with a  $N_2 > 5$  in the modern data are likely to be reliably estimated, whereas taxa with  $N_2 \leq 5$  are rare in the modern data, and the optima for these taxa are probably poorly estimated. The temperature inference model, the analogues and the percentage of rare taxa were calculated using C2 version 1.4.3 /Juggins 2003/, and the modern residual chi-square distances using CANOCO software version 4.0 /Ter Braak and Šmilauer 1998/.

The lowermost samples (below 6.79 m core depth in the Sokli sequence) show low numbers of chironomid head capsules (see Figure 4-1), even after all available material was examined for chironomid remains. These samples were therefore lumped and used as a single sample in the numerical analyses.

Figure 5-1 shows the reconstructed mean July air temperatures based on the chironomid record. Sample-specific prediction errors range between 1.08°C and 1.22°C (i.e. on average 1.15°C). The reconstructed mean July air temperatures are relatively low ( $12.0 \pm 1.15^\circ\text{C}$ ) for the lowermost part of the record (represented by the lumped sample, see above) but they increase steadily to values around  $13.5 \pm 1.15^\circ\text{C}$ . At 6.30 m core depth, temperatures decline to values around  $10.5 \pm 1.15\text{--}11.0 \pm 1.15^\circ\text{C}$  after which they stabilise around  $12.0 \pm 1.15\text{--}13.0 \pm 1.15^\circ\text{C}$  up to 5.30 m core depth. The uppermost three samples show a return to colder conditions with an inferred temperature of  $11.5 \pm 1.15\text{--}12.0 \pm 1.15^\circ\text{C}$ .

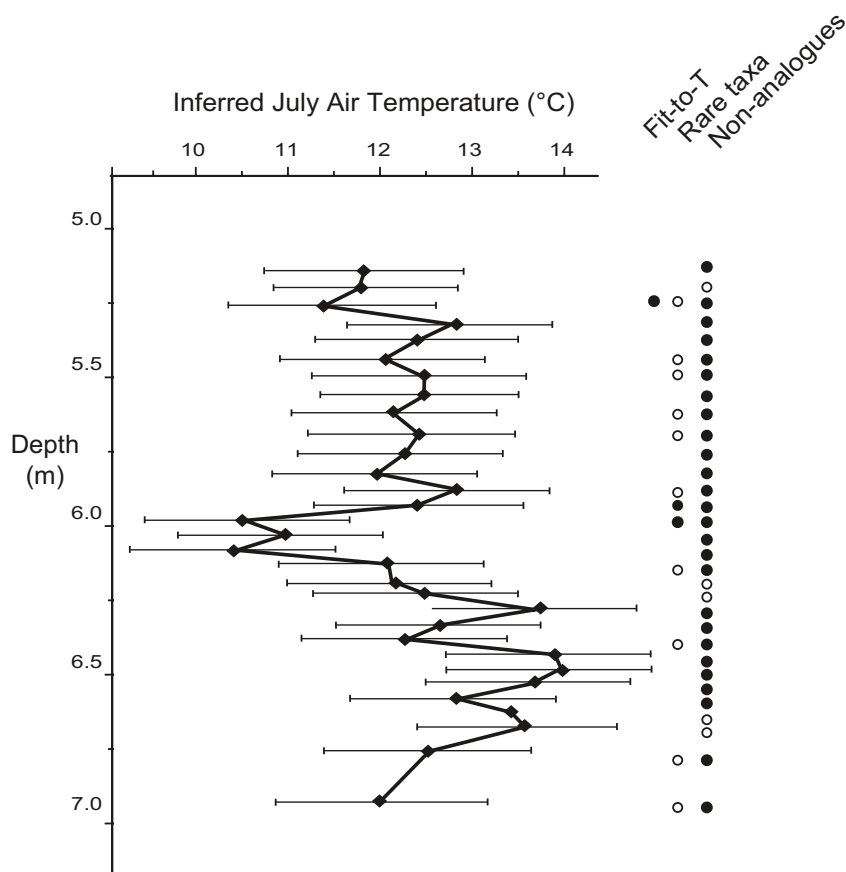


**Figure 5-1.** Chironomid-inferred mean July air temperatures at Sokli, and sample specific error-bars. The open circles indicate samples with no good analogues, and samples with more than 5% abundance of taxa that are rare in the modern training set. The solid circles indicate samples with no close analogues, with more than 10% abundance of taxa that are rare in the modern training set, and samples with a poor fit to temperature.

Since the reconstructed July air temperatures are not near the upper limit of the temperature range of the modern training set (i.e. 15.6°C), the influence of so-called edge effects /Ter Braak and Juggins 1993, Birks 1998/ can be excluded. Furthermore, where under colder climatic conditions the biodiversity tends to be reduced and the same cold-adapted assemblage of chironomids might exist over a wide temperature range /Birks and Birks 2006/, our reconstructed temperatures are in the intermediate to warm range and so are not likely to suffer from this problem.

The cumulative abundance of the six taxa included in the fossil assemblages but absent from the modern calibration set is between 0.0 and 6.9% per sample, whereas on average 98.7% of the identified fossil chironomids were used to obtain paleo-temperature estimates. Most of the identified fossil chironomids were well-represented in the modern training set, as there are only three fossil samples that have an abundance of rare taxa higher than 10%. These samples all have a high abundance of *Paracladius*, a taxon that in the modern training set has an effective number of occurrences (Hills  $N_2$ ) of 4.6, just below our threshold of 5.

Only one sample shows a “poor” fit to temperature and not a single sample has a residual chi-square distance higher than the extreme 5% of the modern samples and therefore none is classified as having a “very poor” fit to temperature. The fossil sample that is classified as having a “poor” fit to temperature is situated in a part of the record where both the chironomid-assemblages as well as the reconstructed temperatures are stable.

No fossil sample has a close analogue in the modern data, and 84% of the fossil samples have no good analogues. This result is surprising, as all the dominant taxa of the fossil record are all well-represented in the Norwegian training set and the training set contains many shallow, macrophyte rich lakes that could potentially provide good analogues for the fossil chironomid-assemblages. Probably, the relative abundances of taxa in the fossil samples are not (well) reflected in the individual training set lakes. Although there are no close modern analogues in the training set, WA-PLS can perform relatively well in poor analogue situations /Birks and Seppä 2004/.

Since there is a good fit to temperature and a high number of fossil taxa that are well-represented in the modern training set, the inferred values are considered to be reliable given the properties of the modern calibration data.

The reconstructed temperatures are surprisingly high, considering that the sediments were deposited in the middle part of the Last Glacial period. The highest reconstructed temperatures are as high as the current mean July air temperature (~ 13°C) at Sokli.

Chironomid studies on both late-glacial and Holocene sediments have produced inferred temperature reconstructions that were in concurrence with other proxy-based temperature estimates /e.g. Heiri and Millet 2005, Magny et al. 2006/, but also reconstructions that showed discrepancies between different sites /e.g. Velle et al. 2005/ or with reconstructions based on different proxies /e.g. Birks and Ammann 2000/. /Larocque and Hall 2003/ elegantly show that in their study there was a close similarity between measured and chironomid-inferred summer temperatures, but they also state that on longer temporal timescales, this relationship might not remain constant. Therefore, each record showing midge-paleo-temperature reconstructions must be interpreted cautiously, and in the context of all palaeoenvironmental data available /Heiri and Lotter 2005, Walker and Cwynar 2006/.

Below, mechanisms that could potentially have influenced the chironomid-inferred temperatures at Sokli are discussed. Botanical and zoological macroremains of aquatic taxa, encountered in the Sokli sediments, however, provide independent evidence for a period of high (minimum) mean July air temperatures, in agreement with the chironomid-based inferences. Elevated minimum mean July air temperatures of ~ 13°C are indicated by findings of macroremains of the aquatic plant *Potamogeton mucronatus* /Brinkkemper et al. 1987/ and the bryozoan *Fredericella indica* in the lower part of the sequence (Figures 4-5 and 4-6). *F. indica* prefers mean summer water temperatures (which are generally a few degrees lower than mean July air temperatures) from 11 to 15°C /Økland and Økland 2001/.

## Sampling design

The fossil chironomid remains recovered in the sediments from the Sokli site are surprisingly well-preserved, considering that an ice sheet has overridden the deposit. Identification of the fossil material was possible to a degree of taxonomic resolution similar to the calibration set. Great care was taken to retrieve the core from the central part of the Sokli basin /Helmens et al. 2000, 2007a/ as was done during the sampling of the lakes in the modern calibration dataset, and to prevent any influence of within-lake variability in chironomid-inferred temperatures as presented in /Heiri et al. 2003b/.

## Lake depth

/Walker and Cwynar 2006/ state that the influence of lake depth on paleo-temperature inferences poses a problem that deserves more attention. Deep, thermally stratified lakes may provide habitats suitable for cold-stenothermous midges, whereas shallow lakes from the same region will not support these species. Paleo-temperature inferences from deep lakes might therefore result in lower temperatures than those inferred from the shallower sites. Both the chironomid-assemblages as well as the botanical macroremains from the lacustrine sediments suggest that a shallow lake was present at the study site throughout the period considered, although the lake might have been relatively deeper during zone S-Ch1 (and DAZ 4, see section 4.1.2). As no drastic increase in littoral macrophyte taxa such as *Carex* spp is reconstructed (see section 4.1.3), we exclude a major influence of lake infilling on the lacustrine habitats available for chironomids.

## Dispersion

/Velle et al. 2005/ conclude that during the Holocene, mobility may not have been a limiting factor for the distribution of chironomids on the Fennoscandian mainland. However, during early MIS 3, there might have been a limited-sized ice-sheet situated close to our study site, possibly forming a major barrier for dispersal from the west (see section 7.3). The lower sediment samples from our record (below 6.79 m core depth) show a low Hill's  $N_2$ -diversity. However, the samples above 6.79 m core depth show relatively high  $N_2$ -diversity, suggesting that after 6.79 m core depth the colonisation of this lake has not been a problem for a wide range of taxa. Even a species with a limited mobility such as *C. ambigua* /Brodersen and Lindegaard 1999/ reached the Sokli basin quickly with respect to the introduction of other chironomid taxa.

Several taxa that reach high abundances only at a later stage in the record already have single occurrences in the lower parts of the record, before finally establishing themselves during a later stage (see for instance *Paracladius*). Therefore, local climate or habitat conditions rather than a restricted dispersion have most likely been the controlling factor for the composition of the chironomid assemblages.

## Decoupling of water temperature and air temperature

Many modern training sets have been designed with the specific goal of providing a tool for reconstructing mean July air temperatures. This, however, does not mean that the authors assume that the chironomid fauna responds exclusively to air temperature /Birks 1998/. In fact, it is likely that chironomids respond to both air and water temperature, as water temperature influences the development of the midges during the relatively long larval stage, whereas air temperature has a direct influence only on the survival and distribution of the winged, short-lived adult stage /Brooks and Birks 2001/.

/Livingstone and Lotter 1998/ found a strong correlation between mean July lake water and air temperatures in Switzerland. However, there are several potential decoupling mechanisms between July air temperature and water temperature, for instance, an increased influence of winter precipitation in the form of snow on the temperature of the lake water /Birks and Birks 2006/, or the influence of glacier-fed streams on a lake /Brooks and Birks 2001/.

In order to investigate whether these potential mechanisms played a role in the former lake, or whether past changes in nutrient availability have influenced the chironomid-based temperature inferences, the application of a single proxy will not suffice. Multi-proxy studies providing multiple lines of evidence for possible changes in climate or environment will help to identify factors influencing the composition of fossil chironomid assemblages.

### 5.1.2 The terrestrial pollen record

A modern pollen-climate data-set consisting of 113 pollen samples from throughout Finland, 161 samples from throughout Norway, and 27 samples from northern Sweden was used to reconstruct mean July air temperature from the Sokli terrestrial pollen and spore assemblages. The modern samples were surface-sediments (0–1 cm) from small- to medium-sized lakes taken with a gravity corer from the deepest part of each lake. In the selection of lakes, lakes were rejected if they had large marginal sedge-swamps, extensively cultivated areas, or obvious signs of disturbance. All samples were analysed to the lowest possible taxonomic level and the data-set contains 156 terrestrial pollen and spore taxa. Modern mean July temperatures were estimated for each lake by a standard interpolation and modelling procedure (see /Seppä and Birks 2001/ for details).

Because of differences between the pollen morphologies of the modern data-set and the Sokli fossil pollen assemblages, taxonomic harmonisation was necessary to make both data-sets comparable. For example, *Betula* and *Betula cf. nana* at Sokli had to be amalgamated into a single *Betula* taxon for comparability with the modern data-set. As a result of these harmonisations, the modern data were reduced to 146 taxa.

Modern pollen-climate transfer functions based on these 146 pollen and spore taxa included in the calculation sum were developed using weighted-averaging partial least squares regression /ter Braak and Juggins 1993/. The ‘minimal adequate model’ /sensu Birks 1998/ was selected to have the lowest number of ‘useful’ components and a good predictive ability, as assessed by leave-one-out cross-validation /ter Braak and Juggins 1993/. The resulting two-component model has a root-mean-square error of prediction (RMSEP) of 1.02°C, an  $r^2$  between predicted and observed values of 0.71, and a maximum bias of 2.31°C. These model statistics compare well with the statistics for the model based on 156 taxa (RMSEP = 0.99°C,  $r^2$  = 0.73, maximum bias = 2.89°C /Birks and Seppä 2004/). All computations were based on square-root transformed percentages in an attempt to stabilise variances /Birks 1995/.

Sample-specific errors were estimated for each fossil sample by Monte Carlo simulation (500 simulations) /Birks 1995/. To highlight the major low-frequency trends in the reconstructions, a LOWESS smoother (locally weighted scatterplot smoother) (span = 0.25 /Cleveland 1979/) was fitted to the reconstructed values.

Numerical evaluation of the Sokli reconstruction followed /Birks 1998/ in terms of the representation of taxa in the fossil data not present in the modern data-set and the lack-of-fit of the fossil samples when fitted passively to a canonical correspondence analysis constrained by mean July temperature of the modern data /Birks et al. 1990/. Any fossil sample whose squared residual distance was larger than the residual distance of the extreme 5% of the modern data is considered to have a “very poor” fit to July temperature and those with values equal to or larger than the extreme 10% are deemed to have a “poor” fit (see /Bigler et al. 2002/ for further details of these evaluation procedures).

The fossil pollen and spore data consisted of 38 taxa, of which 34 were well represented in the modern data-set. The four taxa not present in the modern data (e.g. *Tofieldia*) comprised less than 1% of the total fossil assemblage. Their absence in the modern data would have little or no influence on the temperature reconstructions /Birks 1998/. When the fossil data were fitted passively to the first canonical correspondence analysis of the modern data constrained by mean July air temperature, all the squared residual distances of the fossil samples exceed the residual distances of the 304 modern samples, suggesting that all the fossil samples have a “very poor” fit to mean July temperature. These poor fits suggest that the climate reconstruction should be viewed with caution and as a working hypothesis in need of testing or validating by independent proxies (e.g. terrestrial plant macrofossils).

The mean July air temperatures inferred from the pollen data (Figure 5-2) lie within the range 9.6–12.8°C, with sample-specific errors between 1.22 and 1.74°C (i.e. on average 1.5°C). Despite the uncertainties in the reconstruction, there is a consistent trend of decreasing temperature upward in the sequence from  $12 \pm 1.5^\circ\text{C}$ , or more, to  $10 \pm 1.5^\circ\text{C}$ – $12 \pm 1.5^\circ\text{C}$ , with two small dips in inferred temperature. It should be emphasised that these small dips all lie within the inherent sample-specific errors of the reconstructed values.

Of the terrestrial plant macrofossils present at Sokli (Figure 4-5), *Dryas octopetala*, *Arenaria norvegica*, and *Betula nana* were all confined to the upper part of the lacustrine sequence. These taxa mainly occur in Fennoscandia today in areas where the mean July temperature is 11°C or less, namely in the low-alpine zone /Moen 1999/. Their occurrences support the pollen-based climate reconstructions of 10–12°C ( $\pm 1.5^\circ\text{C}$ ) for the upper part of the sequence.

### 5.1.3 The diatom record

A diatom-mean July air temperature calibration model, based on the relationship of the weighted abundance of modern diatom taxa and the 30-year mean July air temperature of 64 northwestern Fennoscandian lakes /Weckström et al. 2006/, was applied for the climate reconstruction. After the leave-one-out cross-validation procedure, the two-component WA-PLS model performed best with  $r^2 = 0.62$  and a prediction error of 0.96°C. Sample specific error estimates were derived by bootstrap cross-validation with 499 cycles. The general suitability of the modern calibration data set to the fossil data was evaluated by the “goodness-of-fit” and the rare taxa-approaches /e.g. Birks et al. 1990, Brooks and Birks 2001, Engels et al. 2008/. In the goodness-of-fit approach, the fossil samples with a residual distance larger than the residual distance of the extreme 5% in the modern data set were regarded to have a “very poor” fit and fossil samples with residual distances larger than the residual distance of the extreme 10% in the modern set to have a “poor” fit /Birks et al. 1990/. In the rare taxa approach, the percentage of fossil taxa with Hill’s  $N_2$  /Hill 1973/ of less than five in the modern data set was calculated. The temperature optima of these taxa are considered to be poorly estimated in the modern data.

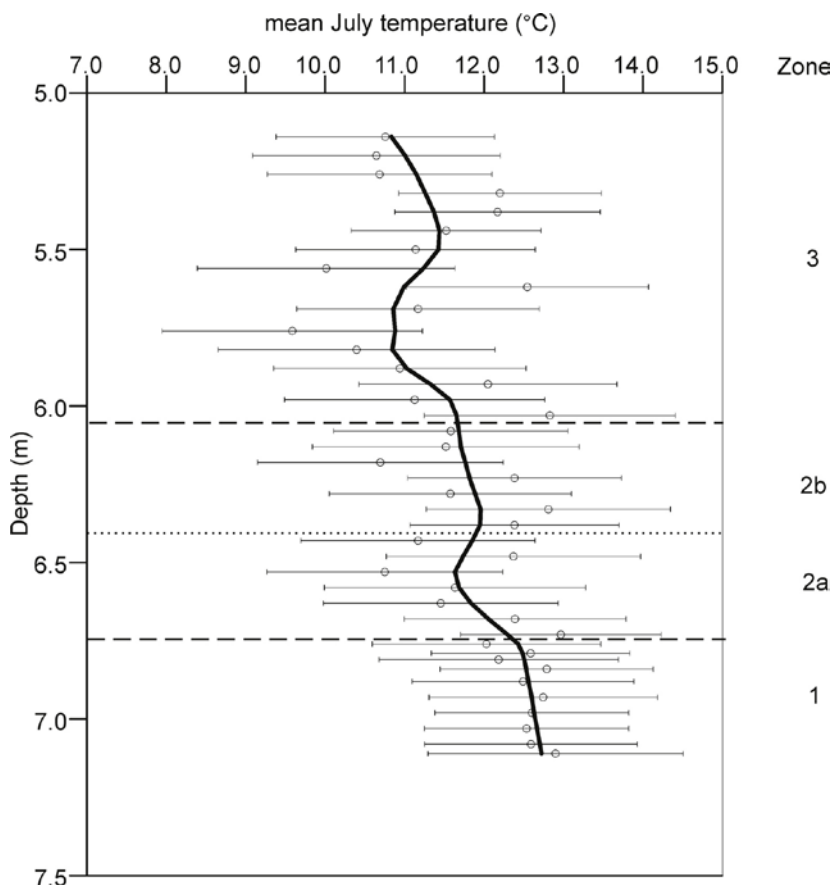


**Figure 5-2.** Pollen-inferred mean July air temperature at Sokli, and sample specific error-bars. The fitted line is a LOWESS (locally weighted scatter plot smoother; span = 0.25) plotted to highlight the main trends in the reconstructed temperatures.

Figure 5-3 shows the reconstructed mean July air temperatures with the sample specific error bars. Of the 211 enumerated fossil diatom taxa 101 were included in the reconstruction. However, these taxa represented 53 to 91% (mean and median 77%) of the total sum of the fossil diatom assemblages. According to the goodness-of-fit analysis, five fossil samples had a “poor” fit to temperature and three samples had a “very poor” fit. All of the fossil samples had an abundance of rare taxa higher than 10% suggesting their poor overall representation in the modern training set. Moreover, 49 out of the 101 taxa included in the reconstruction had a Hill’s  $N_2$  value less than five in the modern data.

As /Anderson 2000/ argues, temperature is not necessarily regarded as the strongest environmental variable affecting the distribution of diatoms. However, /Weckström et al. 1997a, b, 2006/ have shown that temperature is a relatively powerful variable affecting the diatom composition in north-western Fennoscandia. Moreover, /Weckström and Korhola 2001/ demonstrated that in northwestern Fennoscandia, the majority of the most common diatom genera follow a sigmoidal response model along the temperature gradient either increasing or decreasing with temperature.

Due to the relatively poor analogue between the fossil and modern training-set diatom samples, caution must be exercised when interpreting the quantitative temperature fluctuations. In general, however, the diatom-inferred temperature reconstruction reveals the same high temperature values as the chironomid-based temperature reconstruction (Figure 5-1). Both reconstructions show temperatures mainly from ~ 12 to 13°C, which is as high as at present. Although the diatom- and chironomid-based temperature reconstructions are almost inversely correlated during DAZ 4, their

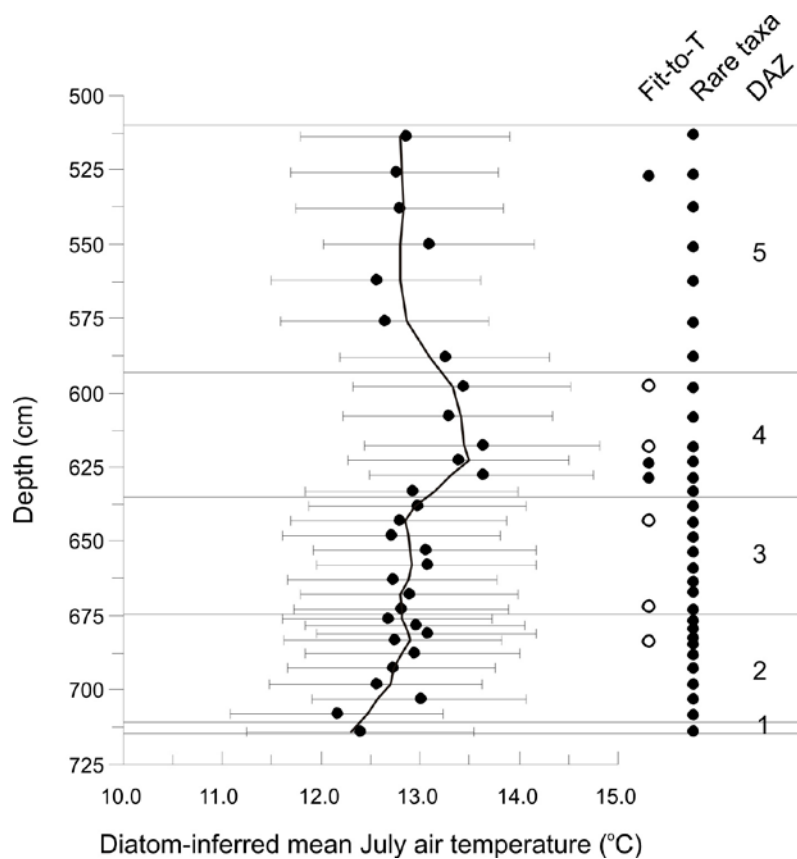


**Figure 5-3.** 7 Diatom-inferred mean July air temperature at Sokli, with a fitted LOWESS smoother (span=0.2; solid line), and sample specific error-bars. According to the goodness-of-fit analysis (Fit-to-T), five fossil samples had a poor fit to temperature (open circles) and three samples had a very poor fit (closed circles). According to rare taxa analysis (Rare taxa) all fossil samples had more than 10% abundance of taxa that are rare in the modern data (closed circles). The five diatom assemblage zones (DAZ) are shown on the right.

sample specific errors are mainly overlapping throughout the core indicating exceptionally high temperatures during MIS 3. This is supported also by the fact that due to the high present July mean temperature at Sokli (~ 13°C) compared to the temperature gradient of our 64-lake training data set (mean and median 11.2°C), the diatom-based temperatures are slightly underestimated. The diatom-based reconstruction suggests that high temperatures already prevailed during the earliest part of lacustrine sedimentation where fossils of chironomids are scarce.

#### 5.1.4 Comparison of the multi-proxy based climate reconstructions

The pollen-based climate reconstructions suggest that mean July air temperatures at Sokli during the time interval studied in this report (early MIS 3) were between 9.6 and 12.8°C ( $\pm 1.5^\circ\text{C}$ ), with highest temperatures recorded for the earliest part of lacustrine sedimentation. Such temperatures today occur at or near the latitudinal or altitudinal tree-line in northern Fennoscandia. The temperatures reconstructed from the fossil chironomid and diatom assemblages range between 10.5 and 14°C ( $\pm 1.15^\circ\text{C}$ ). Elevated mean July air temperatures of minimum ~ 13°C are also reconstructed by other aquatic fossils (aquatic plants and Bryozoa). Thus, the temperature inferences based on terrestrial fossils are consistently lower than temperatures reconstructed from the fossil aquatic assemblages (see Figure 5-4).

One of the possible hypotheses to account for these differences is that the regional terrestrial and the local aquatic systems responded differently to the climatic and landscape features at the time of MIS 3.

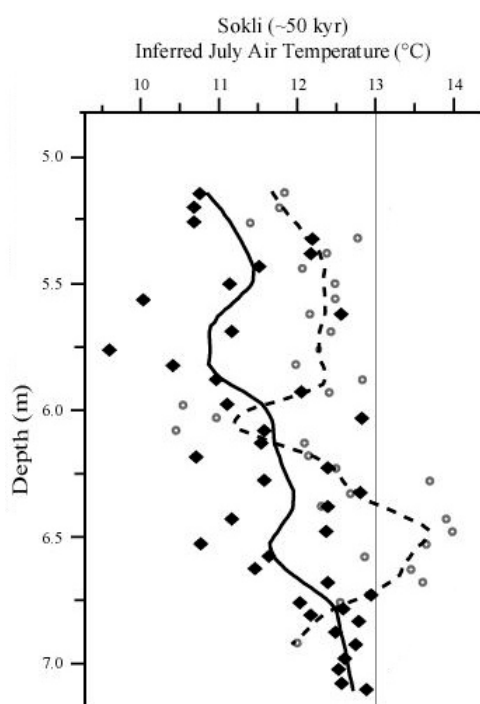


**Figure 5-4.** Terrestrial pollen- (solid quadrangles) and aquatic insect (chironomid; open circles) – inferred mean July air temperatures for the early MIS 3 deposit at Sokli with a locally weighted scatterplot smoother (LOWESS /Cleveland 1979/) applied to the reconstructed values (black line: pollen-based temperature curve (span = 0.25); dashed line: chironomid-based temperature curve (span = 0.20)). Sample-specific prediction errors (not indicated) range between 1.08°C and 1.22°C for the chironomid-based values (see Figure 5-1) and 1.22–1.74°C for the pollen-based values (Figure 5-2). Present-day mean July temperature of ~ 13°C at Sokli is indicated for reference.

## 5.2 Climate model simulations

The LOVECLIM three-dimensional climate model /Driesschaert 2005/, with a spatial resolution of  $5.6^{\circ} \times 5.6^{\circ}$ , was applied to simulate the average MIS 3 interstadial climate. The extent and elevation of the continental ice sheets and other forcings (orbital parameters, atmospheric greenhouse gases and dust content) were modified from full glacial conditions /Roche et al. 2006/.

In agreement with the proxy-based reconstructions, the climate model simulation suggests high mean July temperatures for the sector northeast of the Fennoscandian Ice Sheet for this time period (Figure 5-5). In the model, warm summer conditions are the combined result of enhanced July insolation compared to present ( $+19 \text{ W/m}^2$  /Berger and Loutre 1991/) and northwesterly winds advecting cool, but very dry air from the ice sheet. The winds are produced by a thermal high-pressure cell over the ice sheet which is an extension of the anticyclonal cell situated over the cool northeastern Atlantic Ocean. The combination of high insolation and dry air leads to a strong sensible heat flux and relatively warm conditions near the surface. The climate model simulation was carried out by Drs. Cedric Van Meerbeeck and Dr. Hans Renssen at the Department of Palaeoclimatology and Geomorphology, Vrije Universiteit Amsterdam, The Netherlands.

New data reviewed in section 6, however, indicate that the ice sheet configuration used in the model set-up was too large.

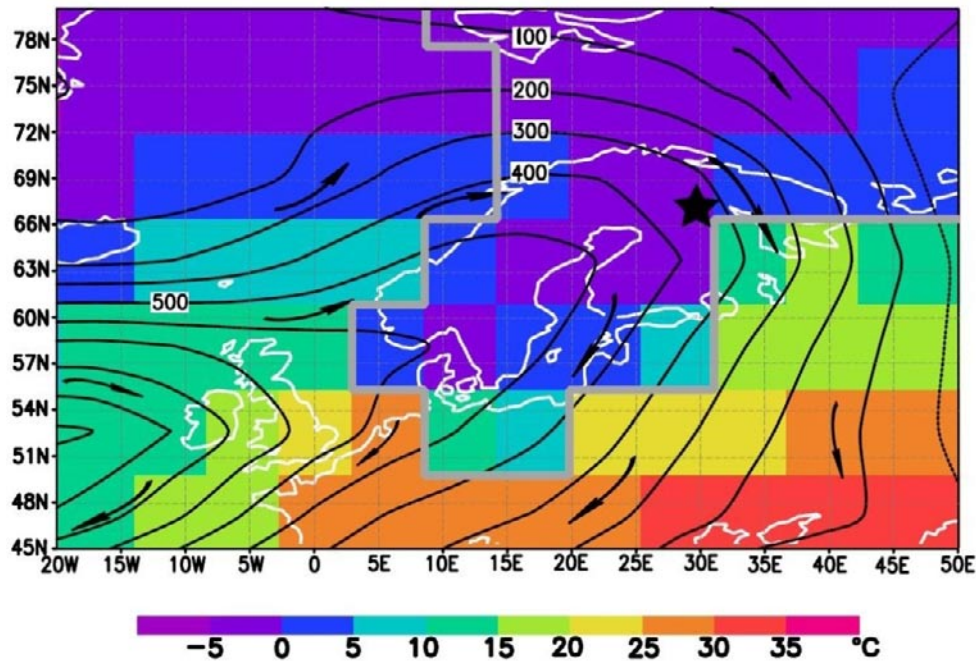


*Figure 5-5. Simulated mean July surface air temperature over the northern and middle part of Europe. Contour lines represent the geopotential height at 800 hPa, while arrows give a schematic view of wind direction in the lower atmosphere. The extent of the prescribed MIS3 Fennoscandian Ice Sheet is indicated in gray; star shows location of Sokli. Note that the model is not suitable for analyzing results at the grid-cell scale because of its low spatial resolution: the model is designed for continental and subcontinental scales.*

## 6 Early MIS 3 lacustrine sequences in Finland

In this section, two recently published, well-dated sediment sequences from eastern and western Finland, including sediments dated to early MIS 3, are summarized with respect to their chronology, vegetation reconstruction and climatic inferences. Results will be compared with the Sokli site in the discussion section 7.

### 6.1 Stratigraphy and dating

#### 6.1.1 Ruunaa (eastern Finland)

/Lunkka et al. 2008/ studied three borehole stratigraphies obtained from the Ruunaa area, eastern Finland (63°25'N, 30°23'E, elevation ~ 140 m.a.s.l.; Figure 6-1). The area is situated just inside the Pieltisjärvi-Kalevala end moraine of Younger Dryas age. A deposit of up to 1.4 m thickness is encountered overlying the bedrock. The deposit consists of cobbles and boulders embedded in a sand/gravel-matrix and are interpreted as a primary till. The till unit is overlain by an up to ~ 4.5 m thick sediment body of clay/silt alternations that becomes more sandy higher up in the unit and was deposited in a lacustrine environment. These lacustrine sediments are overlain by an up to ~ 5.5 m thick sediment unit consisting of several fining-upward cycles of gravels, sands, silts and clays, including ripple laminations and parallel bedding, of probably fluvial origin. The top unit consists of an up to ~ 6 m thick primary till deposit /Lunkka et al. 2008/.



**Figure 6-1.** Northern Europe showing the location of sites discussed in the text in perspective to the MIS 4 (at ~ 65 kyr; solid line) and LGM (~ 20 kyr; dashed line) maximum extents of the Fennoscandian Ice Sheet (according to /Svendsen et al. 2004/).

Three samples were taken from the fluvial current bedded sand units for OSL dating, as these were thought to have been best exposed to light and thus best reset or zeroed. The quartz OSL ages, that were obtained by applying a SAR protocol /Murray and Wintle 2000, 2003/, are very uniform in the order of 50 kyr (uppermost sample) to 52 kyr (lowermost sample), and have sample specific errors of 5–8 kyr. /Lunkka et al. 2008/ acknowledge that some degree of incomplete bleaching can never be completely ruled out, but state that such offsets are smaller than the overall uncertainties calculated for the ages. According to /Murray and Olley 2002/ and /Wallinga 2002/, age offsets of only between zero and a few thousand years have been observed in a wide range of modern fluvial deposits.

The OSL ages and the regional till stratigraphy indicate that the lower till was probably deposited during MIS 4. /Lunkka et al. 2008/ conclude that the overlying laminated sediments were probably deposited in a glacio-lacustrine environment (see below) following deglaciation at around 50 kyr or slightly before.

### **6.1.2 Hitura (western Finland)**

/Salonen et al. 2008/ studied an up to 50 m thick sediment sequence exposed over ~ 240 m in an open pit mine at Hitura, western Finland (63°51'N, 25°03'E, elevation 72 m.a.s.l.; Figure 6-1). The sediment sequence covers bedrock and extends from the Holocene (MIS 1) into the Penultimate Glacial (MIS 6). It was studied in 14 profiles which were correlated lithostratigraphically. A chronology was established based on 12 quartz OSL dates, selecting sorted medium to fine-grained sandy deposits representing possible well-bleached environments (aeolian, soil E-horizon, littoral or fluvial), as well as one AMS <sup>14</sup>C date on a 10 cm long twig.

Sediments in the lower part of the Hitura sequence are dated to the Saalian deglaciation (late MIS 6) and the Eemian Interglacial (MIS 5e), and are interpreted by /Salonen et al. 2008/ as being deposited subglacially (as part of an esker; lowermost unit), and subsequently in glacio-lacustrine, aeolian (with signs of soil formation) and again glacio-lacustrine environments (upper unit).

The middle part of the sequence includes a massive diamicton with a highly variable thickness of a few cm to 5 m, which can be followed along a major part of the exposure. The diamicton is interpreted as basal till overlain by flow till. It contains abundant re-deposited sediment in the form of sorted sediment interclasts that yielded OSL ages ranging from 130–79 kyr. Based on these dates it is suggested that the till unit postdates 79 kyr and was probably deposited during MIS 4. The till is overlain by an up to 4.5 m thick deposit of laminated silt and fine sand, coarsening upwards into alternating layers of plane-parallel bedded medium sand and ripple cross-laminated fine sand, and then into gravel-rich sand showing weakly developed imbrications. The sediments on top of the diamicton are interpreted as representing a regressive succession during deglaciation /Salonen et al. 2008/.

Four OSL datings using single-aliquot measurements on the littoral, more coarse-grained, upper sandy and gravelly sediments, yielded ages between 120–79 kyr. Single-grain measurements on the same samples, however, allowed for the identification of mixed populations of grains from at least two age groups, a younger population (interpreted as representing the sedimentation event) with an age of 55, 61 and 62 kyr and an older population (representing reworked grains derived from previously bleached sediments) dated at 106, 130 and 131 kyr /Salonen et al. 2008/. Strips of allochthonous organic material and small wood fragments found associated with fine-grained sediments in the middle part of the deglacial sequence yielded an AMS <sup>14</sup>C age of > 43 kyr.

The upper part of the Hitura sequence includes a number of diamictons interpreted as belonging to a single glacial depositional sequence recording glacier growth and decay. The uppermost fine-grained sediments (i.e. laminated sand-silt overlain by laminated clays, massive sand and then massive clay) were deposited in glacio-lacustrine and -marine environments during the Early Holocene.

## 6.2 Environmental reconstructions

### 6.2.1 Ruunaa (eastern Finland)

/Lunkka et al. 2008/ analysed a total of five samples for diatom frustules from the laminated clay-silt sediments. Count sums were very low with a total of 53 diatom frustules and 9 diatom fragments that could be identified. Most of the taxa that were identified are diatoms that are typical inhabitants of freshwater environments, and redeposited, marine diatom taxa are few. *Aulacoseira islandica* v. *helvetica* dominates the assemblage, and this taxon is interpreted as a typical inhabitant of relatively large glacio-lacustrine basins /Lunkka et al. 2008/.

A total of six samples from the laminated sediment were analysed for their pollen content. Overall, tree pollen percentages vary between 60–75%. The pollen assemblages are dominated by *Betula*, reaching values of 39–63%. Other tree-pollen that was encountered in the samples included *Pinus* (2–12%), *Alnus* (5–13%) and *Picea* (1–4%). NAP is dominated by *Artemisia* (9–24%) and grasses (2–5%), whereas the abundances of shrubs (e.g. *Betula nana*) and dwarf shrubs are low ( $\leq 4\%$ ). *Corylus* pollen was identified in one sample (4%).

/Lunkka et al. 2008/ note that since many of the pollen are clearly worn and probably reworked, they were most likely transported from the catchment area into the water basin. The authors do not reconstruct the vegetation or vegetation succession from the pollen, only stating that climatic conditions were relatively cold, possibly periglacial.

### 6.2.2 Hitura (western Finland)

Four diatom samples from laminated fine sand and four pollen samples from organic debris, in the lower fine-grained part of the deglacial sequence of early MIS 3 age at Hitura, were analyzed. A minimum count sum of 300 frustules and 300 terrestrial pollen was attempted /Salonen et al. 2008/.

The diatom composition, together with a common occurrence of *Aulacoseira islandica* resting spores, suggests a relatively shallow and cool freshwater environment /Salonen et al. 2008/. The laminated sediments are interpreted as being deposited in a glacial lake. The pollen assemblage, including pollen from deciduous trees like *Carpinus* and from *Larix*, suggests redeposition from Early Weichselian interstadial sediment /Salonen et al. 2008/.

## 7 Discussions

The Sokli record, together with the two records discussed in section 6, provide strong evidence for ice-free conditions in large parts of Finland during the early part of MIS 3. Of the three sites, Sokli and Hitura are located near centrally in relation to the LGM Fennoscandian Ice Sheet (Figure 6-1) whereas Ruunaa is situated more towards the east. The till-covered, deglacial sediment sequences of early MIS 3 age include laminated clay-silt or silt-fine sand sediments interpreted as being of glacio-lacustrine origin. These sediments grade into, or are overlain by, more sandy or sandy-gravelly sediments deposited in a shallow, isolated lake (Sokli, this study), in a littoral environment (Hitura /Salonen et al. 2008/) or in a fluvial environment (Ruunaa /Lunkka et al. 2008/).

### 7.1 Vegetation and climate in Finland during early MIS 3

Of the three sites, the most detailed paleo-ecological data is available for Sokli. The pollen and macrofossil data suggest the local presence of low-arctic shrub tundra vegetation throughout the deposition of the glacio-lacustrine and lacustrine sediments. High values of tree birch pollen (up to 30% of the total sum) in the lower part of the sediment sequence might be a reflection of local pockets of tree *Betula* present in sheltered spots in the Sokli area close to the retreating ice margin. This lower portion of the sequence apparently represents the warmest and moistest part (relatively high representation of spores from ferns (Polypodiaceae)) of the Sokli early MIS 3 sequence. This interpretation is consistent with the pattern of the Greenland millennium-scale Dansgaard-Oeschger interstadials in which abrupt warming is followed by a gradual cooling (Figure 7-1 /e.g. Dansgaard et al. 1993/).

The data from Sokli is in agreement with the pollen data obtained from the Ruunaa site. Although /Lunkka et al. 2008/ are rather cautious in the interpretation of the Ruunaa pollen data, stating that tree pollen might have been reworked from older sediments around the postulated glacio-lacustrine basin, high *Betula* values (up to 60%) suggest the presence of birch forest at this more southerly location. The relatively high percentages of *Artemisia* pollen in the Ruunaa sediments (9–24%) are used by /Lunkka et al. 2008/ to infer the presence of periglacial tundra vegetation. However, the *Artemisia* pollen might as well be a reflection of the open character of the birch forest just following the deglaciation of the area and/or the local presence of this heliophilous, pioneer element on sandy floodplains or dune fields close to the ice margin.

Interestingly, similar pollen assemblages as found at Ruunaa have been encountered in early MIS 3 sediments in a long core from Lake Yamozero (lat. 65°01'N, long. 50°14'E, elevation 213 m.a.s.l.) on the Timan ridge in northern Russia (Figure 6-1 /Henriksen et al. 2007/). Here, an up to 13 m thick sequence of laminated silt has been dated by ten quartz OSL dates (using the SAR protocol) and four infinite AMS <sup>14</sup>C dates (on mostly terrestrial macrofossils) to 42–74 kyr. Two intervals in the lower part of the silt sequence have yielded high pollen concentrations and birch pollen values of up to 45–50%, and finds of spruce stomata in the youngest of the two intervals suggest the local development of open birch forest with stands of spruce /Henriksen et al. 2007/. Yamozero is located outside all Weichselian glacial limits (Figures 1-3 and 6-1), and pollen assemblages from the remaining parts of the MIS 4-3 silt sequence suggest the development of steppe/desert vegetation with increased *Artemisia* and Chenopodiaceae at the expense of dwarf shrubs /Henriksen et al. 2007/.

An important argumentation for the cautious interpretation of the pollen data from the Ruunaa site by /Lunkka et al. 2008/ is that “it is generally accepted that the Middle Weichselian interstadials were tree-less in northwestern Europe /cf. Van Andel and Tzedakis 1996/”. Although records are more scarce from northeastern Europe, they strongly suggest the presence of trees during MIS 3, in accordance with the low-arctic tundra conditions and the proximity of the distributional limits of tree *Betula* and *Pinus* as inferred at Sokli, open birch forest at Ruunaa and open birch forest with spruce at Yamozero. Various sites in the Baltic countries south of Finland (Lithuania, Estonia, and Poland) suggest the presence of boreal forest, or taiga, with *Betula*, *Pinus*, and, in some cases, also *Picea* or *Larix*, during warm intervals early and late in MIS 3 /e.g. Gaigalas et al. 1992, Krzyszkowski et al.

1993, Satkūnas et al. 2003, Granoszewski 2003, Molodkov et al. 2007/. Furthermore, at Lake Nero in central Russia, north of Moscow (Figure 6-1), the presence of the boreal biome (with birch, pine and spruce) has been inferred for MIS 3 /Davydova and Servant-Vildary 1996, Huntley et al. 2003/.

Not only does the presence of trees in Finland during early MIS 3 contrast the inferred MIS 3 tree-less vegetation in northwestern and central Europe, the high, present-day summer temperatures that are consistently reconstructed from aquatic biota in the early MIS 3 sediments at Sokli are striking as well (e.g. Figure 7-1). At present, Sokli is within the northern boreal forest biome with pine and spruce. The absence of these trees during early MIS 3 might be controlled by local factors such as limited soil formation directly following deglaciation, winds from the nearby ice sheet and migrational lags. For instance, spruce is only part of the boreal forest at Sokli since the Late Holocene.

In agreement with the proxy-based climate reconstructions, the climate model simulation (Figure 5-5) suggests high mean July temperatures for the sector northeast of the Fennoscandian Ice Sheet. The high temperatures are attributed to high insolation in combination with dry winds blowing from the ice sheet. The new data reviewed in section 6 (see also Figure 7-2), however, indicate that the ice sheet extent used in the model set-up was too large, diminishing the role of the ice sheet on the recorded high temperatures.

It is notable that recent data from Sokli has revealed fossils of a variety of plants, which currently have considerably more southern distribution ranges, in the gyttja deposit of Early Weichselian (MIS 5c) age. This compelling evidence for summer temperatures at least 3°C higher than at present is related to contemporary orbital forcing /Väliranta et al. 2009/. Warmer-than-present summer temperatures have also been inferred at the high latitude site of Yamozero for the deposit of MIS 5a age /Henriksen et al. 2007/. Summer insolation at the latitudes of Sokli and Yamozero was not much lower during the Early Weichselian (MIS 5a and 5c) than during the Last Interglacial (MIS 5e /Berger and Loutre 1991/.

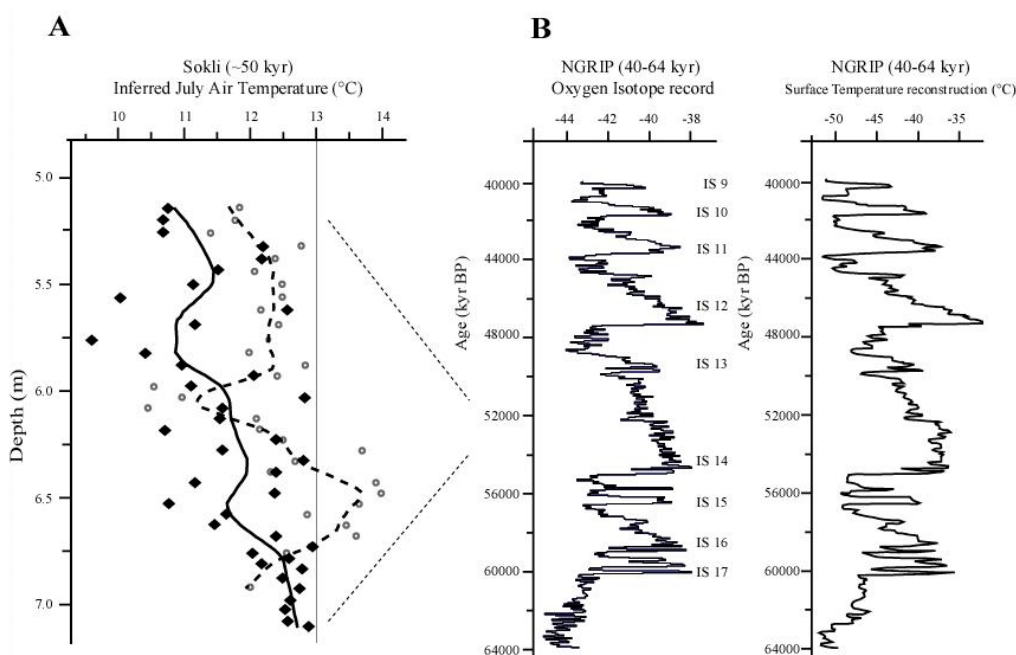


**Figure 7-1.** A) Terrestrial pollen- (black line) and chironomid (dashed line) – inferred mean July air temperatures for the early MIS 3 deposit at Sokli. Sample-specific prediction errors range between  $\pm 1.08$ – $1.22^{\circ}\text{C}$  for the chironomid-based values (see Figure 5-1) and  $\pm 1.22$ – $1.74^{\circ}\text{C}$  for the pollen-based values (Figure 5-2). The lines were produced by with a locally weighted scatterplot smoother (LOWESS, Figure 5-4 /Cleveland 1979/). Present-day mean July temperature of  $\sim 13^{\circ}\text{C}$  at Sokli is indicated for reference. B) Correlation with the NorthGRIP  $\delta^{18}\text{O}_{\text{ice}}$  record from Greenland (left panel /NorthGRIP-members 2004/) and surface temperatures (right panel /Huber et al. 2006/) for the time period 40–64 kyr plotted on the GRIP2001/ss09sea time scale; uncertainties in the temperature reconstruction are  $\sim \pm 3^{\circ}\text{C}$  /Huber et al. 2006). Greenland Interstadials (IS) are marked directly to the right of the oxygen-isotope curve.

## 7.2 Timing and duration of the early MIS 3 ice free interval in Finland

The multiple datings that have been performed at the Finnish sites indicate that the till-covered, deglacial sediment sequences are most probably of early MIS 3 age. Nevertheless, relatively large error limits on the OSL dates and problems related to the OSL method such as incomplete bleaching /Henriksen et al. 2007, Alexanderson et al. 2008, Lunkka et al. 2008, Salonen et al. 2008/, as well as uncertainties at the limit of the radiocarbon dating method and the lack of data for calibration of the radiocarbon ages in this time interval, preclude a precise dating. The dates that have been obtained at the Sokli, Ruunaa and Hitura sites indicate an age of around 50 kyr. Differences of up to several thousands of years between the ice cores from Greenland for the early MIS 3 interval /Johnsen et al. 2001/ furthermore hamper a precise correlation with the Greenland Interstadial (IS) sequence.

In the Greenland records, several interstadials are recognized during early MIS 3, of which IS 14 at about 50 or 55 kyr is the most prominent (Figure 7-1). Warm conditions during IS 14 lasted for about 2,500 years /Huber et al. 2006/. In the speleotherm record from the Austrian Alps, the prominent IS 14 is dated by high-precision U-series thermal ionization mass spectrometry dates to 54.5–52 kyr with uncertainties in the order of 0.1–0.3 kyr /Spötl et al. 2006/.

It can be argued that thinning and gradual retreat of the northeastern margin of the Fennoscandian Ice Sheet from its MIS 4 limit in Russia (Figure 6-1/Svendsen et al. 2004/) might have started during IS 16 in the earliest part of MIS 3, but that only the warming during IS 14 lasted long enough for the Sokli area to become deglaciaded and the dramatic Dansgaard-Oeschger warming event to be registered in the fossil record (see also Figure 7-1). The same argument can be applied to the Ruunaa and Hitura sites. Because of its northern location and therefore most delayed deglaciation, the Sokli site can be expected, however, to only record the younger part of the interstadial.

The early MIS 3 deglacial sequences preserved at Sokli, Ruunaa and Hitura only represent very brief time-windows in the geological record. Direct evidence is lacking to estimate the total time-span with ice free conditions at the sites before the deposition of the uppermost glacial deposits. The analysis of digital elevation data from the Sokli area (Figure 4-7) indicates that the ice margin only had to retreat some 20 km north of Sokli for the early MIS 3 glacial lake to be drained. It is possible that the ice margin remained relatively close to Sokli during deposition of the upper lacustrine sediments, and re-advanced shortly after, maintaining Sokli ice-covered for the remaining part of MIS 3–2. Based on ice-flow configuration, /Salonen et al. 2008/ noted that the till directly overlying the early MIS 3 sediments at Hitura could be correlated with the Jæren stadial at about 45–40 kyr /Lambeck et al. 2006/.

Nevertheless, /Salonen et al. 2008/ as well as /Lunkka et al. 2008/ conclude that the Hitura and Ruunaa areas probably remained ice-free for some 25 kyr to just before the Late Weichselian LGM advance. /Lunkka et al. 2008/ base this conclusion on a series of AMS  $^{14}\text{C}$  dates on mammoth bones from Finland by /Ukkonen et al. 1999/, which suggest that the area at the northern Gulf of Bothnia, north of Hitura, was still ice-free at ~ 33 kyr. However, recently dated mammoth teeth and bones from central Sweden have shown significant discrepancy between the apparent absence of glaciation in the central Swedish uplands and the Baltic basin from 40 to 30 kyr, as indicated by the mammoth data, versus glacial activity in the Baltic basin during the same time interval suggested by OSL-dated geological data from Denmark /Houmark-Nielsen and Kjær 2003, Houmark-Nielsen et al. 2005, Ukkonen et al. 2007/. A compilation of  $^{14}\text{C}$  dates for Sweden in the time range of MIS 3 has revealed that  $^{14}\text{C}$  dates on mammoth tusks and molars diverge in several cases from the age estimates assigned to organic deposits, which indicates that most, if not all  $^{14}\text{C}$  dates on mammoth remains are too young and should likely be regarded as unreliable /Wohlfarth 2009/.

It is notable that the late part of MIS 3 is on average colder than early MIS 3 both in the Greenland, North Atlantic deep-sea and European continental records /e.g. Johnsen et al. 2001, Bond et al. 1993, Henriksen et al. 2007/. This makes it plausible that large parts of Finland became glaciated again in late MIS 3 and remained covered by the Fennoscandian Ice Sheet until the deglaciation in the Early Holocene. Climate-model simulations for late MIS 3 (Greenland Stadial 12 at ~ 44 kyr), with a prescribed restricted MIS 3 Fennoscandian Ice Sheet, have produced a cold and dry climate /Kjellström et al. 2009/. The modelled climate in front of the ice sheet, however, does not exclude the possibility of a larger ice sheet. The global and regional models used in the simulation did not include dynamical modelling of ice sheets and thus an ice sheet cannot form in the models, even if the climate conditions are favourable for ice sheet growth /Kjellström et al. 2009/.

### 7.3 Configuration of the Fennoscandian Ice Sheet during early MIS 3

An extensive data base of geological sections and absolute age determinations (mostly AMS  $^{14}\text{C}$  dates) along the mountainous Norwegian coast has indicated rapid phases of ice retreat (reaching to inland areas) along the western margin of the Fennoscandian Ice Sheet during the late part of MIS 3 and MIS 2 /Olsen et al. 2001/. /Olsen et al. 2001/, however, note that the highly irregular mountainous terrain in Norway, with a densely dissected coastline and deeply incised fjords and valleys, is ideal for rapid ice growth and decay. As such, considerable ice-retreat along the Norwegian coast may therefore have occurred without a major contemporary ice retreat in the continental Baltic region.

In Figure 7-2, the inferred ice-free area at 30 kyr by /Olsen et al. 2001/ is used as the minimum extent of ice-free land along the Norwegian coast during the overall warmer early MIS 3. Based on the geological data reviewed in this report, we have additionally indicated the minimum extent of ice-free land in eastern Fennoscandia during early MIS 3.

Well-dated geological data for MIS 3 has not yet been published for Sweden. A recent study on long records from northern Sweden /Hättstrand 2008/ has presented two alternative chronological interpretations for the age of the sediments. In the first alternative, the till-covered sediment sequence is considered to be of Early Weichselian age. The second alternative places lacustrine sediments in the lower part of the sequence in the Early Weichselian (defined as the Tärendö I Interstadial), whereas those higher up in the sequence are correlated with the early part of MIS 3 (Tärendö II Interstadial).



**Figure 7-2.** Map showing the maximum extension of the Fennoscandian Ice Sheet at ~ 50 kyr. The extent of ice-free land along the Norwegian coast is according to /Olsen et al. 2001/ and corresponds to conditions inferred for the time interval at 30 kyr in the overall colder late MIS 3. Ice-free conditions in major part of Finland are indicated by the Sokli record and other Finnish records reviewed in this report. The ice configuration in Sweden is considered uncertain in the reconstruction.

The Tärendö II Interstadial sediments hold pollen assemblages with *Betula* pollen reaching values of up to 55% suggesting the local presence of birch trees. These pollen assemblages are interrupted by a phase with increased *Artemisia* and grass pollen values which is interpreted as representing arctic steppe vegetation. /Hättestrand 2008/ tentatively correlates the birch forest phases of the Tärendö II Interstadial with IS 14 and 12 in the Greenland record. Based on a bio-stratigraphic correlation with the records in Finland, we consider a MIS 3 age assignment for the Tärendö II Interstadial sediments, however, as unlikely. An MIS 3 age for the Tärendö II sediments would mean that open birch forest developed in northern Sweden, i.e. close to the mountains which served as centers of initial build-up and final decay of the Fennoscandian Ice Sheet, whereas shrub tundra vegetation covered the Sokli area to the east. We consider the conditions in northern Sweden during early MIS 3 as uncertain as long as the Tärendö sediments remain without absolute dating control.

Instead of ice-free conditions in northern Sweden during early MIS 3, one could also tentatively envision a remnant ice sheet in the Scandinavian mountains and east of the mountain range in Sweden, which could have allowed rapid build-up in the continental sector of the Fennoscandian Ice Sheet during late MIS 3 culminating into the LGM ice configuration /Kleman 2008/.

## Acknowledgements

The data on the MIS 3 deposit at Sokli presented in this report would not have been produced, interpreted and integrated without the help of the following persons whom I wish to thank for their great input and enthusiasm throughout the project: (placed in alphabetical order and according to institute) A. Berntsson, P. Kaislahti Tillman, K.N. Jansson, J. Risberg, S. Wastegård and B. Wohlfarth (Stockholm University, Sweden); H.J.B. Birks (University of Bergen, Norway and University College, London, UK); S.J.P. Bohncke, J.A.A. Bos, S. Engels, C.J. Van Meerbeeck and H. Renssen (Vrije Universiteit Amsterdam, Netherlands); S.J. Brooks (The Natural History Museum, London, UK); O. Heiri (Utrecht University, Netherlands); H. Seppä and J. Weckström (University of Helsinki, Finland). My special thanks also to J.O. Näslund (SKB) for the many fruitful discussions.

## References

- Alexanderson H, Eskola K O, Helmens K F, 2008.** Optical dating of a Late Quaternary sediment sequence from Sokli, northern Finland. *Geochronometria*, 32, pp 51–59.
- Anderberg A-L, 1994.** Atlas of seeds and small fruits of Northwest-European plant species with morphological descriptions. Part 4, Resedaceae – Umbelliferae. Stockholm: Swedish Museum of Natural History.
- Andersen B G, Mangerud J, 1989.** The last interglacial-glacial cycle in Fennoscandia. *Quaternary International*, 3/4, pp 21–29.
- Anderson N J, 2000.** Diatoms, temperature and climatic change. *European Journal of Phycology*, 35, pp 307–314.
- Barley E M, Walker I R, Kurek J, Cwynar L C, Mathewes R W, Gajewski K, Finney B P, 2006.** A northwest North American training set: distribution of freshwater midges in relation to air temperature and lake depth. *Journal of Paleolimnology*, 36, pp 295–314.
- Battarbee R W, 1986.** Diatom analysis. In: Berglund B E (ed.). *Handbook of Holocene palaeoecology and palaeohydrology*. Chichester: Wiley, 1986, pp 527–570.
- Bedford A, Jones R T, Lang B, Brooks S, Marshall J D, 2004.** A late-glacial chironomid record from Hawes Water, northwest England. *Journal of Quaternary Science*, 19, pp 281–290.
- Bennett K D, 1996.** Determination of the number of zones in a biostratigraphical sequence. *New Phytologist*, 132, pp 155–170.
- Berger A, Loutre M F, 1991.** Insolation values for the climate of the last 10 million years. *Quaternary Science Reviews*, 10, pp 297–317.
- Berggren G, 1969.** Atlas of seeds and small fruits of Northwest-European plant species with morphological descriptions. Part 2, Cyperaceae. Stockholm: Swedish Museum of Natural History.
- Berggren G, 1981.** Atlas of seeds and small fruits of Northwest-European plant species with morphological descriptions. Part 3, Salicaceae – Cruciferae. Stockholm: Swedish Museum of Natural History.
- Bergman J, Hammerlund D, Hannon G, Barnekow L, Wohlfarth B, 2005.** Deglacial vegetation succession and Holocene tree-limit dynamics in the Scandes Mountains, west-central Sweden: stratigraphic data compared to megafossil evidence. *Review of Palaeobotany and Palynology*, 134, pp 129–151.
- Bigler C, Hall R I, Renberg I, 2000.** A diatom-training set for palaeoclimatic inferences from lakes in northern Sweden. *Verhandlungen der Internationalen Vereinigung für Theoretische und Angewandte Limnologie*, 27, pp 1–9.
- Bigler C, Larocque I, Peglar S M, Birks H J B, Hall R I, 2002.** Quantitative multiproxy assessment of long-term patterns of Holocene environmental change from a small lake near Abisko, northern Sweden. *The Holocene*, 12, pp 481–496.
- Bigler C, Grahn E, Larocque I, Jeziorski A, Hall R I, 2003.** Holocene environmental change at lake Njulla (999 m.a.s.l.), northern Sweden: a comparison with four small nearby lakes along an altitudinal gradient. *Journal of Paleolimnology*, 29, pp 13–29.
- Birks H J B, 1968.** The identification of *Betula nana* pollen. *New Phytologist*, 67, pp 309–314.
- Birks H J B, Birks H H, 1980.** *Quaternary palaeoecology*. Edward Arnold, London.
- Birks H J B, Gordon A D, 1985.** *Numerical methods in quaternary pollen analysis*. London: Academic Press.
- Birks H J B, Line J M, Juggins S, Stevenson A C, ter Braak C J F, 1990.** Diatoms and pH reconstruction. *Philosophical Transactions of the Royal Society of London. Series B, Biological Sciences*, 327, pp 263–278.

- Birks H J B, 1995.** Quantitative palaeoenvironmental reconstructions. In: Maddy D, Brew J S (eds.). *Statistical modelling of quaternary science data*. Cambridge: Quaternary Research Association, (Technical Guide 5), 1995, pp 161–254.
- Birks H J B, 1998.** Numerical tools in palaeolimnology – progress, potentialities, and problems. *Journal of Paleolimnology*, 20, pp 307–322.
- Birks H H, 2000.** Aquatic macrophyte vegetation development in Kråkenes Lake, western Norway, during the late-glacial and early Holocene. *Journal of Paleolimnology*, 23, pp 7–19.
- Birks H H, Ammann B, 2000.** Two terrestrial records of rapid climatic change during the glacial-Holocene transition (14,000–9,000 calendar years BP) from Europe. *Proceedings of National Academy of Science*, 97, pp 1390–1394.
- Birks H J B, 2003.** Quantitative palaeoenvironmental reconstructions from Holocene biological data. In: Mackay A, Battarbee R W, Birks H J B, Oldfield F (eds.). *Global change in the Holocene*. London: Arnold, 2003, pp 107–123.
- Birks H J B, Seppä H, 2004.** Pollen-based reconstructions of late-Quaternary climate in Europe – progress, problems, and pitfalls. *Acta Palaeobotanica*, 44, pp 317–334.
- Birks H H, Birks H J B, 2006.** Multi-proxy studies in palaeolimnology. *Vegetation History and Archaeobotany*, 15, pp 235–251.
- Bjune A E, Birks H J B, Seppä H, 2004.** Holocene vegetation and climate history on a continental–oceanic transect in northern Fennoscandia based on pollen and plant macrofossils from lakes situated at or near the present tree-line. *Boreas*, 33, pp 211–223.
- Blackmore S, Steinmann J A J, Hoen P P, Punt W, 2003.** The Northwest European pollen flora, 65: Betulaceae and Corylaceae. *Review of Palaeobotany and Palynology*, 123, pp 71–98.
- Bond G, Broecker W, Johnsen S, McManus J, Labeyrie L, Jouzel J, Bonani G, 1993.** Correlations between climate records from North Atlantic sediments and Greenland ice. *Nature*, 365, pp 143–147.
- Bos J A A, Bohncke S J P, Janssen C R, 2006.** Lake-level fluctuations and small-scale vegetation patterns during the late glacial in the Netherlands. *Journal of Paleolimnology*, 35, pp 211–238.
- Bos J A A, Helmens K F, Bohncke S J P, Seppä H, Birks H J B, 2009.** Flora, vegetation, and climate at Sokli, north-eastern Fennoscandia, during the Weichselian Middle Pleniglacial. *Boreas*, 38, pp 335–348.
- Boulton G S, Dongelmans P, Punkari M, Broadgate M, 2001.** Palaeoglaciology of an ice sheet through a glacial cycle: the European ice sheet through the Weichselian. *Quaternary Science Reviews*, 20, pp 591–625.
- Brinkkemper O, Van Geel B, Wiegers J, 1987.** Palaeoecological study of a Middle Pleniglacial deposit from Tilligte, the Netherlands. *Review of Palaeobotany and Palynology*, 51, pp 235–269.
- Brodersen K P, Lindegaard C, 1999.** Mass occurrence and sporadic distribution of *Corynocera ambigua* Zetterstedt (Diptera, Chironomidae) in Danish lakes. Neo- and palaeolimnological records. *Journal of Paleolimnology*, 22, pp 41–52.
- Brooks S J, Birks H J B, 2000.** Chironomid-inferred Late-glacial air temperatures at Whitrig Bog, south-east Scotland. *Journal of Quaternary Science*, 15, pp 759–764.
- Brooks S J, Birks H J B, 2001.** Chironomid-inferred air temperatures from Lateglacial and Holocene sites in northwest Europe: progress and problems. *Quaternary Science Reviews*, 20, pp 1723–1741.
- Brooks S J, 2006.** Fossil midges (Diptera: Chironomidae) as palaeoclimatic indicators for the Eurasian region. *Quaternary Science Reviews*, 25, pp 1894–1910.
- Cappers R T J, 1993.** The identification of Potamogetonaceae fruits found in the Netherlands. *Acta Botanica Neerlandica*, 42, pp 447–460.
- Chappell J, Shackleton N J, 1986.** Oxygen isotopes and sea level. *Nature*, 324, pp 137–140.
- Cholnoky B J, 1968.** Die ökologie der Diatomeen in Binnengewässern. *Lehre*: Cramer.

- Cleve-Euler A, 1951–1955.** Die Diatomeen von Schweden und Finnland, Teil I–V. Kungliga Svenska Vetenskapsakademiens handlingar, Serie 4, band 2:1 (1951), band 3:3 (1952), band 4:1 (1953), band 4:5 (1953), band 5:4 (1955).
- Cleveland W S, 1979.** Robust locally weighted regression and smoothing scatterplots. *Journal of the American Statistical Association*, 74, pp 829–836.
- Corner G D, Yevzerov V Y, Kolka V V, Möller J, 1999.** Isolation basin stratigraphy and Holocene relative sea-level change at the Norwegian-Russian border north of Nikel, northwest Russia. *Boreas*, 28, pp 146–166.
- Cremer H, Van de Vijver B, 2006.** On *Pliocaeenicus costatus* (Bacillariophyceae) in Lake El'gytgyn, east Siberia. *European Journal of Phycology*, 41, pp 169–178.
- Cushing E J, 1964.** Redeposited pollen in Late-Wisconsin pollen spectra from east-central Minnesota. *American Journal of Science*, 262, pp 1075–1078.
- Dansgaard W, Johnsen S J, Clausen H B, Dahl-Jensen D, Gundestrup N S, Hammer C U, Hvidberg C S, Steffensen J P, Sveinbjörnsdóttir A E, Jouzel J, Bond G, 1993.** Evidence for general instability of past climate from a 250-kyr ice-core record. *Nature*, 364, pp 218–220.
- Davies S J, Metcalfe S E, Bernal-Brooks F, Chacón-Torres A, Farmer J G, MacKenzie A B, Newton A J, 2005.** Lake sediment record sensitivity of two hydrologically closed upland lakes in Mexico to human impact. *Ambio*, 34, pp 470–475.
- Davydova N N, Servant-Vildary S, 1996.** Late pleistocene and holocene history of the lakes in the Kola Peninsula, Karelia and the North-Western part of the East European plain. *Quaternary Science Reviews*, 15, pp 997–1012.
- Donner J, 1995.** *The Quaternary history of Scandinavia*. Cambridge: Cambridge University Press.
- Donner J, 1996.** The Early and Middle Weichselian interstadials in the central area of the Scandinavian glaciations. *Quaternary Science Reviews*, 15, pp 471–479.
- Douglas M S V, Smol J P, 1995.** Paleolimnological significance of observed distribution patterns of chrysophyte cysts in Arctic pond environments. *Journal of Paleolimnology*, 13, pp 1–5.
- Driesschaert E, 2005.** Climate change over the next millennia using LOVECLIM, a new Earth system model including the polar ice sheets. Ph. D. thesis. Université Catholique de Louvain-la-Neuve.
- Engels S, Bohncke S J P, Bos J A A, Brooks S J, Heiri O, Helmens K F, 2008.** Chironomid-based palaeotemperature estimates for northeast Finland during Oxygen Isotope Stage 3. *Journal of Palaeolimnology*, 40, pp 49–61.
- Fægri K, Iversen J, 1989.** *Textbook of pollen analysis*. 4th edition by Fægri, K, Kaland P E, Krzywinski K. Chichester: Wiley.
- Forsström L, 1990.** Occurrence of larch (*Larix*) in Fennoscandia during the Eemian interglacial and the Brørup interstadial according to pollen analytical data. *Boreas* 19, pp 241–248.
- Fuchs M, Straub J, Zöller L, 2005.** Residual luminescence signals of recent river flood sediments: a comparison between quartz and feldspar of fine- and coarse-grain sediments. *Ancient TL*, 23, pp 25–30.
- Gaigalas A, Serebryanny L, Valueva M, 1992.** Middle Valdaian forest environments at Birzai, northern Lithuania. *Boreas*, 21, pp 289–293.
- Godfrey-Smith D I, Huntley D J, Chen W-H, 1988.** Optical dating studies of quartz and feldspar sediment extracts. *Quaternary Science Reviews*, 7, pp 373–380.
- Granoszewski W, 2003.** Late Pleistocene vegetation history and climatic changes at Horoszki Duże, eastern Poland: a palaeobotanical study. *Acta Palaeobotanica Supplementum*, 4, pp 3–95.
- Grimm E C, 1991–2004.** TILIA, TILIA.GRAPH, and TGView. Springfield: Illinois State Museum, Research and Collections Center.
- Haapasaari M, 1988.** The oligotrophic heath vegetation of northern Fennoscandia and its zonation. *Acta Botanica Fennica*, 135.

- Hannon G, Gaillard M-J, 1997.** The plant macrofossil record of past lake-level changes. *Journal of Paleolimnology*, 18, pp 15–28.
- Hansen L, Funder S, Murray A S, Mejdahl V, 1999.** Luminescence dating of the last Weichselian glacier advance in East Greenland. *Quaternary Geochronology*, 18, pp 179–190.
- Haworth E Y, 1988.** Distribution of diatom taxa of the old genus *Melosira* (now mainly *Aulacoseira*) in Cumbrian waters. In: Round F E (ed.). *Algae and the aquatic environment*. Bristol: Biopress, 1988, pp 139–165.
- Heiri O, Lotter A F, Hausmann S, Kienast F, 2003a.** A chironomid-based Holocene summer air temperature reconstruction from the Swiss Alps. *Holocene*, 13, pp 477–484.
- Heiri O, Birks H J B, Brooks S J, Velle G, Willassen E, 2003b.** Effects of within-lake variability on fossil assemblages on quantitative chironomid-inferred temperature reconstructions. *Palaeogeography, Palaeoclimatology, Palaeoecology*, 199, pp 95–106.
- Heiri O, Ekrem T, Willassen E, 2004.** Larval head capsules of European *Micropsectra*, *Paratanytarsus* and *Tanytarsus* (Diptera: Chironomidae: Tanytarsini). Version 1.0.
- Heiri O, Lotter A F, 2005.** Holocene and Lateglacial summer temperature reconstruction in the Swiss Alps based on fossil assemblages of aquatic organisms: a review. *Boreas*, 34, pp 506–516.
- Heiri O, Millet L, 2005.** Reconstruction of Late Glacial summer temperatures from chironomid assemblages in Lac Lautrey (Jura, France). *Journal of Quaternary Science*, 20, pp 33–44.
- Helmens K F, Räsänen M E, Johansson P, Jungner H, Korjonen K, 2000.** The last interglacial-glacial cycle in NE Fennoscandia: a nearly continuous record from Sokli (Finnish Lapland). *Quaternary Science Reviews*, 19, pp 1605–1623.
- Helmens K F, Johansson P W, Räsänen M E, Alexanderson H, Eskola K O, 2007a.** Ice-free intervals continuing into Marine Isotope Stage 3 at Sokli in the central area of the Fennoscandian glaciations. *Bulletin of the Geological Society of Finland*, 79, pp 17–39.
- Helmens K F, Bos J A A, Engels S, Van Meerbeek C J, Bohncke S J P, Renssen H, Heiri O, Brooks S J, Seppä H, Birks H J B, Wohlfarth B, 2007b.** Present-day temperatures in northern Scandinavia during the last glaciation. *Geology*, 35, pp 987–990.
- Helmens K F, Risberg J, Jansson K N, Weckström J, Berntsson A, Tillman P K, Johansson P W, Wastegård S, 2009.** Early MIS 3 glacial lake evolution, ice-marginal retreat pattern and climate at Sokli (northeastern Fennoscandia). *Quaternary Science Reviews*, 28, pp 1880–1894.
- Helmens K F, Engels S (in revision).** Ice-free conditions during early Marine Isotope Stage 3: lacustrine records from eastern Fennoscandia. *Boreas*.
- Henriksen M, Mangerud J, Matiouchkov A, Murray A S, Paus A, Svendsen J I, 2007.** Intriguing climatic shifts in a 90 kyr old lake record from northern Russia. *Boreas*, 37, pp 20–37.
- Hill M O, 1973.** Diversity and evenness: a unifying notation and its consequences. *Ecology*, 54, pp 427–432.
- Hirvas H, 1991.** Pleistocene stratigraphy of Finnish Lapland. Geological Survey of Finland, Bulletin 354.
- Houmark-Nielsen M, Kjær K H, 2003.** Southwest Scandinavia, 40–15 kyr BP: palaeogeography and environmental change. *Journal of Quaternary Science*, 18, pp 1–18.
- Houmark-Nielsen M, Krüger J, Kjær K H, 2005.** De seneste 150.000 år i Danmark. *Geovidenskab – Geologi og geografi*, 2, pp 1–20.
- Huber C, Leuenberger M, Spahni R, Flückiger J, Schwander J, Stocker T F, Johnsen S, Landais A, Jouzel J, 2006.** Isotope calibrated Greenland temperature record over marine Isotope Stage 3 and its relation to CH<sub>4</sub>. *Earth and Planetary Science Letters* 243, pp 504–519.
- Huntley B, Alfano M J, Allen J R M, Pollard D, Tzedakis P C, de Beaulieu J-L, Gröger E, Watts B, 2003.** European vegetation during Marine Oxygen Isotope Stage-3. *Quaternary Research* 59, pp 195–212.

- Hyvärinen H, 1975.** Absolute and relative pollen diagrams from northernmost Fennoscandia. *Fennia*, 142, pp 1–23.
- Hättestrand M, 2008.** Vegetation and climate during Weichselian ice free intervals in northern Sweden. *Dissertations from the Department of Physical Geography and Quaternary Geology (Stockholm university)*, 15.
- Hättestrand C, Clark C D, 2006.** Reconstructing the pattern and style of deglaciation of Kola Peninsula, NE Fennoscandian Ice Sheet. In: Knight P G (ed.). *Glaciology and Earth's Changing Environment*. Oxford: Blackwell, 2006, pp 199–201.
- Ilyashuk E A, Ilyashuk B P, Hammarlund D, Larocque I, 2005.** Holocene climatic and environmental changes inferred from midge records (Diptera: Chironomidae, Chaoboridae, Ceratopogonidae) at Lake Berkut, southern Kola Peninsula, Russia. *Holocene*, 15, pp 897–914.
- Iivonen E, 1973.** Eem-Kerrostuma Savukosken Soklilla. *Geologi*, 25, pp 81–84.
- Jansson K N, 2003.** Early Holocene glacial lakes and ice marginal retreat pattern in Labrador/Ungava, Canada. *Palaeogeography, Palaeoclimatology, Palaeoecology*, 193, pp 473–501.
- Johansson P W, 1995.** The deglaciation in the eastern part of the Weichselian ice divide in Finnish Lapland. *Geological Survey of Finland, Bulletin* 383.
- Johansson P W, Kujansuu R, 2005.** Deglasiatio. In: Johansson P W, Kujansuu R (eds.). *Pohjois-Suomen maaperä: maaperäkartojen 1:400 000 selitys*. Espoo: Geologian tutkimuskeskus, 2005, pp 149–156.
- Johansson P W, 2007.** Weichselian and Saalian esker systems in north Finland. *INQUA 2007 abstracts. Quaternary International*, 167–168 (Supplement), p 195.
- Johnsen S J, Clausen H B, Dansgaard W, Fuhrer K, Gundestrup N, Hammer C U, Iversen P, Jouzel J, Stauffer B, Steffensen J P, 1992.** Irregular glacial interstadials recorded in a new Greenland ice core. *Nature*, 359, pp 311–313.
- Johnsen S J, Dahl-Jensen D, Gundestrup N, Steffensen J P, Clausen H B, Miller H, Masson-Delmotte V, Sveinbjörnsdóttir A E, White J, 2001.** Oxygen isotope and palaeotemperature records from six Greenland ice-core stations: Camp Century, Dye-3, GRIP, GISP2, Renland and NorthGRIP. *Journal of Quaternary Science*, 16, pp 299–307.
- Jones V J, Birks H J B, 2004.** Lake-sediment records of recent environmental change on Svalbard: results of diatom analysis. *Journal of Paleolimnology*, 31, pp 445–466.
- Juggins S, 2003.** C2 user guide. Software for ecological and palaeoecological data analysis and visualisation. Newcastle upon Tyne: University of Newcastle.
- Juggins S, 2007.** C2 Version 1.5 User guide. Software for ecological and palaeoecological data analysis and visualisation. Newcastle upon Tyne: Newcastle University.
- Khursevich G K, 1994.** Morphology and taxonomy of some centric diatom species from the miocenen sediments of the Dzhilinda nad Tunkin hollows. In: Kociolek J P (ed.). *Proceedings of the 11th International Diatom Symposium*. San Francisco: California Academy of Sciences, pp 269–280.
- Kienel U, Siegert C, Hahne J, 1999.** Late Quaternary palaeoenvironmental reconstructions from a permafrost sequence (North Siberian Lowland, SE Taymyr Peninsula) – a multidisciplinary case study. *Boreas*, 28, pp 181–193.
- Kjellström E, Brandefelt J, Näslund J-O, Smith B, Strandberg G, Wohlfarth B, 2009.** Climate conditions in Sweden in a 100,000-year time perspective. SKB TR-09-04, Svensk Kärnbränslehantering AB.
- Kleman J, Hättestrand C, Borgström I, Stroeven A, 1997.** Fennoscandian palaeoglaciology reconstructed using a glacial geological inversion model. *Journal of Glaciology*, 43, pp 283–299.
- Kleman J, Hättestrand C, Clarhäll A, 1999.** Zooming in on frozen-bed patches: scale-dependent controls on Fennoscandian ice sheet basal thermal zonation. *Annals of Glaciology*, 28, pp 189–194.

- Kleman J, 2008.** The elusive MIS 3 ice sheet extents – geomorphological constraints, glaciological reasoning and research strategies. In: Näslund J-O, Wohlfarth B (eds.). Fennoscandian paleo-environment and ice sheet dynamics during Marine Isotope Stage (MIS) 3. 2008, pp 19–20. SKB R-08-79, Svensk Kärnbränslehantering AB.
- Kolstrup E, 1980.** Climate and stratigraphy in Northwestern Europe between 30,000 BP and 13,000 BP, with special reference to the Netherlands. Mededelingen van de Rijks Geologische Dienst, 32, pp 181–253.
- Kolstrup E, 1982.** Late-glacial pollen diagrams from Hjelm and Draved Mose (Denmark) with a suggestion of the possibility of drought during the Earlier Dryas. Review of Palaeobotany and Palynology, 36, pp 35–63.
- Korhola A, Tikkanen M, 1996.** The early postglacial history of Lake Sirkkajärvi, southern Finland, with implications to the “G stage” of the Baltic. Geografiska annaler, 78A, pp 235–245.
- Korhola A, Weckström J, Nyman M, 1999.** Predicting the long-term acidification trends in small subarctic lakes using diatoms. Journal of Applied Ecology, 36, pp 1021–1035.
- Korhola A, Weckström J, 2004.** Paleolimnological studies in Arctic Fennoscandia and the Kola Peninsula (Russia). In: Pienitz R, Douglas M S V, Smol J P (eds.). Long-term environmental change in Arctic and Antarctic lakes, Vol. 8. Dordrecht: Springer, 2004, pp 381–418.
- Korpela K, 1969.** Die Weichsel-eiszeit und ihr Interstadial in Peräpohjola (nördliches Nordfinnland) im Licht von submoränen Sedimenten. Annales Academiae Scientiarum Fennicae A. III, 99, pp 1–108.
- Krammer K, Lange-Bertalot H, 1986.** Bacillariophyceae 1. Teil Naviculaceae. In: Ettl H, Gerloff J, Heynig H, Mollenhauser D (eds.). Süßwasserflora von Mitteleuropa. Bd 2/1. Stuttgart: Fischer.
- Krammer K, Lange-Bertalot H, 1988.** Bacillariophyceae 2. Teil Bacillariaceae, Epithemiaceae, Surirellaceae. In: Ettl H, Gerloff J, Heynig H, Mollenhauser D (eds.). Süßwasserflora von Mitteleuropa. Bd 2/2. Stuttgart: Fischer.
- Krammer K, Lange-Bertalot H, 1991a.** Bacillariophyceae 3. Teil Centrales, Fragilariaceae, Eunotiaceae. In: Ettl H, Gerloff J, Heynig H, Mollenhauser D (eds.). Süßwasserflora von Mitteleuropa. Bd 2/3. Stuttgart: Fischer.
- Krammer K, Lange-Bertalot H, 1991b.** Bacillariophyceae 4. Teil Achnanthaceae. Kritische Ergänzungen zu Navicula (Lineolate) und Gomphonema. In: Ettl H, Gerloff J, Heynig H, Mollenhauser D (eds.). Süßwasserflora von Mitteleuropa. Bd 2/4. Stuttgart: Fischer.
- Krzyszowski D, Balwierz Z, Pyszyński W, 1993.** Aspects of Weichselian Middle Pleniglacial stratigraphy and vegetation in central Poland. Geologie en Mijnbouw, 72, pp 131–142.
- Kujansuu R, Eriksson B, Grönlund T, 1998.** Lake Inarijärvi, northern Finland: sedimentation and late quaternary evolution. Geological Survey of Finland, Report of Investigation 143.
- Körber-Grohne U, 1964.** Bestimmungsschlüssel für subfossile Juncus-Samen und Gramineen-Früchte. Probleme der Küstenforschung im Südlichen Nordseegebiet, 7, pp 1–47.
- Körber-Grohne U, 1991.** Bestimmungsschlüssel für subfossile Gramineen-Früchte. Probleme der Küstenforschung im Südlichen Nordseegebiet, 18, pp 169–234.
- Lagerbäck R, 1988.** The Veiki moraines in northern Sweden – widespread evidence of an Early Weichselian deglaciation. Boreas 17(4): 469–486.
- Lagerbäck R, Robertsson A-M, 1988.** Kettle holes – stratigraphical archives for Weichselian geology and palaeo-environment in northernmost Sweden. Boreas, 17, pp 439–468.
- Laing T E, Pienitz R, Smol J P, 1999.** Freshwater diatom assemblages from 23 lakes located near Norilsk, Siberia: a comparison with assemblages from other circumpolar treeline regions. Diatom Research, 14, pp 285–305.
- Lambeck K, Purcell A, Funder S, Kjær K H, Larsen E, Möller P, 2006.** Constraints on the Late Saalian to early Middle Weichselian ice sheet of Eurasia from field data and rebound modelling. Boreas, 35, pp 539–575.

- Larocque I, Hall R I, 2003.** Chironomids as quantitative indicators of mean July air temperature: validation by comparison with century-long meteorological records from northern Sweden. *Journal of Paleolimnology*, 29, pp 475–493.
- Linsley B K, 1996.** Oxygen-isotope record of sea level and climate variations in the Sulu Sea over the past 150,000 years. *Nature*, 380, pp 234–237.
- Livingstone D M, Lotter A F, 1998.** The relationship between air and water temperatures in lakes of the Swiss Plateau: a case study with palaeolimnological implications. *Journal of Paleolimnology*, 19, pp 181–198.
- Lotter A F, Juggins S, 1991.** POLPROF, TRAN and ZONE: programs for plotting, editing and zoning pollen and diatom data. Inqua-Subcommission for the study of the Holocene, Working Group on Data-Handling Methods, Newsletter 6, pp 4–6.
- Lotter A F, Pienitz R, Schmidt R, 1999.** Diatoms as indicators of environmental change near arctic and alpine treeline. In: Stoemer E F, Smol J P (eds.). *The diatoms: applications for the environmental and earth sciences*. Cambridge: Cambridge University Press, 1999, pp 205–226.
- Lundqvist J, 1992.** Glacial stratigraphy in Sweden. Geological Survey of Finland, Special Paper 15, pp 43–59.
- Lunkka J P, Murray A, Korpela K, 2008.** Weichselian sediment succession at Ruunaa, Finland, indicating a Mid-Weichselian ice-free interstadial in eastern Fennoscandia. *Boreas*, 37, pp 234–244.
- Magny M, Aalbersberg G, Bégeot C, Benoit-Ruffaldi P, Bossuet G, Disnar J R, Heiri O, Laggoun-Defarge F, Mazier F, Millet L, Peyron O, Vanni re B, Walter-Simonnet A V, 2006.** Environmental and climatic changes in the Jura mountains (eastern France) during the Lateglacial-Holocene transition: a multi-proxy record from Lake Lautrey. *Quaternary Science Reviews*, 25, pp 414–445.
- Makarchenko E A, Makarchenko M A, 1999.** Chironomidae. In: Tsalolikhin S J (ed.). *Key to freshwater invertebrates of Russia and adjacent lands*. St. Petersburg: Zoological Institute RAS, pp 670–857.
- Mangerud J, 1991.** The Scandinavian ice sheet through the last interglacial/glacial cycle. In: Frenzel B (ed.). *Klimageschichtliche Probleme der letzten 130000 Jahre*. Stuttgart: Fischer, 1991, pp 307–330.
- Martinson D G, Pisias W G, Hays J D, Imbrie J, Moore T C Jr, Shackleton N J, 1987.** Age dating of the orbital theory of the ice ages: development of a high-resolution 0 to 300,000-year chronostratigraphy. *Quaternary Research*, 27, pp 1–29.
- Moen A, 1999.** National Atlas of Norway: vegetation. H nefoss: Norwegian Mapping Authority.
- Moller Pillot H K M, 1984.** De larven der nederlandse Chironomidae (Diptera) (Inleiding, Tanypodinae & Chironomini). *Nederlandse Faunistische Mededelingen*, 1A.
- Molodkov A, Bolikhovskaya N, Miidel A, Ploom K, 2007.** The sedimentary sequence recovered from the Voka outcrops, northeastern Estonia: implications for late Pleistocene stratigraphy. *Estonian Journal of Earth Science*, 56, pp 47–62.
- Moore P D, Webb J A, Collinson M E, 1991.** *Pollen analysis*. 2nd ed. Oxford: Blackwell Scientific.
- Murray A S, Wintle A G, 2000.** Luminescence dating of quartz using an improved single-aliquot regenerative-dose protocol. *Radiation Measurements*, 32, pp 57–73.
- Murray A S, Olley J M, 2002.** Precision and accuracy in the optically stimulated luminescence dating of sedimentary quartz: a status review. *Geochronometria*, 21, pp 1–17.
- Murray A S, Wintle A G, 2003.** The single aliquot regenerative dose protocol: potential for improvements in reliability. *Radiation Measurements*, 37, pp 377–381.
- M kel  E M, 1996.** Size distinctions between *Betula* pollen types – a review. *Grana*, 35, pp 248–256.

- Mölder K, Tynni R, 1967–1973.** Über Finnlands rezente und subfossile Diatomeen I–VI. *Comptes Rendus de la Société géologique de Finlande* N:o XXXIX, pp 199–217 (1967), Geological Society of Finland, Bulletin 40, pp 151–170 (1968), Bulletin 41, pp 235–251 (1969), Bulletin 42, pp 129–144 (1970), Bulletin 43, pp 203–220 (1971), Bulletin 44, pp 141–149 (1972), Bulletin 45, pp 159–179 (1973).
- Niemelä J, Tynni J, 1979.** Interglacial and interstadial sediments in the Pohjanmaa region, Finland. Geological Survey of Finland, Bulletin 302.
- North Greenland Ice Core Project members, 2004.** High-resolution record of Northern Hemisphere climate extending into the last interglacial record. *Nature*, 431, pp 147–151.
- Oberdorfer E. 1994.** Pflanzensoziologische Exkursionsflora. 7. Auflage. Stuttgart: Ulmer.
- Oksanen L, Virtanen R, 1995.** Topographic, altitudinal, and regional patterns in continental and suboceanic heath vegetation of northern Fennoscandia. *Acta Botanica Fennica*, 153, pp 1–80.
- Oliver D R, Roussel M E, 1983.** The insects and arachnids of Canada. Part 11. The genera of larval midges of Canada. Diptera: Chironomidae. Ottawa: Agriculture Canada.
- Olsen L, Sveian H, Bergström B, 2001.** Rapid adjustments of the western part of the Scandinavian Ice Sheet during the Mid and Late Weichselian – a new model. *Norsk Geologisk Tidsskrift*, 81, pp 93–118.
- Philibert A, Praire Y, 2002.** Is the introduction of benthic species necessary for open-water chemical reconstruction in diatom-based transfer functions? *Canadian Journal of Fisheries and Aquatic Sciences*, 59, pp 938–951.
- Prentice I C, 1978.** Modern pollen spectra from lake sediments in Finland and Finnmark, north Norway. *Boreas*, 7, pp 131–153.
- Påsse T, Robertsson A-M, Miller U, Klingberg F, 1988.** A late Pleistocene sequence at Margreteberg, southwestern Sweden. *Boreas*, 17, pp 141–163.
- Rieradevall M, Brooks S J, 2001.** An identification guide to subfossil Tanypodinae larvae (Insecta: Diptera: Chironomidae) based on cephalic setation. *Journal of Paleolimnology*, 25, pp 81–99.
- Risberg J, Sandgren P, Andrén E, 1996.** Early Holocene shore displacement and evidence of irregular isostatic uplift northwest of Lake Vänern, western Sweden. *Journal of Paleolimnology*, 15, pp 47–63.
- Roche D M, Dokken T M, Goosse H, Renssen H, Weber S L, 2006.** Climate of the last glacial maximum: sensitivity studies and model-data comparison with the LOVECLIM coupled model: *Climate of the Past Discussions*, 2, pp 1105–1153.
- Round F E, Håkansson H, 1992.** Cyclotelloid species from a diatomite in the Harz Mountains, Germany, including *Pliocaenicus* gen. nov. *Diatom Research*, 7, pp 109–125.
- Rühland K, Smol J P, Pienitz R, 2003.** Ecology and spatial distributions of surface-sediment diatoms from 77 lakes in the subarctic Canadian treeline region. *Canadian Journal of Botany*, 81, pp 57–73.
- Salonen V-P, Kaakinen A, Kultti S, Miettinen A, Eskola K O, Lunkka J P, 2008.** Middle Weichselian glacial event in the central part of the Scandinavian Ice Sheet recorded in the Hitura pit, Ostrobothnia, Finland. *Boreas*, 37, pp 38–54.
- Satkunas J, Grigriemė A, Velichkevich F, Robertsson A-M, Sandgren P, 2003.** Upper Pleistocene stratigraphy at the Medininkai site, eastern Lithuania: a continuous record of the Eemian–Weichselian sequence. *Boreas*, 32, pp 627–641.
- Schmid P E, 1993.** A key to the larval Chironomidae and their instars from Austrian danube region streams and rivers with particular reference to a numerical taxonomic approach. Part I. Diamesinae, Prodiamesinae and Orthoclaadiinae. *Wasser und Abwasser Supplement* 3/93.
- Selby K A, O'Brien C E, Brown A G, Stuijts I, 2005.** A multi-proxy study of Holocene lake development, lake settlement and vegetation history in central Ireland. *Journal of Quaternary Science*, 20, pp 147–168.

- Seppä H, Weckström J, 1999.** Holocene vegetational and limnological changes in the Fennoscandian tree-line area as documented by pollen and diatom records from Lake Tsuolbmajavri, Finland. *Ecoscience*, 6, pp 621–635.
- Seppä H, Birks H J B, 2001.** July mean temperature and annual precipitation trends during the Holocene in the Fennoscandian tree-line area: pollen-based climate reconstructions. *The Holocene*, 11, pp 527–539.
- Seppä H, Nyman M, Korhola A, Weckström J, 2002.** Changes of tree-lines and alpine vegetation in relation to post-glacial climate dynamics in northern Fennoscandia based on pollen and chironomid records. *Journal of Quaternary Science*, 17, pp 287–301.
- Seppä H, Birks H J B, Odland A, Poska A, Veski S, 2004.** Modern pollen-climate calibration set from northern Europe: developing and testing a tool for palaeoclimatological reconstructions. *Journal of Biogeography*, 31, pp 251–267.
- Shackleton N J, 1987.** Oxygen isotopes, ice volume and sea level. *Quaternary Science Reviews*, 6, pp 183–190.
- Sirocko K, Seelos K, Schaber K, Rein B, Dreher F, Diehl M, Lehne R, Jäger K, Krbetschek M, Degering D, 2005.** A late Eemian aridity pulse in central Europe during the last glacial inception. *Nature*, 436, pp 833–836.
- Siver P A, Kling H, 1997.** Morphological observations of *Aulacoseira* using scanning electron microscopy. *Canadian Journal of Botany*, 75, pp 1807–1835.
- Spötl C, Mangini A, Richards D A, 2006.** Chronology and paleoenvironment of Marine Isotope Stage 3 from two high-elevation speleothems, Austrian Alps. *Quaternary Science Reviews*, 25, pp 1127–1136.
- Stachura-Suchples K, Khursevich G, 2007.** On the genus *Pliocaenicus* Round and Håkansson (Bacillariophyceae) from the northern hemisphere. In: Kusber W-H Jahn R. (eds.). *Proceedings of the 1<sup>st</sup> Central European Diatom Meeting 2007*. Berlin: BGBM, 2007, pp 155–158.
- Svendsen J I, Alexanderson H, Astakhov V I, Demidov I, Dowdeswell J A, Funder S, Gataullin V, Henriksen M, Hjort C, Houmark-Nielsen M, Hubberten H W, Ingolfsson O, Jakobsson M, Kjær K H, Larsen E, Lokrantz H, Lunkka J P, Lysa A, Mangerud J, Matiouchkov A, Murray A, Möller P, Niessen F, Nikolskaya O, Polyak L, Saarnisto M, Siegert C, Siegert M J, Spielhagen R F, Stein R. 2004.** Late Quaternary ice sheet history of northern Eurasia. *Quaternary Science Reviews*, 23, pp 1229–1271.
- ter Braak C J F, Juggins S, 1993.** Weighted averaging partial least squares regression (WA-PLS): an improved method for reconstructing environmental variables from species assemblages. *Hydrobiologia*, 269–270, pp 485–502.
- ter Braak C J F, Šmilauer P, 1998.** *CANOCO reference manual and user's guide to Canoco for Windows*. Wageningen: Centre for Biometry.
- Terasmäe J, 1951.** On the pollen morphology of *Betula nana*. *Svensk botanisk tidskrift*, 45, pp 358–361.
- Tynni R, 1975–1980.** Über Finnlands rezente und subfossile Diatomeen VIII–XI. *Geological Survey of Finland, Bulletin 274 (1975), Bulletin 284 (1976), Bulletin 296 (1978), Bulletin 312 (1980)*.
- Tynni R, 1982.** The reflection of geological evolution in Tertiary and interglacial diatoms and silicoflagellates in Finnish Lapland. *Geological Survey of Finland, Bulletin 320*.
- Ukkonen P, Lunkka J P, Jungner H, Donner J, 1999.** New radiocarbon dates from Finnish mammoths indicating large ice-free areas in Fennoscandia during the Middle Weichselian. *Journal of Quaternary Science*, 14, pp 711–714.
- Ukkonen P, Arppe L, Houmark-Nielsen M, Kjær K H, Karhu J A, 2007.** MIS 3 mammoth remains from Sweden-implications for faunal history, palaeoclimate and glaciation history. *Quaternary Science Reviews*, 26, pp 3081–3098.

- Usinger H, 1977.** Bölling-Interstadials und Laacher Bimstuff in einem neuen Spätglazial-profil aus dem Vallensgård Mose/Bornholm. Mit pollen-größenstatistischer Trennung der Birken. *Danmark Geologiske Undersøgelse, Årbog 1977*, pp 5–29.
- Van Andel T H, Tzedaskis P C, 1996.** Palaeolithic landscapes of Europe and environs, 150,000–25,000 years ago: an overview. *Quaternary Science Reviews*, 15, pp 481–500.
- van der Meijden R, 2005.** Heukels' flora van Nederland. Groningen: Wolters-Noordhoff.
- van Geel B, Hallewas D P, Pals J P, 1983.** A Late Holocene deposit under the Westfriese dijk near Enkhuizen (Prov. of Noord-Holland, The Netherlands): palaeoecological and archaeological aspects. *Review of Palaeobotany and Palynology*, 38, pp 269–335.
- van Geel B, Coope G R, van der Hammen T, 1989.** Palaeoecology and stratigraphy of the Lateglacial type section at Usselo (The Netherlands). *Review of Palaeobotany and Palynology*, 60, pp 25–129.
- Vartiainen H, 1980.** The petrography, mineralogy and petrochemistry of the Sokli carbonatite massif, northern Finland. *Geological Survey of Finland, Bulletin 313*.
- Velle G, Brooks S J, Birks H J B, Willassen E, 2005.** Chironomids as a tool for inferring Holocene climate: an assessment based on six sites in southern Scandinavia. *Quaternary Science Reviews*, 24, pp 1429–1462.
- Väliranta M, 2006.** Terrestrial plant macrofossil records; possible indicators of past lake-level fluctuations in north-eastern European Russia and Finnish Lapland? *Acta Palaeobotanica*, 46, pp 235–243.
- Väliranta M, Birks H H, Helmens K F, Engels S, Piirainen M, 2009.** Early Weichselian interstadial (MIS 5c) summer temperatures were higher than today in northern Fennoscandia. *Quaternary Science Reviews*, 28, pp 777–782.
- Walker I R, Smol J P, Engstrom D R, Birks H J B, 1991.** An assessment of Chironomidae as quantitative indicators of past climatic change. *Canadian Journal of Fisheries and Aquatic Sciences*, 48, pp 975–987.
- Walker M J C, Coope G R, Sheldrick C, Turney C S M, Lowe J J, Blockley S P E, Harkness D D, 2003.** Devensian Lateglacial environmental changes in Britain: a multi-proxy record from Llanilid, South Wales, UK. *Quaternary Science Reviews*, 22, pp 475–520.
- Walker I R, Cwynar L C, 2006.** Midges and palaeotemperature reconstruction – the North American experience. *Quaternary Science Reviews*, 25, pp 1911–1925.
- Wallinga J, 2002.** Optically stimulated luminescence dating of fluvial deposits: a review. *Boreas*, 31, pp 303–322.
- Wastegård S, Rasmussen T L, Kuijpers A, Nielsen T, van Weering T C E, 2006.** Composition and origin of ash zones from Marine Isotope Stages 3 and 2 in the North Atlantic. *Quaternary Science Reviews*, 25, pp 2409–2419.
- Weckström J, Korhola A, Blom T, 1997a.** The relationship between diatoms and water temperature in thirty subarctic Fennoscandian lakes. *Arctic and Alpine Research*, 29, pp 75–92.
- Weckström J, Korhola A, Blom T, 1997b.** Diatoms as quantitative indicators of pH and water temperature in subarctic Fennoscandian lakes. *Hydrobiologia*, 347, pp 171–184.
- Weckström J, Korhola A, 2001.** Patterns in the distribution, composition and diversity of diatom assemblages in relation to ecoclimatic factors in Arctic Lapland. *Journal of Biogeography*, 28, pp 31–45.
- Weckström J, Snyder J A, Korhola A, Laing T E, MacDonald G M, 2003.** Diatom inferred acidity history of 32 lakes on the Kola Peninsula, Russia. *Water, Air, and Soil Pollution*, 149, pp 339–361.
- Weckström J, Korhola A, Erästö P, Holmström L, 2006.** Temperature patterns over the past eight centuries in northern Fennoscandia inferred from sedimentary diatoms. *Quaternary Research*, 66, pp 78–86.

- Weeda E J, Westra J, Westra C, Westra T, 1987.** Nederlandse oecologische flora: wilde planten en hun relaties 2. Deventer: de Lange/Van Leer.
- Weeda E J, Westra J, Westra C, Westra T, 1994.** Nederlandse oecologische flora: wilde planten en hun relaties 5. Eindhoven: Lecturis BV.
- Whitmore T J, 1989.** Florida diatom assemblages as indicators of trophic state and pH. *Limnology and Oceanography*, 34, pp 882–895.
- Wiederholm T (ed), 1983.** Chironomidae of the Holarctic region. Keys and diagnoses. Part I. Larvae. *Entomologica Scandinavica*, Supplement, 19.
- Wohlfarth B, Veres D, Ampel L, Lacourse T, Blaauw M, Andrieu-Ponel V, Kéravis D, Lallier-Vergès E, Björck S, Davies S M, de Beaulieu J-L, Risberg J, Hormes A, Kasper H U, Possnert G, Reille M, Thouveny N, Zander A, 2008.** Rapid ecosystem response to abrupt climate changes during the last glacial period in western Europe, 40–16 ka. *Geology*, 36, pp 407–410.
- Wohlfarth B, 2009.** Ice-free conditions in Fennoscandia during Marine Oxygen Isotope Stage 3? SKB TR-09-12, Svensk Kärnbränslehantering AB.
- Økland K A, Økland J, 2000.** Freshwater bryozoans (Bryozoa) of Norway: distribution and ecology of *Cristatella mucedo* and *Paludicella articulata*. *Hydrobiologia*, 421, pp 1–24.
- Økland K A, Økland J, 2001.** Freshwater bryozoans (Bryozoa) of Norway II: distribution and ecology of two species of *Fredericella*. *Hydrobiologia*, 459, pp 103–123.
- Økland K A, Økland J, 2005.** Freshwater bryozoans (Bryozoa) of Norway V: review and comparative discussion of the distribution and ecology of the 10 species recorded. *Hydrobiologia*, 534, pp 31–55.

**List of chironomid-taxa encountered in the MIS 3 sediments at Sokli**

Taxonomy follows /Brooks et al. 2007/ unless indicated otherwise.

*Ablabesmyia*  
*Chaetocladius piger*-type  
*Chironomus anthracinus*-type  
*Chironomus plumosus*-type  
*Cladopelma lateralis*-type  
*Cladotanytarsus mancus* type I  
*Corynocera ambigua*  
*Corynoneura ?carriana*-type  
*Corynoneura coronata*-type  
*Corynoneura lobata*-type  
*Corynoneura scutellata*-type  
*Cricotopus (Isocladius) trifasciatus*-type  
*Cricotopus (Isocladius) intersectus*-type  
*Cryptochironomus*  
*Diamesa* spp.  
*Dicrotendipes nervosus*-type  
*Endochironomus albipennis*-type  
*Endochironomus impar*-type  
*Eukiefferiella*  
*Georthocladius*  
*Glyptotendipes barbipes*-type  
*Heterotrissocladius marcidus*-type  
*Heterotrissocladius grimshawi*-type  
*Limnophyes*  
*Metriocnemus* spp.  
*Microchironomus*  
*Microtendipes pedellus*-type  
*Micropsectra radialis*-type  
*Micropsectra insignilobus*-type  
*Monodiamesa*  
*Orthocladius oliveri*-type  
*Pagastiella orophila*  
*Parachironomus arcuatus* (after /Moller Pillot 1984/)  
*Paracladius*  
*Paracladopelma*  
*Parakiefferiella bathophila*-type  
*Parakiefferiella fennica*-type  
*Parakiefferiella nigra*-type  
*Parametriocnemus/Paraphaenocladius*  
*Paratendipes* spp.  
*Paratanytarsus penicillatus*-type  
*Phaenopsectra flavipes*-type

*Polypedilum nubeculosum*-type  
*Polypedilum pedestre*-type  
*Potthastia gaedii* (after /Oliver and Roussel 1983/)  
*Procladius*  
*Prodiamesa*  
*Psectrocladius sordidellus*-type  
*Pseudochironomus*  
*Pseudodiamesa*  
*Pseudosmittia*  
*Rheotanytarsus* spp.  
*Sergentia coracina*-type  
*Smittia*  
*Stempellina*  
*Stempellinella/Zavrelia*  
*Stictochironomus*  
*Synorthocladius*  
*Tanytarsus nemorosus*-type  
*Tanytarsus mendax*-type  
*Tanytarsus pallidicornis*-type I  
*Tanytarsus lugens*-type  
*Thiennemanniella*  
*Thienemannimyia*

**List of diatom-taxa encountered in the MIS 3 sediments at Sokli**

**Planktonic taxa**

*Actinocyclus* spp Ehrenberg  
*Aulacoseira ambigua* (Grunow) Simonsen  
*Aulacoseira granulata* (Ehrenberg) Simonsen  
*Aulacoseira islandica* (O. Müller) Simonsen  
*Aulacoseira laevissima* (Grunow) Krammer  
*Aulacoseira subartica* (O. Müller) Haworth  
*Cyclostephanos dubius* (Fricke) Round  
*Cyclotella comensis* Grunow in Van Heurck  
*Cyclotella hakanssoniae* Wendker  
*Cyclotella michiganiana* Skvortzow  
*Cyclotella radiosa* (Grunow) Lemmermann  
*Cyclotella schumannii* (Grunow) Håkansson  
*Stephanodiscus medius* Håkansson  
*Stephanodiscus neoastraea* Håkansson & Hickel  
*Stephanodiscus parvus* Stoermer & Håkansson  
*Stephanodiscus* spp Ehrenberg

**Tychoplanktonic taxa**

*Aulacoseira distans* v. *distans* (Ehrenberg) Simonsen  
*Aulacoseira italica* v. *valida* (Grunow) Simonsen  
*Aulacoseira lirata* v. *lacustris* (Grunow) Ross  
*Aulacoseira lirata* v. *lirata* (Ehrenberg) Ross  
*Aulacoseira tenuior* (Grunow) Krammer  
*Aulacoseira tethera* Haworth  
*Cocconeis neodiminuta* Krammer  
*Cyclotella iris* Brun et Héribaud  
*Cyclotella krammeri* Håkansson  
*Diatoma vulgare* Bory  
*Fragilaria capucina* Desmazières  
*Fragilaria capucina* v. *mesolepta* (Rabenhorst) Rabenhorst  
*Synedra ulna* (Nitzsch) Ehrenberg  
*Tabellaria flocculosa* (Roth) Kützing  
*Tabellaria* spp Ehrenberg

**Benthic taxa**

*Achnanthes calcar* Cleve  
*Achnanthes conspicua* A. Mayer  
*Achnanthes holstii* Cleve  
*Achnanthes joursacense* Héribaud  
*Achnanthes lanceolata* (Brébisson) Grunow  
*Achnanthes lanceolata* ssp. *lanceolata* Brébisson ex Kützing  
*Achnanthes lanceolata* ssp. *robusta* (Hustedt) Lange-Bertalot

*Achnanthes oestrupii* (Cleve-Euler) Hustedt  
*Achnanthes rupestoides* Hohn  
*Achnanthes* spp Bory  
*Achnanthes stewartii* Patrick  
*Amphora aequalis* Krammer  
*Amphora libyca* Ehrenberg  
*Amphora ovalis* (Kützing) Kützing  
*Amphora* spp Ehrenberg in Kützing  
*Anomoeoneis sphaerophora* (Ehrenberg) Pfitzer  
*Aulacoseira distans* v. *alpigena* Grunow in Van Heurck  
*Aulacoseira distans* v. *nivalis* (W. Smith) Haworth  
*Aulacoseira italica* (Ehrenberg) Simonsen  
*Aulacoseira pfaffiana* (Reinsch) Krammer  
*Brachysira follis* (Ehrenberg) Ross in Hartley  
*Brachysira zellensis* (Grunow) Round & D. G. Mann  
*Caloneis bacillum* (Grunow) Cleve  
*Caloneis silicula* (Ehrenberg) Cleve  
*Campylodiscus noricus* Ehrenberg  
*Campylodiscus noricus* v. *hibernicus* (Ehrenberg) Grunow  
*Cocconeis disculus* (Schumann) Cleve in Cleve & Jentzsch  
*Cocconeis placentula* Ehrenberg  
*Cocconeis placentula* v. *lineata* (Ehrenberg) Van Heurck  
*Cocconeis placentula* v. *placentula* Ehrenberg  
*Cyclotella ocellata* Pantocsek  
*Cymatopleura elliptica* (Brébisson) W. Smith  
*Cymatopleura elliptica* v. *hibernica* (W. Smith) Van Heurck  
*Cymbella affinis* Kützing  
*Cymbella cistula* (Ehrenberg) Kirchner  
*Cymbella cuspidata* Kützing  
*Cymbella ehrenbergii* Kützing  
*Cymbella elginensis* Krammer  
*Cymbella gracilis* (Ehrenberg) Kützing  
*Cymbella hebredica* (Grunow in Cleve) Cleve  
*Cymbella hybrida* Grunow in Cleve & Möller  
*Cymbella lata* Grunow in Cleve  
*Cymbella mesiana* Chohnoky  
*Cymbella minuta* Hilse ex Rabenhorst  
*Cymbella paucistriata* Cleve-Euler  
*Cymbella prostrata* (Berkeley) Cleve  
*Cymbella proxima* Reimer in Patrick and Reimer  
*Cymbella silesiaca* Bleisch in Rabenhorst  
*Cymbella* spp Agardh  
*Cymbella subaequalis* Grunow in Van Heurck  
*Denticula kuetzingii* Grunow  
*Diatoma ehrenbergii* Kützing  
*Didymosphenia geminata* (Lyngbye) M. Schmidth

*Diploneis domblittensis* (Grunow) Cleve  
*Diploneis elliptica* v. *elliptica* (Kützing) Cleve  
*Diploneis finnica* (Ehrenberg) Cleve  
*Diploneis ovalis* (Hilse) Cleve  
*Diploneis* spp Ehrenberg  
*Epithemia adnata* (Kützing) Brébisson  
*Epithemia frickei* Krammer  
*Epithemia hyndmannii* W. Smith  
*Epithemia sorex* Kützing  
*Epithemia* spp Brébisson ex Kützing  
*Epithemia turgida* (Ehrenberg) Kützing  
*Eunotia arcus* Ehrenberg  
*Eunotia circumborealis* Lange-Bertalot & Nörpel  
*Eunotia exigua* (Brébisson) Rabenhorst  
*Eunotia faba* Ehrenberg  
*Eunotia implicata* Nörpel, Lange-Bertalot & Alles  
*Eunotia lapponica* Grunow  
*Eunotia monodon* Ehrenberg  
*Eunotia pectinalis* v. *undulata* (Ralfs) Rabenhorst  
*Eunotia praerupta* Ehrenberg  
*Eunotia serra* Ehrenberg  
*Eunotia serra* v. *diadema* (Ehrenberg) Patrick  
*Eunotia soleirolii* (Kützing) Rabenhorst  
*Eunotia* spp Ehrenberg  
*Eunotia triodon* Ehrenberg  
*Fragilaria biceps* (Kützing) Lange-Bertalot  
*Fragilaria brevistriata* Grunow in Van Heurck  
*Fragilaria constricta* Ehrenberg  
*Fragilaria construens* (Ehrenberg) Grunow  
*Fragilaria construens* v. *binodis* (Ehrenberg) Hustedt  
*Fragilaria construens* v. *construens* (Ehrenberg) Hustedt  
*Fragilaria construens* v. *venter* (Ehrenberg) Hustedt  
*Fragilaria dilatata* (Brébisson) Lange-Bertalot  
*Fragilaria elliptica* Schumann  
*Fragilaria exigua* Grunow in Cleve & Möller  
*Fragilaria fasciculata* (C. Agardh) Lange-Bertalot  
*Fragilaria lancettula* Schumann (sensu Grunow)  
*Fragilaria lapponica* Grunow in Van Heurck  
*Fragilaria leptostauron* v. *dubia* (Grunow) Hustedt  
*Fragilaria leptostauron* v. *leptostauron* (Ehrenberg) Hustedt  
*Fragilaria neoproducta* Lange-Bertalot  
*Fragilaria nitzschioides* Grunow in Van Heurck  
*Fragilaria pinnata* Ehrenberg  
*Fragilaria pseudoconstruens* Marciniak  
*Fragilaria* spp Lyngbye  
*Frustulia rhomboides* v. *rhomboides* (Ehrenberg) De Toni

*Gomphonema acuminatum* v. *acuminatum* Ehrenberg  
*Gomphonema angustatum* (Kützing) Rabenhorst  
*Gomphonema angustum* Agardh  
*Gomphonema clavatum* Ehrenberg  
*Gomphonema gracile* Ehrenberg  
*Gomphonema grovei* M. Schmidt  
*Gomphonema lagerheimii* A. Cleve  
*Gomphonema olivaceum* (Hornemann) Brébisson  
*Gomphonema parvulum* v. *parvulum* (Kützing) Kützing  
*Gomphonema* spp Agardh  
*Gomphonema subtile* Ehrenberg  
*Gomphonema truncatum* Ehrenberg  
*Gyrosigma acuminatum* (Kützing) Rabenhorst  
*Gyrosigma* spp Hassall  
*Navicula absoluta* Hustedt  
*Navicula cari* Ehrenberg  
*Navicula cuspidata* (Kützing) Kützing  
*Navicula gastrum* (Ehrenberg) Kützing  
*Navicula jentzschii* Grunow  
*Navicula laterostrata* Hustedt  
*Navicula placentula* (Ehrenberg) Kützing  
*Navicula protracta* (Grunow) Cleve  
*Navicula pupula* Kützing  
*Navicula pusilla* W. Smith  
*Navicula radiosa* Kützing  
*Navicula scutelloides* W. Smith ex. Gregory  
*Navicula slesvicensis* Grunow in Van Heurck  
*Navicula* spp Bory  
*Navicula striolata* (Grunow) Lange-Bertalot  
*Navicula tuscula* Ehrenberg  
*Navicula vulpina* Kützing  
*Neidium ampliatum* (Ehrenberg) Krammer  
*Neidium bisulcatum* v. *bisulcatum* (Lagerstedt) Cleve  
*Neidium calvum* Østrup  
*Neidium decoratum* Brun  
*Neidium* spp Pfitzer  
*Nitzschia angustata* v. *angustata* (W. Smith) Grunow in Cleve & Grunow  
*Nitzschia epithemoides* v. *disputata* (Carter) Lange-Bertalot  
*Nitzschia levidensis* (W. Smith) Grunow in Van Heurck  
*Nitzschia levidensis* v. *victoriae* (Grunow) Cholnoky  
*Nitzschia* spp Hassall  
*Opephora martyi* Héribaud  
*Pinnularia alpina* W. Smith  
*Pinnularia borealis* Ehrenberg  
*Pinnularia brevicostata* Cleve

*Pinnularia gibba* Ehrenberg  
*Pinnularia hemiptera* v. *hemiptera* (Kützing) Rabenhorst  
*Pinnularia lata* (Brébisson) Rabenhorst  
*Pinnularia maior* v. *maior* (Kützing) Rabenhorst  
*Pinnularia mesolepta* (Ehrenberg) W. Smith  
*Pinnularia microstauron* (Ehrenberg) Cleve  
*Pinnularia nobilis* (Ehrenberg) Ehrenberg  
*Pinnularia pulchra* v. *angusta* (Cleve) Krammer  
*Pinnularia* spp Ehrenberg  
*Pinnularia streptoraphe* Cleve  
*Pinnularia subrostrata* (A. Cleve) Cleve-Euler  
*Pinnularia viridis* (Nitzsch) Ehrenberg  
*Rhopalodia gibba* v. *gibba* (Ehrenberg) O. Müller  
*Stauroneis acuta* W. Smith  
*Stauroneis anceps* v. *anceps* Ehrenberg  
*Stauroneis dilatata* Ehrenberg  
*Stauroneis javanica* (Grunow) Cleve  
*Stauroneis legumen* (Ehrenberg) Kützing  
*Stauroneis phoenicenteron* v. *phoenicenteron* (Nitzsch) Ehrenberg  
*Stauroneis* spp Ehrenberg  
*Surirella linearis* v. *linearis* W. Smith  
*Synedra parasitica* (W. Smith) Hustedt  
*Tetracyclus ellipticus* (Ehrenberg) Grunow  
*Tetracyclus ellipticus* v. *clypeus* (Ehrenberg) Hustedt  
*Tetracyclus emarginatus* (Ehrenberg) W. Smith  
*Tetracyclus lacustris* Ralfs  
*Tetracyclus lacustris* v. *strumosa* (Ehrenberg) Hustedt  
*Tetracyclus* spp Ralfs

### **Aerophilous taxa**

*Achnanthes exigua* Grunow  
*Caloneis aerophila* Bock  
*Cymbella aspera* (Ehrenberg) Peragallo  
*Cymbella sinuata* Gregory  
*Ellerbeckia arenaria* (Moore) Crawford  
*Eunotia diodon* Ehrenberg  
*Eunotia fallax* A. Cleve  
*Hantzschia amphioxys* (Ehrenberg) Grunow in Cleve & Grunow  
*Melosira dickiei* (Thwaies) Kützing  
*Navicula mutica* Kützing  
*Orthoseira circularis* (Ehrenberg) Crawford  
*Orthoseira roseana* (Rabenhorst) O'Meara  
*Stauroneis agrestis* Petersen

**Rheophilous taxa**

*Achnanthes montana* Krasske

*Aulacoseira italica* f. *crenulata* (Ehrenberg) Ross in Hartley

*Cymbella naviculiformis* (Auerswald) Cleve

*Diatoma mesodon* (Ehrenberg) Kützing

*Eunotia* cf. *minor* (Kützing) Grunow

*Hannaea arcus* v. *arcus* (Ehrenberg) Patrick

*Meridion circulare* v. *circulare* (Greville) Agardh

**Reworked/Tertiary taxa**

*Aulacoseira* cf. *canadensis* (Hustedt) Simonsen

*Campylodiscus echeneis* Ehrenberg

*Coscinodiscus* spp Ehrenberg

*Fragilaria triangulata* Moisseva

*Hemiaulus* spp Ehrenberg

*Paralia sulcata* (Ehrenberg) Cleve

*Pliocaenicos costatus* (Loginova, Lupikina. & Khursevich) Round & Håkansson

*Stephanopyxis* spp Ehrenberg

*Triceratium* spp Ehrenberg

**Unknown ecology**

*Cyclotella* spp (Kützing) Brébisson

*Melosira* spp Agardh

*Surirella* spp Turpin

Varia

